Identification and Characterization of Histone H3K36 Demethylases in *Drosophila melanogaster*

Thesis

Identification and Characterization of Histone H3K36 Demethylases in *Drosophila melanogaster*

Chia-Hui Lin M.Sc.

Submitted in partial fulfillment of the requirements for
the degree of Doctor of Philosophy

Stowers Institute for Medical Research

The Open University

18 April 2011

Date of Submission: 15 April 2011
Date of Award: 17 July 2011

ProQuest LLC.
789 East Eisenhower Parkway
P.O. Box 1346
Ann Arbor, MI 48106 – 1346

ABSTRACT

Covalent modifications of histones, such as acetylation, methylation, phosphorylation and ubiquitination, have an important role in regulating gene expression. Histone methylation is implicated in both gene activation and repression depending on the methylation site and the state of methylation (Li et al., 2007a). Historically, histone methylation was considered to be a static modification. Recent discoveries of histone demethylases demonstrate that histone methylation is reversible. Numerous studies have shown that dynamic regulation of histone methylation plays an important role in many cellular processes (Cloos et al., 2008). However, mechanisms governing the targeting and regulation of histone demethylation remain elusive.

In this thesis, I identified two *Drosophila melanogaster* JmjC domain-containing proteins, dKDM4A and dDKM4B, which are histone H3K36 demethylases. Affinity purification and mass spectrometry analysis revealed that Heterochromatin Protein 1a (HP1a) associates with dKDM4A. I found that the chromoshadow domain of HP1a and a HP1-interacting motif within dKDM4A are responsible for this interaction. HP1a stimulates the histone H3K36 demethylation activity of dKDM4A and this stimulation depends on HP1a binding to the H3K9me. Loss of HP1a leads to increased level of histone H3K36me3. By chromatin immunoprecipitation using an antibody against H3K36me3 in wild type and dKDM4A mutant embryos, I identified candidate target genes of dKDM4A. A subset of dKDM4A target genes are also shown to be bound by HP1a, suggesting dKDM4A-HP1a complex may function in regulating H3K36 levels at these genes.

TABLE OF CONTENTS

LIST OF FIGURES

LIST OF TABLES

ABBREVIATIONS

% (v/v) .....ml per 100ml (volume/volume)
aa.....amino acid
ALL-1 .....acute lymphoblastic leukemia
ALR-1 .....ALL-1 related gene
AR.....androgen receptor
ARID .....AT rich interaction domain
ASCL2.....Achaete scute-like homologue 2
Ash1.....absent small or homeotic discs1
bp .....base pair
BHC.....BRAF-HDAC complex
Bre1 .....Brefeldin A sensitivity 1
BSA .....bovine serum albumin
CBP.....CREB binding protein
CD.....chromo domain
cDNA.....complimentary deoxyribonucleic acid
ChIP.....chromatin immunoprecipitation
Cht3 .....Chitinase 3
Clr4 .....Cryptic loci regulator 4
COMPASS ....Complex proteins associated with Set1
CSD .....chromo shadow domain
C-terminal.....Carboxy terminal
Da .....Dalton
DNA .....deoxyribonucleic acid
Dot1 .....disruptor of telomeric silencing
dRAF .....dRING-associated factors
DTT .....dithiothreitol
ESC.....extra sex combs
Eu-HMTase1 .euchromatic histone methyltransferase 1
E(Z).....Enhancer of Zeste
Ezh2.....enhancer of zest homolog 2
FAD .....flavin adenine dinucleotide
FPKM .....fragments per kilobase per million fragments mapped
GAL4.....positive regulator of galactose inducible genes 4
Gcn5 .....General control nonderepressible 5
GNAT.....Gcn5-related N-acetyltransferase
GO .....gene ontology
HAT.....histone acetyltransferase

HDAC.....histone deacetylase complexes
HKMT .....Histone lysine methyltransferase
Hox .....homeobox
HP1 .....Heterochromatin Protein 1
IP.....immunoprecipitation
JARID1 .....JumonjiC and ARID domain protein 2
JHDM .....JmjC domain-containing histone demethylase 1
JmjC.....Jumonji C
Kb .....kilobase
KDa.....kilodalton
KDM.....lysine demethylase
LRR .....leucine-rich repeats
LSD1.....lysine specific demethylase 1
M.....molar
MDa.....megadalton
mg.....milligram
min.....minute
ml .....millilitre
MLA .....methyl-lysine analog
MLL.....mixed-lineage leukaemia or myeloid / lymphoid leukaemia
mM .....millimolar
MPA .....mycophenolic acid
MRG15.....MORF4-related genes on chromosomes 15
mRNA.....messenger RNA
MSL.....male specific lethal
MudPIT.....multidimensional protein identification technology
MYST.....named for members MOZ, Ybf2/Sas3, Sas2, and Tip60
nm.....nanometer
NP-40.....Nonidet P-40
NRD.....Nucleosome remodelling and deacetylating complex
NSD1 .....nuclear receptor SET domain protein 1
N-terminal.....amino terminal
nvd .....neverland
ORC.....origin recognition complex
ORF .....open reading frame
Paf1 .....RNA polymerase II-associated factor 1
PAGE.....polyacrylamide gel electrophoresis
PBS .....phosphate buffered saline
PC .....Polycomb
PCR.....polymerase chain reaction
PEV.....position effect variegation
PHD .....Plant Homeo Domain
PHF.....PHD finger protein

PRC1.....polycomb repressive complex-1
PRMT .....Protein arginine mehtyltransferase
PTB.....Polypyrimidine tract binding protein
qPCR.....quantitative polymerase chain reaction
Rad6.....Radiation sensitive 6
RBP2.....Retinoblastoma binding protein 2
REST .....RE-1 silencing transcription factor
RNA.....ribonucleic acid
Rpd3S .....reduced potassium dependency 3 small
rpm.....revolutions per minute
rRNA .....ribosomal RNA
RT-qPCR .....reverse transcription followed by quantitative PCR
SAM .....S-adenosylmethionine
SETDB1 .....SET domain bifurcated 1
Scp1 .....Sarcoplasmic calcium-binding protein 1
SD.....standard deviation
SDS.....sodium dodecyl sulphate
SET .....Suppressor of variegation 3-9, Enhancer of zeste, Trithorax
Su(var)2-5.....Suppressor of variegation 2-5
Su(var)3-9.....Suppressor of variegation 3-9
SUZ12.....suppressor of zeste-12
Swi6..... mating type switching 6
SWIRM.....named for its presence in the proteins Swi3, Rsc8, and
.....Moira
Trx .....trithorax
TSGA.....testis-specific gene A
µM .....micromolar
UTX.....ubiquitously transcribed tetratricopeptide repeat, X chromosome
UTY .....ubiquitously transcribed tetratricopeptide repeat, X chromosome
wupA .....wings up A
XLMR.....X-linked mental retardation

ACKNOWLEDGEMENTS

I would like to thank my advisor Jerry for giving me the opportunity to work in his lab and for his guidance and support. I appreciate his patience and encouragement especially when the project did not go smoothly. I would like to thank all members in the Workman lab, past and present, for their advice and encouragement. I have learned many techniques from them and had many discussions about science with them. In particular, I want to thank Bing, who helped me a lot and also gave a lot of input to this project. I also want to thank Tamaki and Vikki, who taught me a lot of techniques and fly genetics. I want to thank Susan Abmayr for helpful discussions about fly work, and members of her lab for sharing reagents.

I want to thank people in core facilities, including Media Prep, Molecular Biology, Proteomics, Microscopy Center, Bioinformatics, and Tissue Culture, in Stowers Institute. In particular, I want to thank Ying Zhang for analyzing MudPIT results, Hua Li, Ariel Paulson and Chris Seidel for analyzing genomic data.

I want to thank my thesis committee, Ali Shilatifard, Joan Conaway, Robb Krumlauf, and Susan Abmayr, for helpful suggestions and discussions on this project.

Last, but not least, I would like to thank my parents and my sister for their support and encouragement.

Chapter 1 Introduction

1.1 Chromatin

In eukaryotic cells, about two meters of DNA is packed into a condensed structure known as chromatin. DNA wraps around an octamer of histone proteins and further organizes into the higher order chromatin structures. The compact structure of chromatin is important in regulation of gene transcription by restricting DNA accessibility. Although the structure of chromatin is condensed, it is also dynamic, which is regulated by histone modification and nucleosome remodeling.

1.2 Core Histones and the Nucleosomes

The basic unit of chromatin is the nucleosome, which consists of 146 base pairs of DNA wrapped around a histone octamer of histones H2A, H2B, H3 and H4 (Kornberg and Lorch, 1999). Through crystallographic analysis, the shape of the histone octamer has been described as a wedge or a flat disk (Klug et al., 1980), as well as a tripartite assembly with a central $(H3\text{-}H4)_2$ tetramer flanked by two H2A-H2B dimers, forming a left-handed superhelix (Arents et al., 1991; Burlingame et al., 1985). Each of the core histone proteins shares a common motif, histone fold, which consists of a long central helix flanked by a loop segment and a shorter helix on either side (Arents and Moudrianakis, 1995). The histone fold domain provides DNA binding sites on histones, and is involved in the formation of histone heterodimers via a handshake motif, in which two histone chains clasps each other through the head-to-tail association (Arents et al., 1991; Arents and Moudrianakis, 1995). The tetramer of $(H3\text{-}H4)_2$ is formed through the interaction of the two copies of H3, while the octamer is completed by the assembly of H2A-H2B dimers through two H4-H2B associations. The histone octamer is only stable at high salt

conditions or when wrapped with DNA due to the fact that the interface of H4-H2B interaction is more hydrophobic than that of H3-H3 interaction (Luger et al., 1997).

In each nucleosome, 146 base pairs of DNA wraps in 1.65 turns around the core histones in a left-handed superhelix with 7.6 turns of DNA helix in each superhelical turn (Richmond et al., 1984). The central 12 turns of the DNA helix contact the positively charged surface of the octamer as the path of the DNA helix around the octamer coincides with the path of histone-positive charges on the surface of the octamer (Richmond et al., 1984). Each histone heterodimer is associated with 27-28 base pairs of DNA, leaving 4 base pairs linkers between them. Additional DNA interactions are provided by the N-terminal tails of H3 and H2B, which project through the minor groove of the helix, and by the N-terminal tail of H2A, which binds the minor groove on the outside of the superhelix (Luger et al., 1997).

1.3 Linker Histone H1 and Higher order Chromatin Structure

In metazoans, linker histones, such as histone H1, bind to nucleosomes and 20 base pairs of linker DNA, forming the chromatosome (Simpson, 1978). The linker histone is composed of an unstructured long N-terminal domain and a long C-terminal domain, flanking a globular domain (Allan et al., 1980). The globular domain contains at least two DNA-binding sites, which allow the linker histone to bridge DNA molecules (Thomas et al., 1992). Linker histones bind to nucleosomes at the entry and exit sites of the nucleosomal DNA (Hayes et al., 1994), which increases the micrococcal nuclease protection of nucleosome to 168 base pairs (Noll and Kornberg, 1977).

The primary structure of chromatin is composed of a 10 nm-diameter nucleosome arrays, which can be observed as a "beads-on-a-string" conformation under low salt condition (Thoma et al., 1979). The addition of divalent cation causes a heterogeneous population of folded arrays, including the secondary chromatin structure, a compact 30 nm fiber

(reviewed in (Horn and Peterson, 2002)). The folding of 30 nm chromatin fiber is stabilized by binding of linker histones, which can convert the heterogeneous population of folded arrays to homogeneous and fully-compacted arrays (Carruthers et al., 1998). It has also been found that the removal of N-terminal tails of core histones blocks condensation of chromatin even in the presence of linker histones, suggesting that interactions between histone tails also contribute to the establishment of condensed chromatin structure (Carruthers and Hansen, 2000).

The structure of the compacted 30nm chromatin has been studied and there are two different basic models for its structure: the one-start helix, or solenoid, and the two-start helix. In the one-start helix model, 6 consecutive nucleosomes containing linker histones are arranged to complete a helical turn, so each nucleosome (N) contacts with its neighboring nucleosomes (N+1 and N-1) . In the two-start helix model, nucleosomes are stacked in a zig-zag arrangement, in which linker DNA connects between two stacked rows of nucleosomes, so the nearest neighbors of a nuecleosome (N) are nucleosome N-2 and N+2 (reviewed in (van Holde and Zlatanova, 2007)). The 30 nm chromatin fibers are further compacted into 100 nm-300 nm thick mitotic chromosomes (Belmont et al., 1987).

1.4 Post-translational Modifications of Histones

Histone modifications were first reported in the early 1960s (Allfrey et al., 1964). It was speculated that modifications of histone tails could affect chromatin structure after the structure of the nucleosome was solved, in which highly basic histone N-terminal tails were found to protrude from the nucleosome and make contacts with DNA (Luger et al., 1997). It is now known that many different modifications occur at specific residues of the histone tails and within the globular domains (Table1-1) (reviewed in ((Kouzarides, 2007)). The most studied histone modifications include acetylation, methylation, phosphorylation and ubiquitination. These modifications not only directly affect the accessibility of histone-

bound DNA, but also recruit proteins or complexes to regulate gene transcription. It has also been reported that cross-regulations occur between different modifications, either *in cis* (on one histone) or *in trans* (between histones) (reviewed in (Latham and Dent, 2007)). For example, histone H3S10 phosphorylation promotes acetylation of histone H3K14 (Lo et al., 2000), while it blocks acetylation and methylation of histone H3K9 to prevent heterochromatin protein 1, HP1, binding (Edmondson et al., 2002; Fischle et al., 2005). The cross-talk between histone modifications *in trans* was seen between histone H2B and H3. Monoubiquitination of histone H2BK123 is required for methylation of histone H3K4 and H3K79 (Shilatifard, 2006). A "histone code" hypothesis was proposed that modifications of histones provide epigenetic markers for gene expression, and combinations of histone modifications generate different readouts which are translated into biological functions (Jenuwein and Allis, 2001).

Table 1-1 Modifications identified on histones and their functions.

Modification	Residues modified	Functions
Acetylation	K	Transcription, repair, replication, condensation
Methylation	K and R	Transcription, repair
Phosphorylation	S and T	Transcription, repair, condensation
Ubiquitination	K	Transcription, repair
Sumoylation	K	Transcription
ADP ribosylation	E	Transcription
Deimination	R to Citrulline	Transcription
Proline Isomerization	P (cis to trans)	Transcription

1.4.1 Histone Acetylation

When Allfrey and colleagues first found that histones can be acetylated, they proposed that it might be involved in regulation of gene transcription (Allfrey et al., 1964). Later it was found that acetylation is related to active gene transcription (Hebbes et al., 1994; Hebbes et al., 1988). There are two hypotheses on how histone acetylation regulates gene transcription. First, histone acetylation neutralizes the positive charge of the lysine residues on histone tails, which weaken the interactions between DNA and histones, resulting in a more open chromatin structure for the binding of the transcription machinery (Ausio and van Holde, 1986; Hong et al., 1993). The second hypothesis proposed that the acetylation marks provide binding sites for factors and complexes which regulate gene transcription (Syntichaki et al., 2000). This modification is carried out by histone acetyltransferases (HATs), which catalyze the transfer of an acetyl group from acetyl-CoA to the ε-amino group of the lysine residues on the N-terminal tails of histones. The direct link of histone acetylation and gene activation came when the homolog of yeast transcription activator Gcn5 was isolated as a histone acetyltransferase in *Tetrahymena* (Brownell et al., 1996). There are two classes of HATs: nuclear type A HATs and cytoplasmic type B HATs. The type B HATs acetylate free histones before they are assembled into chromatin (Parthun et al., 1996). The type A HATs acetylate histones in the form of chromatin, thus they are linked to transcription activation (Brownell and Allis, 1996). The type A HATs include Gcn5-related N-acetyltransferases (GNATs), MYST HATs, CBP/p300 HATs, the general transcription factor HATs and the nuclear hormone-related HATs (reviewed in (Carrozza et al., 2003)). Histone acetylation is reversible and the reaction is catalyzed by histone deacetylases (HDACs) (Table 1-2).

Table 1-2 Different classes of histone deacetylases (HDACs)

Class	*S. cerevisiae*	Mammals	Localization
Class I	Rpd3	HDAC1, 2, 3 and 8	nucleus
Class IIa	Hda1	HDAC4, 5, 7and 9	nucleus and cytoplasm
IIb		HDAC6 and 10	cytoplasm
Class III	Sir2	SIRT1, 2, 3, 4, 5, 6 and 7	nucleus, cytoplasm, or mitochondria
Class IV		HDAC11	nucleus

1.4.2 Histone Methylation

Histone methylation is found on histone H3 and H4 (Table 1-3). The stability and slow turnover rate of methyl groups observed in early studies led to the belief that histone methylation was a static and irreversible modification (Borun et al., 1972; Byvoet, 1972). However, recent discoveries of numerous histone demethylases have shown that histone methylation is dynamically regulated (Klose et al., 2006a). Methylation of histone lysines is mediated by histone lysine methyltransferases (HKMTs), which catalyze the transfer of a methyl group from S-adenosylmethionine (SAM) to the ε-amino group of the lysine residues. Histone lysines can be mono-, di- or trimethylated, and histone methylation can be involved in gene activation or gene silencing (Li et al., 2007a). In general, methylation at histone H3K4, K36 and K79 is associated with active transcription, while methylation at histone H3K9, K27 and H4K20 is linked to gene silencing (Martin and Zhang, 2005). Histone methylation also occurs at arginine residues of histone H3 and H4 in higher eukaryotes. Histone arginine can be mono- or di-methylated, which is mediated by protein arginine methyltransferases (PRMTs). PRMTs catalyze the transfer of a methyl group from SAM to the ω-guanidino group of arginine residues (Shilatifard, 2006). Several protein motifs, such as chromodomain, tudor domain, PHD finger domain and WD40-repeat domain, have been found to bind to methylated lysines (Bannister et al., 2001; Huyen et al., 2004; Li et al., 2006; Pena et al., 2006; Shi et al., 2006; Wysocka et al., 2005). The specific interactions between methylated lysine residues and proteins with those motifs result in different biological outcomes.

Table 1-3 Histone methyltransferases and their site specificities

Site specificity	Histone Methyltransferase		
	S. cerevisiae	*D. melanogaster*	*Mammals*
H3K4	Set1	Trx, Ash1	Set9/7, ALL-1, MLL, ALR-1/2, ALR, Set1
H3K9	-	Su(var)3-9, Ash1, SETDB1	Suv39h1/2, G9a, Eu-HMTase1, ESET, SETDB1
H3K27	-	E(Z)	Ezh2
H3K36	Set2	dSet2, dMes4	Set2/HYPB, NSD1, Smyd2
H3K79	Dot1	dDot1/grappa	Dot1L
H4K20	-	PR-Set7/SET8, Ash1, SUV4-20	PR-Set7/SET8, Suv4-20h1/2
H3R2	-	-	CARM1
H3R17	-	-	CARM1
H3R26	-	-	CARM1
H4R3	-	-	PRMT1

Unlike HATs, histone methyltransferases are more specific for their target residues. The first HKMTs identified are the mammalian Suv39h and its *S. pombe* homolog, Clr4, which catalyze the methylation of histone H3K9 (Rea et al., 2000). Most of the HKMTs contain a SET domain, named after *Drosophila Su(var)3-9*, *Enhancer of zeste (E(z))* and *trithorax (trx)*. An exception is the Dot1 enzyme, a histone H3K79 methyltransferase, which does not contain a SET domain (Feng et al., 2002; van Leeuwen et al., 2002). Although multiple HKMTs have been found to target the same histone lysine residue, each HKMT has specificity on its target genes and the degree of methylation carried out, thus regulating different cellular process. For example, the mammalian histone H3K9 methyltransferases include Suv39h1, Suv39h2, G9a and SETDB1. Suv39h1 and Suv39h2 catalyze trimethylation of histone H3K9 at heterochromatin, while G9a mediates mono- and di-methylation and SETDB1 mediates tri-methylation of histone H3K9 at euchromatic regions (Shilatifard, 2006) .

Suv39h1-mediated histone H3K9 methylation at heterochromatin was found to be involved in the formation of heterochromatin. The methylated histone H3K9 provides a binding site for the chromodomain-containing heterochromatin protein HP1 (Bannister et

al., 2001; Lachner et al., 2001). G9a and SETDB1-mediated H3K9 methylation contributes to HP1-mediated gene silencing at euchromatin (Rice et al., 2003; Schultz et al., 2002). However, a recent study showed that tri-methylated histone H3K9 and HP1γ are enriched at the coding region of active genes, suggesting that they might also be involved in active transcription (Vakoc et al., 2005). Histone H3K27 is methylated by E(Z) (or EZH2) complex, which consists of a SET domain-containing protein E(Z), ESC (extra sex combs) and SUZ12 (suppressor of zeste-12) (Cao et al., 2002; Czermin et al., 2002; Kuzmichev et al., 2002; Muller et al., 2002). Methylated histone H3K27 provides a binding site for a chromodomain-containing protein, Polycomb (Pc), which is a subunit of PRC1 (polycomb repressive complex-1) (Min et al., 2003). It is required for the H2A ubiquitination by another component, Ring1B, of PRC1 (Cao et al., 2005). Histone H3K27 methylation has been linked to Hox gene silencing, X inactivation and pluripotency of stem cells (Cao and Zhang, 2004). Histone H4K20 methylation is also a marker of heterochromatin. Two SET-domain-containing proteins, Suv4-20h1 and Suv4-20h2, catalyze H4K20 tri-methylation at pericentric regions (Schotta et al., 2004). SET8/PR-Set7 mediates the mono-methylation of H4K20, which is required in cell cycle regulation (Fang et al., 2002; Karachentsev et al., 2005; Nishioka et al., 2002).

Methylated histone H3K4 and K36 are hallmarks of actively transcribe genes. Tri-methylated histone H3K4 is enriched at the 5' region of genes and is mediated by Set1/MLL protein. Set1 is a subunit of COMPASS (complex proteins associated with Set1), which is associated with early elongating RNA polymerase II via the Paf1 complex (Shilatifard, 2006). Set2-mediated trimethylation of histone H3K36 is enriched at 3' of coding regions of actively transcribed genes and has been shown to be involved in transcription elongation (Li et al., 2007a). Methylation of histone H3K79 is catalyzed by Dot1 when histone H3 is assembled in the chromatin, and is required for proper telomeric-

associated gene silencing by preventing the spread of Sir protein complexes (Ng et al., 2003; van Leeuwen et al., 2002).

1.4.3 Histone Phosphorylation

Histone phosphorylation is correlated with several cellular events, including mitosis and meiosis chromosome condensation, DNA repair and gene transcription. Histone phosphorylation occurs at serines, threonines and tyrosines on histone tails and the globular regions. It is mediated by kinases and is removed by phosphatases (reviewed in (Iizuka and Smith, 2003; Nowak and Corces, 2004)). Phosphorylation of histone H3S10 and H3S28 were found to be involved in chromosome condensation during mitosis (Goto et al., 1999; Wei et al., 1999). It was also found that histone H3 is rapidly phosphorylated during the induction of *c-fos* and *c-jun* genes, suggesting a role in gene activation (Mahadevan et al., 1991). Indeed, it was later found that phosphorylation of histone H3S10 can promote the acetylation of histone H3K9 and H3K14 mediated by Gcn5 (Lo et al., 2001; Lo et al., 2000). Histone H1 phosphorylation was also found to regulate transcription of specific genes through a different mechanism. Phosphorylation creates localized negative charge patch, which increases the rate of H1 dissociation from chromatin (Dou et al., 2002; Dou and Gorovsky, 2002). Phosphorylation of the C-terminal domains of mammalian H2AX, yeast H2A and fly H2Av is required for DNA repair in response to double strand breaks (Celeste et al., 2002; Downs et al., 2000; Madigan et al., 2002).

1.4.4 Histone Ubiquitination

Ubiquitin is a 76 amino acid protein conjugated to substrate proteins in a reaction involving three enzymes: an E1 activating enzyme, an E2 conjugating enzyme and an E3 ligase (reviewed in (Hochstrasser, 1996)). Polyubiquitinated substrates are subject to degradation by the 26S proteasome, while monoubiquitination regulates the localization

and activity of proteins (reviewed in (Hicke, 2001)). Monoubiquitination of histones has been reported for histone H2A (Goldknopf et al., 1975), H2B (Thorne et al., 1987), H3 (Chen et al., 1998) and H1 (Pham and Sauer, 2000). Monoubiquitination of yeast histone H2B at lysine 123 is mediated by the E2 enzyme Rad6 and the E3 ubiquin ligase Bre1 (Hwang et al., 2003; Wood et al., 2003). Loss of H2B ubiquitination in yeast causes defects in cell growth and sporulation (Robzyk et al., 2000). H2B monoubiquitination is required for methylation of histone H3K4 and K79, two histone marks of active transcription (Shilatifard, 2006). It has been reported that H2B ubiquitination regulates the binding of the Cps35 subunit of COMPASS, the complex mediating histone H3K4 methylation in yeast, which is essential for the methyltransferase activity (Lee et al., 2007a). In humans, H2A ubiquitination is mediated by PRC1 subunit Ring1B, and 2A-HUB E3 ligases, which are associated with gene silencing (Cao et al., 2005; Wang et al., 2004; Zhou et al., 2008). H2A ubiquitination is present at the promoters of PRC1 target genes in a Ring1B-dependent manner (Cao et al., 2005; Wang et al., 2004). Methylation of histone H3K27 mediated by PRC2 is required for H2A monoubiquitination (Cao et al., 2005).

1.5 Histone H3K36 Methylation

Histone H3K36me3 is enriched at the 3' end of actively transcribed genes (Bannister et al., 2005; Pokholok et al., 2005). In *S. cerevisiae*, H3K36 methylation is catalyzed by a sole enzyme, Set2, which associates with the elongating form of RNA polymerase II (Krogan et al., 2003; Li et al., 2003; Schaft et al., 2003; Xiao et al., 2003). The methylated H3K36 nucleosomes are recognized by the combinatorial action of two subunits, Eaf3 and Rco1, of the Rpd3S histone deacetylase complex (Li et al., 2007b), and are required for the activity of Rpd3S following its recruitment to transcribed genes by the phosphorylated RNA polymeraseII C-terminal domain (Drouin et al., 2010; Govind et al., 2010). The

recruitment of Rpd3S to coding regions results in a hypoacetylated chromatin environment within ORFs, which prevents intragenic transcription initiation at cryptic promoters (Carrozza et al., 2005; Joshi and Struhl, 2005; Keogh et al., 2005).

Through genome-wide analysis of histone modifications in higher eukaryotes, it has been shown that histone H3K36me3 is not only enriched at coding region of actively transcribed genes as seen in yeasts, the pattern of enrichment is also highly correlated to exonic regions (Andersson et al., 2009; Dhami et al., 2010; Hon et al., 2009; Kolasinska-Zwierz et al., 2009). Moreover, alternatively spliced exons show lower levels of H3K36me3 than constitutively expressed exons, suggesting exon marking of H3K36me3 is related to alternative splicing (Kolasinska-Zwierz et al., 2009). A recent study of PTB (polypyrimidine tract binding protein)-dependent alternative spliced genes found that the high level of H3K36me3 along the alternatively spliced exon attracts MRG15, a chromatin-binding factor specifically recognizing H3K36me3, which recruits the PTB splicing factor, thus inducing exon skipping (Luco et al., 2010).

A role for H3K36 methylation in *Drosophila* dosage compensation has recently been reported (Bell et al., 2008; Larschan et al., 2007). Dosage compensation is an essential process to equalize the expression level of X chromosome-linked genes between males and females. In *Drosophila*, it is mediated by the MSL (male-specific lethal) complex, which upregulates the transcription of genes on the X chromosome in males by twofold (Straub and Becker, 2007). The MSL complex is recruited to active genes on X chromosome through binding to H3K36me3 by the chromo domain of its subunit, MSL3 (Bell et al., 2008; Larschan et al., 2007; Sural et al., 2008). The H3K36me3-dependent recruitment of the MSL complex is required for the spreading of the MSL complex to its target genes following the initial recognition of chromatin entry sites (Sural et al., 2008).

1.6 Histone Demethylases

Unlike other histone modifications, histone methylation was considered to be a static modification because the N-CH_3 bond is highly stable thermodynamically and the half-life of the methylated lysine is similar to that of histones. Histone replacement or histone tail clipping were believed to be the possible mechanisms to remove methylation marks. Reaction mechanisms for removal of methyl group by enzymatic demethylation was first proposed in 2002 (Bannister et al., 2002), and it was not until 2004 that the first histone demethylase, LSD1 (lysine-specific demethylase 1) /KDM1A, was identified (Shi et al., 2004). LSD1 demethylates di- and mono-methylated histone H3K4 (K4me2/me1) or K9 (K9me2/me1) through a flavin adenine dinucleotide (FAD)-dependent oxidative reaction (Metzger et al., 2005; Shi et al., 2004). In 2006, the first JmjC domain-containing demethylase, JHDM1/KDM2A, was identified as a histone H3K36 demethylase (Tsukada et al., 2006). Since this initial discovery, a cluster of Jumonji C (JmjC) domain-containing proteins have been identified as histone demethylases that can specifically remove methyl groups from histone H3K4, K9, K27, K36, R2, H4K20 and R3 (Table 1-4) (Agger et al., 2008; Pedersen and Helin, 2010).

Table 1-4 The histone demethylase families and their substrate specificities

	H. sapiens	Specifity	*D. melanogaster*	*S. cerevisiae*
KDM1	**KDM1A/LSD1**	**H3K4me2/me1 H3K9me2/me1**	**Su(var)3-3/CG17149**	
	KDM1B/LSD2	**H3K4me2/me1**		
KDM2	**KDM2A/JHDM1A**	**H3K36me2/me1**		
	KDM2B/JHDM1B	**H3K36me2/me1 H3K4me3**	**dKDM2/CG11033**	**Jhd1**
KDM3	**KDM3A/JHDM2A** KDM3B/JHDM2B JHDM2C	**H3K9me2/me1**	CG8165	
KDM4	**KDM4A/JMJD2A KDM4B/JMJD2B KDM4C/JMJD2C KDM4D/JMJD2D**	**H3K36me3/me2 H3K9me3/me2 H1.4K26me3.me2**	**dKDM4A/CG15835 dKDM4B/CG33182**	**Rph1** Gis1
KDM5	**KDM5A/JARID1A KDM5B/JARID1B KDM5C/JARID1C KDM5D/JARID1D**	**H3K4me3/me2**	**Lid/CG9088**	**Jhd2** Ecm5
KDM6	**KDM6A/UTX KDM6B/JMJD3** UTY	**H3K27me3/me2**	**UTX/CG5640**	
PHF	**KDM7/KIAA1718 PHF8**	**H3K9me2/me1 H3K27me2 H4K20me1**		
	PHF2	**H3K9me1**		
KDM8	**JMJD5**	**H3K36me2**		
JMJD6	**JMJD6**	**H3R2 H4R3**	PSR/CG5383	

Proteins with known demethylation activity are shown in bold.

1.6.1 LSD1

LSD1/KDM1A, also known as p110b, BHC110, KIAA0601, was previously identified as a subunit of several co-repressor complexes, including NRD (Tong et al., 1998), CoREST (You et al., 2001), BHC (BRAF–HDAC complex) (Hakimi et al., 2002) and CtBP co-repressor complex (Shi et al., 2003). The C-terminal domain of LSD1 shares significant sequence homology with FAD-dependent amine oxidases. The SWIRM domain at the N-terminus of LSD1 has been found in several proteins involved in chromatin regulation (Aravind and Iyer, 2002). In 2004, Shi and colleagues demonstrated that LSD1 can demethylate histone H3K4me2/me1 (Shi et al., 2004). It uses FAD as a co-factor to catalyze the oxidation of amino groups of the di- or mono-methylated lysine, generating imine intermediates which spontaneously hydrolyze to produce formaldehyde and a mono- or unmethylated lysine (Figure 1-1A). The demethylation reaction catalyzed by LSD1

requires a protonated nitrogen as a hydrogen donor, limiting its substrates to di- and mono-methylated residues.

The enzymatic activity and specificity of LSD1 have been shown to be regulated by its associated proteins, including CoREST (Lee et al., 2005; Shi et al., 2005), BHC80 (Shi et al., 2005) and androgen receptor (AR) (Metzger et al., 2005). CoREST stimulates the demethylation activity of LSD1 on histone H3K4me2/me1 and also promotes demethylation activity on nucleosomes, while LSD1 alone shows no activity towards nucleosomal substrates. In contrast, BHC80 inhibits the demethylation activity of LSD1. When LSD1 is in complex with AR, it functions as a transcriptional activator and demethylates histone H3K9me.

1.6.2 The JmjC Domain Protein Family

Jumonji, cruciform in Japanese, was first identified in a gene trap study in mice. The gene was named Jumonji because an abnormal cross-like neural groove is formed on the neural plate in mice with a gene trap inserted in Jumonji locus (Takeuchi et al., 1995). The JmjC domain was defined by the conserved sequences in Jumonji (Jarid2), Smcx (Jarid1C) and RBP2 (Jarid1A) (Balciunas and Ronne, 2000; Clissold and Ponting, 2001; Takeuchi et al., 1995). There are 27 JmjC domain-containing proteins within the human genome, and they are highly conserved from yeast to human. The mechanism of histone demethylation by JmjC domain-containing proteins was first proposed in 2005 based on the oxidative demethylation reaction of DNA by bacterial AlkB protein (Trewick et al., 2005).

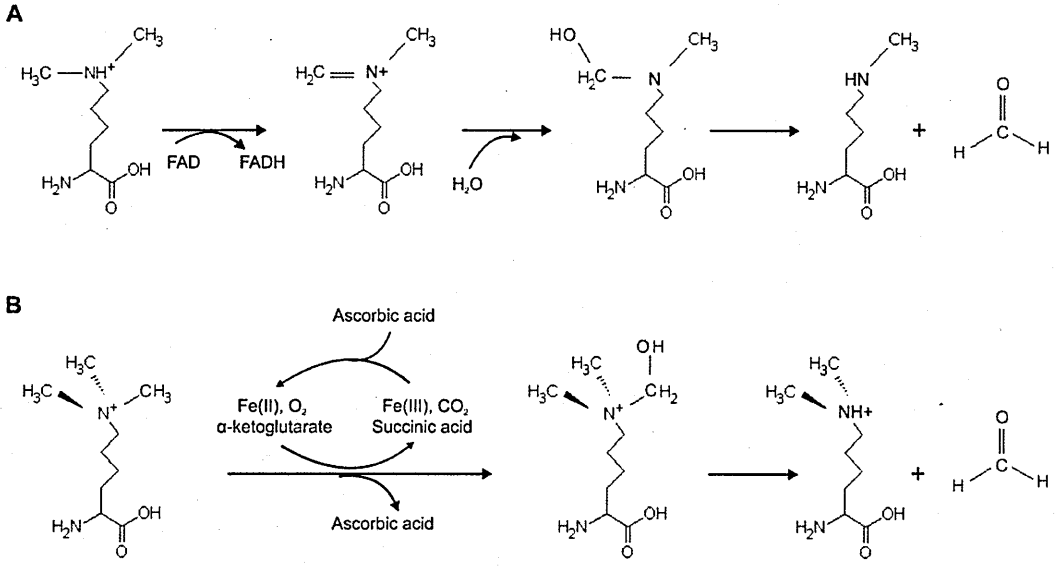

Figure 1-1 Chemical mechanisms of histone lysine demethylation by LSD1 and JmjC family proteins.

(A) LSD1 requires FAD as a cofactor to catalyze an amine oxidation of the protonated nitrogen, creating an imine intermediate, which is hydrolyzed to release formaldehyde, resulting in a mono-methylated lysine.
(B) JmjC domain-containing demethylases mediate the demethylation reaction by an oxidative mechanism, which requires Fe (II) and α-ketoglutarate as cofactors. Demethylation occurs by hydroxylation of the methyl group, resulting in an unstable hydroxymethyl intermediate, which is spontaneously released as formaldehyde.

JHDM1A/KDM2A was the first identified JmjC domain-containing demethylase, which specifically demethylates mono- and di-methylated histone H3K36. JmjC domain-containing demethylases remove methyl groups from histones by an oxidative reaction which requires Fe (II) and α-ketoglutarate as cofactors (Figure 1-1B) (Tsukada et al., 2006). Unlike LSD1, this reaction mechanism allows JmjC domain-containing demethylases to act on all three states of methylated lysines. Soon after the publication of JHDM1, several groups identified JMJD2/KDM4, the first demethylase capable of demethylating tri-methylated lysines, H3K36me3/me2 and/or H3K9me3/me2 (Cloos et al., 2006; Fodor et al., 2006; Klose et al., 2006b; Whetstine et al., 2006).

Based on the alignment of JmjC domains, the JmjC domain-containing proteins can be grouped into different subfamilies (Klose et al., 2006a). In most cases, proteins within the same subfamily have the same specificity for histone demethylation.

1.6.2.1 KDM2 Family

There are two human proteins, KDM2A/JHDM1A/FBXL11 and KDM2B/JHDM1B/FBXL10, in the KDM2 family. Homologs of KDM2 can be found from budding yeast to humans. The human, mouse and fly KDM2 orthologs contain an F-box domain, a CXXC zinc-finger domain and leucine-rich repeats (LRRs) in addition to the JmjC domain. KDM2A was the first identified JmjC domain-containing demethylase, which demethylates di- and mono-methylated histone H3K36 (Tsukada et al., 2006). KDM2B was also reported to have demethylation activity on H3K36me2/me1 (He et al., 2008; Tsukada et al., 2006), while H3K4me3-specific demethylase activity was also observed (Frescas et al., 2007).

1.6.2.2 KDM3 Family

KDM3A/JMJD1A/JHDM2A/TSGA (testis-specific gene A) was originally identified as a male germ-specific transcript (Hoog et al., 1991). It was later reported to be an H3K9me2/me1 demethylase and acts as a coactivator of androgen receptor (AR) (Yamane et al., 2006). The biological function of KDM3A has been linked to spermatogenesis as it positively regulates the expression of two genes, Tnp1 and Prm1, by removing H3K9 methyl marks from their promoters. Tnp1 and Prm1 are involved in sperm chromatin condensation and maturation during spermiogenesis (Okada et al., 2007). There are two other human proteins, KDM3B/JMJD1B/JHDM2B and JMJD1C/JHDM2C/TRIP8 (thyroid receptor interacting protein8), that belong to this family, however, their enzymatic activities have not been reported yet.

1.6.2.3 KDM4 Family

The KDM4 family consists of four human proteins, KDM4A/JMJD2A, KDM4B/JMJD2B, KDM4C/JMJD2C and KDM4D/JMJD2D. While KDM4D only contains JmjC and JmjN domains, other KDM4 proteins also contain PHD and Tudor domains. KDM4 proteins have demethylation activity on histone H3K36me3/me2 and/or H3K9me3/me2, as the specificity varies between family members (Cloos et al., 2006; Fodor et al., 2006; Klose et al., 2006b; Whetstine et al., 2006). It has recently been reported that KDM4 proteins also have demethylation activity on H1.4K26me3/me2 (Trojer et al., 2009). Overexpression of KDM4A-C results in decreased level of H3K9me3 at pericentric heterochromatin and abrogates the recruitment of HP1 (Cloos et al., 2006; Fodor et al., 2006; Klose et al., 2006b). Amplification of the KDM4B and KDM4C locus has been seen in multiple cancers, and KDM4A-C were also found to be overexpressed in cancer cells, suggesting roles in tumor development (Liu et al., 2009; Northcott et al., 2009; Yang et al., 2001). Moreover, KDM4C has been found to positively regulate Nanog gene expression by removing repressive H3K9me3 marks at the promoter, and is critical for ES cell self-renewal (Loh et al., 2007).

1.6.2.4 KDM5 Family

KDM5 proteins all have demethylation activity on histone H3K4me3/me2 (Christensen et al., 2007; Iwase et al., 2007; Klose et al., 2007b; Lee et al., 2007b; Tahiliani et al., 2007; Yamane et al., 2007). There are four human proteins in this family, KDM5A/JARID1A/RBP2, KDM5B/JARID1B/PLU-1, KDM5C/JARID1C/SMCX and KDM5D/JARID1D/SMCY. Homologs of KDM5 proteins can be found from yeast to human. In higher eukaryotes, KDM5 proteins contain JmjN, JmjC domains, Bright/Arid (AT-rich interactive domain), PHD and C5HC2 zinc-finger domains. KDM5A was originally identified as an RB binding protein (Defeo-Jones et al., 1991). It has been shown

that KDM5A acts as a repressor on genes involved in differentiation, while pRB binding converts KDM5A to a transcriptional activator (Benevolenskaya et al., 2005). Indeed, KDM5A was found to mediate transcriptional repression of Hox genes in ES cells through demethylating H3K4me3 (Christensen et al., 2007). KDM5B displays a restricted expression pattern in normal adult tissue and is highly expressed in breast and prostate cancers (Lu et al., 1999; Xiang et al., 2007). It has been reported that the demethylation activity of KDM5B plays an important role in proliferation of breast cancer cell lines through repression of tumor suppressor genes (Yamane et al., 2007). The function of KDM5C has been linked to brain development. Mutations in KDM5C are frequently identified in patients with XLMR (X-linked mental retardation) (Jensen et al., 2005). KDM5C was found to function with REST in gene silencing of REST target genes (Tahiliani et al., 2007). KDM5D was found to associate with polycomb-like protein Ring6a/MBLR and mediate gene repression (Lee et al., 2007b).

1.6.2.5 KDM6 Family

KDM6 family consists of KDM6A/UTX, KDM6B/JMJD3 and UTY in mammalian cells. KDM6A and KDM6B have demethylation activity on histone H3K27me3/me2, while no activity has been reported for UTY (Agger et al., 2007; De Santa et al., 2007; Lan et al., 2007; Lee et al., 2007c). There are UTX orthologs from worms to human. UTX and UTY contain TPR (tetratricopeptide repeat) domains in addition to JmjC domain, whereas KDM6B/JMJD3 lacks the TPR domain. The TPR domain is a structural motif that has been implicated in mediating protein-protein interactions (Blatch and Lassle, 1999). Indeed, it has been reported that UTX forms part of different H3K4-methyltransferase complexes (Cho et al., 2007; Issaeva et al., 2007; Lee et al., 2007c). The presence of UTX in H3K4 HMT complexes suggests a model in which UTX coordinates with the H3K4 methyltransferase by removing the repressive H3K27me3, leading to transcriptional activation. UTX has been found to be recruited to HOX loci upon differentiation,

indicating the important role of UTX during development (Agger et al., 2007; Lan et al., 2007; Lee et al., 2007c). KDM6B has also been reported to be required during epidermal differentiation (Sen et al., 2008). It has also been demonstrated that KDM6B is involved in transcriptional activation of INK4A-ARF, which encodes tumor suppressor proteins $p16^{INK4A}$ and $p14^{ARF}$, suggesting its function in tumor suppression (Agger et al., 2009; Barradas et al., 2009).

1.6.2.6 PHF Family

Three mammalian proteins, KDM7/KIAA1718, PHF8 and PHF2, comprise the PHF subfamily. They all contain a PHD finger domain in addition to the JmjC domain. It has recently been reported that KDM7 and PHF8 can demethylate H3K9me1/me2, H3K27me2 and H4K20me1. KDM7 and PHF8 positively regulate gene transcription through removing the repressive histone methylation marks (Liu et al., 2010; Qi et al., 2010; Tsukada et al., 2010). KDM7 has been shown to be required during brain development (Tsukada et al., 2010) PHF8 regulates genes involved in neural and craniofacial development and in cell cycle progression (Liu et al., 2010; Qi et al., 2010). Mutations in PHF8 have also been found in XLMR patients (Laumonnier et al., 2005). It has been reported that PHF8 interacts with another XLMR protein, ZNF711, which binds to a subset of PHF8 target genes, suggesting that PHF8 is involved in XLMR (Kleine-Kohlbrecher et al., 2010). PHF2 has demethylation activity on H3K9me1 and is required for rDNA expression. It has also been shown that the PHD finger domain is required for the function of PHF proteins through its binding to H3K4me2/me3.

1.6.2.7 JMJD6

JMJD6/PSR/PTDSR (phosphotidylserine receptor) is the first identified demethylase specific to arginine residues. It demethylates histone H3R2me2 and H4R3me2 (Chang et al., 2007). Although the function of JMJD6 as an arginine demethylase is still unclear, it

has previously been found to be required for differentiation during embryogenesis (Bose et al., 2004; Schneider et al., 2004). More recently, it has been shown that JMJD6 has lysyl hydroxylation activity towards the splicing factor U2AF65, suggesting a role of JMJD6 in regulation of RNA splicing (Webby et al., 2009).

1.6.2.8 KDM8

KDM8/JMJD5 has recently been reported as an H3K36me2 demethylase. It lacks additional domains other than the JmjC domain. KDM8 was found to be overexpressed in tumors and is required for proliferation of a cancer cell line through regulation of cyclin A1 expression (Hsia et al., 2010).

1.7 Heterochromatin Protein 1

Heterochromatin protein 1 (HP1 or HP1a) was first identified in *Drosophila melanogaster* as a nonhistone chromosome binding protein, which is encoded by the *Su(var)2-5* gene. It was found that HP1 functions as a dominant suppressor of position effect variegation (PEV). PEV is a mosaic pattern of gene expression that occurs when a euchromatic gene is translocated to a position next to or within the heterochromatin (Weiler and Wakimoto, 1995). A mutation which causes missplicing of HP1 suppresses the silencing effect in PEV (Eissenberg et al., 1990). On polytene chromosome of *Drosophila melanogaster*, it has been shown that HP1 is mainly located at the pericentric heterochromatin, and is also detected at fourth chromosome, telomeres and about 200 sites along the euchromatin, (Fanti et al., 2003; James et al., 1989).

HP1 contains an N-terminal chromo domain (CD), a C-terminal chromoshadow domain (CSD) and a hinge region between the two domains (Aasland and Stewart, 1995; Paro and Hogness, 1991). The chromo (chromosome organization modifier) domain was first identified as a 37 amino acids domain that was highly conserved between Polycomb (PC)

and HP1 (Paro and Hogness, 1991). Despite they share a highly conserved domain, PC and HP1 bind to distinct regions on the chromatin (James et al., 1989; Zink and Paro, 1989). The CD of HP1 recognizes di- and tri-methylated histone H3K9 through a hydrophobic binding pocket formed by aromatic residues (Bannister et al., 2001; Jacobs and Khorasanizadeh, 2002; Lachner et al., 2001; Nielsen et al., 2002). The chromo shadow domain can only be found in HP1 family proteins, and is very similar to the chromo domain (Aasland and Stewart, 1995). The CSD of HP1 is responsible for dimerization of HP1 proteins and interactions with HP1 binding proteins (Cowieson et al., 2000; Li et al., 2002), and it is required for the nuclear localization of HP1 (Fanti et al., 1998). The hinge region is less conserved and variable in length between HP1 proteins from the same species and from different species. It has been shown that the hinge region binds to RNA and the linker histone, and these interactions are important for the localization and the function of HP1 (Muchardt et al., 2002; Nielsen et al., 2001). In addition, posttranslational modifications within the hinge region, especially phosphorylation and SUMOylation, are also critical to HP1 targeting (Badugu et al., 2005; Lomberk et al., 2006; Maison et al., 2011; Zhao et al., 2001).

The most known function of HP1 is the establishment and maintenance of high-order structure of heterochromatin. The establishment of heterochromatin involves HP1 and Su(var)3-9. Su(var)3-9, another dominant suppressor of PEV, is a SET domain-containing histone methyltransferase mediating histone H3K9 methylation (Czermin et al., 2001). It is enriched in the heterochromatin (Aagaard et al., 1999; Schotta et al., 2002), and physically interacts with HP1 (Schotta et al., 2002). It has been shown that Su(var)3-9 is required for HP1 recruitment to histone H3K9me2 in vivo (Stewart et al., 2005). A model for the spreading of heterochromatin has been proposed , in which HP1 binds to Su(var3-9)-mediated histone H3K9me2 through its CD, and the CSD recruits additional Su(var)3-9 through protein-protein interaction, resulting the propagation of K9 methylation along the

chromosome and the spreading of HP1 (Lachner et al., 2001). The spreading of heterochromatin has been shown to be involved in gene silencing. Transgenes placed within heterochromatin region were silenced (Wallrath and Elgin, 1995). It has been shown that the compact structure of heterochromatin established by HP1 prevents the binding of transcription factors resulting in gene silencing (Cryderman et al., 1999). Targeting of HP1 to euchromatin also causes gene silencing and closed chromatin structure similar to the heterochromatin (Danzer and Wallrath, 2004). In addition to its role in heterochromatin formation, HP1 is also required for telomere capping and the telomere transcriptional silencing (Fanti et al., 1998; Perrini et al., 2004).

Recently, HP1 has been shown to be involved in transcriptional activation of some heterochromatic and euchromatic genes. It was found that HP1 is required for transcription of genes located in the pericentric heterochromatin (Lu et al., 2000). The expression of these genes is lost when placed into euchromatin, suggesting that their expression relies on the heterochromatic environment (Wakimoto and Hearn, 1990). Immunostaining of *Drosophila* polytene chromosome reveals that HP1 is located at about 200 sites on euchromatin, suggesting HP1 might function in regulating gene expression of euchromatic genes (Fanti et al., 2003). Indeed, HP1 was found to be associated with developmentally regulated and heat-shock induced chromosome puffs. HP1 is recruited to the coding region of Hsp70 upon heat shock and is positively involved in Hsp70 gene activity (Piacentini et al., 2003). Microarray analysis showed that several euchromatic genes were downregulated in HP1 mutant larvae or HP1-knockdown cells, suggesting HP1 has a positive role in regulating gene expression at euchromatin (Cryderman et al., 2005; De Lucia et al., 2005). In addition to the role of HP1 in gene activation, HP1 has been reported to be involved in sex-specific gene regulation (Liu et al., 2005; Spierer et al., 2005). The loss of HP1a in *Su(var)2-5* mutants results in bloated X chromosomes in males, suggesting a role in regulating X-linked gene expression in flies (Spierer et al., 2005). Despite these findings,

the molecular mechanism by which HP1 regulates active transcription remains largely unknown.

1.8 Thesis Overview

My project began by investigating the enzymatic activity of *Drosophila* orthologs of histone H3K36 demethylases. In chapter 3, I demonstrated that the *Drosophila* orthologs of KDM4, dKDM4A and dKDM4B, have histone demethylation activity both in vitro and in vivo. In chapter 4, I sought to identify proteins associated with dKDM4A or dKDM4B by MudPIT analysis following the affinity purification. While I did not find specific protein partners of dKDM4B, I found that HP1a was present in the dKDM4A purification. This interaction is further confirmed by in vitro binding assays. I also found that the association of HP1a stimulates the demethylation activity of dKDM4A. In chapter 5, I performed genome-wide analysis, including RNA-seq and ChIP-on-chip, to identify target genes of KDM4A and explore biological functions of dKDM4A. In the last chapter, I summarized and discussed our findings, and examined the future directions.

Chapter 2 Materials and Methods

2.1 Plasmids and Antibodies

The full length cDNAs of dKDM4A, dKDM4B, HP1a, HP1b and HP1c were cloned into the S2 cell expression vectors pRmHa3-CHA_2FL_2 (Guelman et al., 2006a) or pBacPAK8 containing FLAG or HA tag for overexpression in insect cells. H195A and V423A mutations of dKDM4A, H186A mutation of dKDM4B and V26M, I191E and W200A mutations of HP1a were generated using the Quik Change II XL Site-Directed Mutagenesis Kit (Stratagene).

Anti-FLAG-HRP antibody (A8592), anti-FLAG M2-agarose (F2426), anti-HA agarose (A2095) were purchased from Sigma. Anti-HA-HRP antibody (12013819001) and anti-HA rat monoclonal antibody (3F10) (1867423) used in immunofluorescence analysis were from Roche. Anti-H3K36me3 (ab9050), anti-H3K36me2 (ab9049), anti-H3K36me1 (ab9048), anti-H3K9me3 (ab8898), anti-H3K9me2 (ab1220), anti-H3K9me1 (ab9045), anti-H3K4me2 (ab7766), anti-histone H4 (ab7311) and anti-histone H3 (ab1791) antibodies were from Abcam. Anti-H3K36me2 antibody (07-369) was from Upstate. Anti-HP1a (291C) was from Covance, anti-HP1a monoclonal antibody (C1A9) was from Developmental Studies Hybridoma Bank (DSHB). To generate anti-dKDM4A antibody, rabbits were immunized with synthetic peptide CVPEPSSAPKRYDFNTEAVVRV conjugated with KLH (keyhole limpet hemocyanin) (Pocono Rabbit Farm and Laboratory Inc.)

2.2 Fly Stocks and Crosses

2.2.1 Mutant fly stocks

The KG04636 P element insertion mutant (y[1] w[67c23]; P{y[+mDint2] w[BR.E.BR]=SUPor-P}Kdm4A[KG04636]) was obtained from Bloomington Stock Center at Indiana University (stock number 13828). Fly stocks Su(var)2-5^{04}/Cyo-GFP and Su(var)2-5^{05}/Cyo-GFP were provided by Dr. Sarah Elgin (Washington University, St. Louis, MO).

2.2.2 Overexpression of dKDM4A in Salivary Glands

The full length cDNAs of dKDM4A or dKDM4A-V423A were cloned into pUAST vector containing a C-terminal HA and FLAG tag. Transgenic fly lines, UAS-*Kdm4A-HA_1FLAG_2* (*w; P{w[+mC]=[UAS-Kdm4A-HA_1FLAG_2]}*) and UAS-*Kdm4A-V423A-HA_1FLAG_2* (*w; P{w[+mC]=[UAS-Kdm4A-V423A-HA_1FLAG_2]}*) were generated by Genetic Services. To overexpress HAFLAG-tagged dKDM4A or dKDM4A-V423A in salivary glands, transgenic flies were crossed to the Sgs3-GAL4 (*w[1118]; P{w[+mC]=Sgs3-GAL4.PD}TP1*) stock (Bloomington stock number 6870) (Brand and Perrimon, 1993).

2.2.3 Precise Excision of P element KG04636

The P element KG04636 was mobilized by crossing the stock (y[1] w[67c23]; P{y[+mDint2] w[BR.E.BR]=SUPor-P}Kdm4A[KG04636]) to y[1]w[*];CyO,H{w[+mc]=PΔ2-3}Hop2.1/Bc[1]Egfr[E1] flies. Males of KG04646/transposase PΔ2-3 were crossed to a CyO balanced stock. P element excision was screened by the eye color, and further confirmed by PCR. PCR products were sequenced to confirm the precise excision.

2.2.4 Rescue of dKDM4A Mutant with FLAG-dKDM4A

To generate the genomic construct of dKDM4A, a fragment containing the genomic dKDM4A locus including about 1.6 KB upstream of 5'UTR and 220 bp downstream of 3'UTR of dKDM4A was amplified from the genomic DNA of Oregon R flies. A double FLAG tags were added at the C-terminus of dKDM4A. The fragment was cloned into pCa4B vector (Markstein et al., 2008). Site specific integration at attP40 landing site (2L 25C7) (Markstein et al., 2008) was carried out by Genetic Services. To rescue the KG04636 P element insertion mutant, the transgene (FLAG-dKDM4A) on the second chromosome was recombined to the chromosome carrying KG04636 insertion. In these flies, FLAG-tagged dKDM4A is expressed under the control of its own promoter in the absence of the endogenous dKDM4A.

2.3 Phylogenetic Analysis

Alignments of JmjC domains of KDM4A orthologs were performed using ClustalX (Thompson et al., 1997), followed by the Boxshade server (http://www.ch.embnet.org/software/BOX_form.html).

2.4 Purification of Recombinant Proteins from Insect Cells

cDNAs of dKDM4A, dKDM4B, HP1a, HP1b, HP1c and derivatives were subcloned into vector pBacPAK8 carrying a N-terminal FLAG or HA tag. Recombinant baculoviruses were generated and manipulated according to manufacture suggestion (BacPAK expression system (Clontech)). Sf21 insect cells were cultured at 27 °C in the Sf-900 II SFM (Invitrogen) supplemented with 10 % FBS (SAFC biosciences), and penicillin-streptomycin (Invitrogen). 48 hours after infection, cells were collected and washed with ice-cold PBS, before lysed in 20 ml of ice-cold lysis buffer (50 mM HEPES-NaOH (pH 7.9), 500 mM NaCl, 2 mM $MgCl_2$, 0.2 % Triton X-100, 10 % (v/v) glycerol, 0.5 mM EDTA and

protease inhibitors). Cell lysates were clarified by ultracentrifugation at 40,000 rpm for 30 min at 4 °C, and were subsequently incubated with anti-FLAG (M2), or anti-HA-agarose beads overnight at 4 °C. The beads were washed three times with lysis buffer, and bound proteins were eluted twice with 1 column volume of elution buffer (0.5 mg/ml triple FLAG or HA peptide in 50 mM HEPES-NaOH (pH 7.9), 100 mM NaCl, 2 mM $MgCl_2$, 0.02 % NP-40 and 10 % (v/v) glycerol).

2.5 MLA Histones Preparation

Recombinant *Xenopus* histone H3 containing point mutations K36C and C110A was expressed in BL21 codon plus-RIL (Stratagene) cells and purified as described (Li et al., 2005) for alkylation reaction. Methyl-lysine analog (MLA) histones were prepared as described (Simon et al., 2007). Basically, the cysteine residue is converted into analogs of mono-, di or tri-methylated lysine by treatment with different alkylating agents. For tri-methylated lysine analogs (Kc me3), (2-bromoethyl) trimethylammonium bromide (Aldrich) was added in the alkylation reaction; for mono-methylated lysine analogs (Kc me1), (2-chloroethyl)-methylammonium chloride (Karl Industries, Inc) was added in the reaction.

2.6 Histone Demethylation Assay

HeLa core histones or chemically modified histone H3 (MLA) were incubated with recombinant dKDM4A, dKDM4B or native complex in histone demethylation assay buffer (50 mM HEPES-KOH pH7.9, 100 uM $Fe(NH_4)_2(SO_4)_2$, 1 mM α-ketoglutarate, 2 mM Ascorbate) in a final volume of 10 µl for 1 hour at 37 °C. The reaction mixture was analyzed by western blot using histone methylation specific antibodies.

2.7 In vitro Binding Assay

Recombinant HA-HP1a, HP1b, HP1c or HP1a mutants and FLAG-dKDM4A, its mutant dKDM4A-V423A, or dKDM4B were mixed in the buffer containing 50mM HEPES-NaOH (pH 7.9), 150 mM NaCl, 2 mM $MgCl_2$, 0.05 % Triton X-100, 10 % (v/v) glycerol, 0.5mM EDTA, 1mM PMSF and 0.1 μg/μl BSA or 500μg of Sf21 cell lysate overnight at 4 °C and then incubated with anti-HA agarose beads (Sigma) for 2 hour at 4 °C. The beads were washed 4 times using the same buffer described above and eluted by boiling in SDS-PAGE sample buffer. The eluate and 2 % of the input were analyzed by western blot using anti-FLAG and anti-HA antibodies.

2.8 Immunofluorescence Analysis of S2 cells

Stable S2 cell lines expressing HAFLAG-tagged dKDM4A or the mutant dKDM4AH195A were seeded on CultureSlide (BD Bioscience) and induced for 1 day with 100 μM $CuSO_4$. Cells were fixed in 4 % paraformaldehyde for 15 min, washed twice with PBS, and permeabilized in 0.5 % Triton X-100 in PBS for 5 min. Permeabilized cells were washed with buffer containing 0.1 M Tris-HCl (pH7.5), 150 mM NaCl and 0.05 % Tween 20, and blocked in 4 % milk in PBS for 30 min. Slides were incubated with primary antibody overnight at 4 °C using histone methylation specific antibodies at a dilution of 1:500 and anti-HA (3F10) antibody at a dilution of 1:1500. After three times of wash, cells were stained with Cy2 or Cy3-conjugated secondary antibody (Jackson ImmunoResearch) for 1 hour. Cells were washed three times and stained with 4', 6-diamidino-2-phenylindole dihydrochloride (DAPI) in PBS for 30 min, washed twice with PBS and mounted on glass slides, then visualized by a confocal laser scanning microscope (LSM-510 META, Zeiss).

2.9 Purification of Native Complexes from S2 cells and Mass Spectrometry

Affinity Purification was performed as previously described (Suganuma et al., 2008). Briefly, 4 liters of *Drosophila* S2 stable cells were grown and induced with 100 μM $CuSO_4$ for one day. Cells were collected and washed with ice-cold PBS, before lysed with the lysis buffer containing 10 mM HEPES-KOH (pH7.9), 1.5 mM $MgCl_2$, 10 mM KCl, 1 % NP-40, 1 mM DTT and 1 mM PMSF. Nnuclei were pelleted by centrifugation at 5,000 rpm for 5 min at 4 °C and extracted using a buffer containing 20 mM HEPES-NaOH (pH7.9), 420 mM NaCl, 1.5 mM $MgCl_2$, 0.2 mM EDTA, 25 % (v/v) glycerol, 1 mM DTT and 1 mM PMSF. Nuclear extracts were centrifuged at 14,000 rpm for 15min at 4 °C and then ultracentrafuged at 45,000 rpm for 1.5 hours at 4 °C. The NaCl concentration of the extract was subsequently adjusted to 300 mM. Nuclear extracts were incubated with anti-FLAG (M2) agarose beads (Sigma) overnight at 4 °C. The beads were washed three times for 10 min in washing buffer (10 mM HEPES-NaOH (pH 7.9), 300 mM NaCl, 10 mM KCl, 1.5 mM $MgCl_2$, 0.2 % Triton X-100, 1 mM PMSF). The complexes were eluted from the beads with elution buffer (0.5 mg/ml triple FLAG peptide in 10mM HEPES-NaOH (pH 7.9), 100 mM NaCl, 1.5 mM $MgCl_2$, 0.05 % Triton X-100 and protease inhibitor). MudPIT analysis of the affinity-purified complexes was carried out as previously described (Guelman et al., 2006b).

2.10 Superose 6 Chromatography

The eluate of FLAG purification of native dKDM4A complex from S2 cells or recombinant dKDM4A-HP1a complex from Sf21 insect cells were loaded on the Superose 6 HR 10/30 size exclusion column (Amersham Bioscience) containing 40mM HEPES (pH 7.5) , 350 mM NaCl, 10 % (v/v) glycerol and 0.1 % (v/v) Tween 20. 500 μl- fractions were collected and the fraction profiles were analyzed by western blot analysis. The Superose 6

column was calibrated with Blue Dextran 2000 (2 MDa), Thyroglobulin (669 KDa), Ferritin (440 KDa), Aldolase (158 KDa), Conalbumin (75 KDa) and Ovalbumin (44 KDa).

2.11 Knockdown of dKDM4A in S2 Cells by dsRNA

Primers containing T7 sequence tagged at the 5' end were used to amplify dKDM4A and LacZ fragments. PCR products were gel-purified and served as templates to generate dsRNA with MEGAscript T7 kit (Ambion) following manufacturer's instruction. 1μg of dsRNA was transfected into S2 cells using Effectene (Qiagen). After 4 days of RNAi treatment, histones were acid-extracted from S2 cells and analyzed by western blot. Primers for RNAi knockdown of dKDM4A and LacZ in S2 Cells:

2.12 Immunostaining of Polytene Chromosomes

The third instar larvae were dissected in PBS supplemented with 0.1 % TritonX-100. Salivary glands were fixed first in solution 1 (phosphate-buffered saline (PBS), 3.7 % paraformaldehyde and 1 % Triton X-100) and then in solution 2 (3.7 % paraformaldehyde, 50 % acetic acid). The chromosomes were spread on poly-L-lysine coated microscope slides. Anti-HP1 antibody was used at 1:50 and anti-HA antibody was used at 1:100. Cy3 and Cy3-conjugated secondary antibodies were used at 1:400. Images were taken on a confocal laser scanning microscope (LSM-510 META, Zeiss).

2.13 Chromatin Immunoprecipitation

Chromatin immunoprecipitation (ChIP) was performed from staged 2-4 hours embryos collected in population cages as described in (Sandmann et al., 2006) with modifications:

2.13.1 Preparation of Chromatin Extracts

Embryos were dechorionated in 50 % commercial bleach at room temperature for 2 min, washed with distilled water, and then transferred to 15 ml PBT (PBS with 0.1 % Triton). Embryos were cross-linked with 1.8% formaldehyde in 2.3 ml fixation buffer (50 mM Hepes pH 8.0, 1 mM EDTA, 0.5 mM, EGTA, 100 mM NaCl) and 7.5 ml heptane for 15 min with vigorous shaking. Embryos were pelleted by centrifugation at 500g for 1 min. Cross-linking was stopped by replacing the buffer with 125 mM glycine in 15 ml PBT. Embryos were washed with ice-cold PBT, frozen by liquid nitrogen and stored at -80 °C. Multiple collections were done to obtain sufficient embryos. Embryos were homogenized in 5 ml A1 buffer (15 mM Hepes pH 7.5, 15 mM NaCl, 60 mM, KCl, 4 mM MgCl, 0.5 % Triton X-100, 0.5 mM DTT and protease inhibitors) with Dounce homogenizer (three strokes each). The homogenate was transferred to a 15-ml tube and centrifuged for 1 min, 500g at 4°C. The supernatant was discarded and the pellet was washed three times in 5 ml A1 buffer and once in 5 ml A2 buffer (15 mM Hepes pH 7.5, 140 mM NaCl, 1 mM EDTA, 0.5 mM EGTA, 1 % Triton X-100, 0.1 % sodium deoxycholate, 1 % SDS, 0.5 % N-lauroylsarcosine and protease inhibitors) at 4° C. Nuclei were resuspended in A2 buffer and sonicated 7 times for 12 seconds, 30 % power. Spin at 4 °C for 10 min at high speed and transfer supernatant to a fresh tube. About 700ug to1mg of chromatin was used for each IP.

2.13.2 Chromatin Immunoprecipitation and DNA Purification

1.5 ug of anti-H3K36me3 antibody (ab9050), 3 ul of anti-HP1a (Covance 291C) were used in the IP. After incubated with the antibody overnight at 4 °C, Dynal magnetic beads (Invitrogen) pre-washed with 0.5 % BSA (w/v) in PBS were added to the IP sample and incubate for 2 hours at 4 °C, followed by 4 times of wash with RIPA buffer (50 mM Hepes pH 7.5, 0.5 M LiCl, 1 mM EDTA, 1 % NP-40, 0.7 % sodium deoxycholate) and once with

50mM NaCl in TE. Bound complexes were eluted twice with 200 µl of elution buffer (50mM Tris pH 8.0, 10 mM EDTA, 1 % SDS) at 65 °C for 30min. The eluate were treated with RNase A (0.2 µg/µl) for 1 hour at 37 °C followed by Protinase K treatment (0.2 µg/µl) for 1 hour at 55 °C. Crosslinks were reversed by incubating samples at 65 °C overnight.

DNA was extracted twice with phenol:chloroform:isoamylalcohol and once with chloroform, followed by ethanol precipitation with 30 µg glycogen as a carrier. DNA pellets were resuspended in 120 µl of 10 mM Tris-HCl (pH 8.0) and analyze by real-time PCR, or in 60 µl of 10mM Tris-HCl (pH 8.0) for ChIP-chip analysis.

2.13.3 Preparation of Input DNA

50 µl of the chromatin extracts were used as input. The input chromatin was supplemented with 350 µl of elution buffer and treated with Protinase K (0.2 µg/µl) for 1 hour at 55 °C, followed by 65 °C overnight to reverse the crosslink. It was treated with RNase A for 1 hour at 37 °C following phenol:chloroform:isoamylalcohol extraction. DNA was then extracted and precipitated as described above and was resuspended in 50 µl of 10mM Tris-HCl (pH 8.0).

2.14 ChIP-chip Analysis

Two biological replicate of H3K36me3 ChIPs were performed in dKDM4A mutant (P element insertion) and wild type (Precise excision of P element) embryos. The amplification and labeling of immunoprecipitated DNA and input DNA were performed as described in (Lee et al., 2006) by Karin Zueckert-Gaudenz and Brian Fleharty in the molecular biology core facility. The cy5-labeled IP DNA and Cy3-labeled input DNA were hybridized to *Drosophila* whole genome ChIP-on-chip microarrays (Agilent) using Agilent CGH protocol and reagents. Two slides of 244K microarrays containing probes

tiled across whole *Drosophila* genome with 233 nt average spacing. The scanned array data were analyzed by Ariel Paulson in the bioinformatics core facility. Basically, peaks were called on the ratio track (mt/WT) using a double-threshold method. Track was smoothed using a 5-probe MA , then peaks were called using a candidate threshold of 1SD outside the mean and a peak threshold of 2SD outside the mean (+ or -), a minimum run of 3 probes, max gap = 1000bp. In other words, any contiguous run of more than 3 probes, with heights at or beyond 1SD, and having no internal gaps > 1000 bp, becomes a candidate. Any candidate with at least one probe at or beyond 2SD gets called a peak. To find positive peaks (increased K36me3 levels in the dKDM4A mutant) which are consistently present in both replicate, only peaks that are positive, overlapping a peak in the other replicate, and contain more positive probes than negative in the mutant data are retained.

2.15 Preparation of RNA and cDNA

S2 cells or dechorionated 2-4 hours embryos were homogenized in 1ml of Trizol (Invitrogen). RNA was purified according to the manufacturer's protocol. cDNA was generated using Superscript III First-Strand Synthesis kit according to the manufacturer's protocol.

2.16 RNA-seq Analysis

RNA extracted from 2-4 hours embryos was submitted to Karin Zueckert-Gaudenz in the molecular biology core facility for library preparation. Libraries were prepared using mRNA-seq sample preparation kit (Illumina) according to the manufacturer's protocol. Briefly, mRNA was purified from total RNA using poly-T oligo-attached magnetic beads. The mRNA was then fragmented and reverse transcribed into the first strand cDNA using reverse transcriptase and random primers, followed by synthesis of the second strand. Next,

DNA end-repair and A-tailing was performed. The adapters were ligated to the ends of the DNA fragments, and the products were purified, followed by cDNA amplification using primers that anneal to the ends of the adapters. Sequencing was performed on the Illumina Genome Analyzer.

The differential gene expression analysis was carried out by Hua Li in the bioinformatics core facility. Briefly, we used Tophat (Trapnell et al., 2009) to align reads to dmel-r.5.29 (Flybase). Gene expression values were obtained using Cufflinks (Trapnell et al., 2010) with default parameters. Genes with the maximum gene expression across four samples being less than 3 FPKM (fragments per kilobase of transcript per million fragments mapped) were excluded. Then, raw FPKM values were log2 transformed. We applied t-test to compare expression differences between two wild type samples and mutant samples. P-values are adjusted using BH-FDR (Benjamini et al., 1995).

GO term analysis was performed using DAVID (http://david.abcc.ncifcrf.gov/) (Huang da et al., 2009).

Chapter 3 Identification of Histone H3K36 Demethylases in *Drosophila melanogaster*

3.1 Introduction

Histone H3K36 methylation has been shown to be involved in transcription elongation (Carrozza et al., 2005; Joshi and Struhl, 2005; Keogh et al., 2005), alternative splicing (Kolasinska-Zwierz et al., 2009; Luco et al., 2010) and dosage compensation (Bell et al., 2008; Larschan et al., 2007). Set2 is the sole enzyme responsible for all three methylation states of histone H3K36 in budding yeasts (Strahl et al., 2002). Histone H3K36me3 is catalyzed by dSet2 (dHypb) in flies (Bell et al., 2007; Larschan et al., 2007) and HYPB/Setd2 in mammals (Edmunds et al., 2008; Sun et al., 2005), whereas K36me2 is mediated by dMes-4 (NSD homolog) in flies (Bell et al., 2007) and NSD family proteins in mammals (Li et al., 2009; Lucio-Eterovic et al., 2010). H3K36 methylation is also subject to dynamic regulation. While mono- and di-methylated H3K36 is demethylated by JHDM1/KDM2 (Tsukada et al., 2006), H3K36me3 can be demethylated by JMJD2A/KDM4A, which is also able to remove di- and tri-methylation from H3K9 (Klose et al., 2006b; Whetstine et al., 2006).

JHDM1A/KDM2A was named FBXL11 when it was first identified as an F-box-containing protein in bioinformatic studies (Cenciarelli et al., 1999; Winston et al., 1999). The CxxC Zinc finger domain of KDM2A recognizes nonmethylated CpG islands, which results in a depletion of H3K36me2 at these elements (Blackledge et al., 2010). It has been reported that KDM2A binds to rRNA promoters in nucleoli and represses the transcription of rRNA in response to starvation (Tanaka et al., 2010). The mammalian paralog of KDM2A, KDM2B/FBXL10, is also a histone H3K36 demethylase and functions in regulating cell proliferation (He et al., 2008). Overexpression of the yeast homolog of

KDM2, Jhd1, leads to a subtle 3' shift of H3K36me2 while knockout of KDM2 causes subtle 5' shift of H3K36me2, suggesting a role of Jhd1 in fine-tuning the distribution of H3K36me2 (Fang et al., 2007). The Drosophila homolog dKDM2 was found in a dRING-containing complex, dRAF (dRING-associated factors), along with dRING and PSC. Genetic interaction studies showed that dKDM2 functions as an enhancer of Polycomb and as a suppressor of trx and ash1. dKDM2 not only regulates the level of H3K36me2, but is also required for efficient H2A ubiquitination mediated by dRING/PSC, implicating a novel *trans*-histone regulation (Lagarou et al., 2008).

The JMJD2/KDM4 family consists of four genes, JMJD2A/KDM4A, JMJD2B/KDM4B, JMJD2C/KDM4C and JMJD2D/KDM4D, in the human and mouse genome. JMJD2A/KDM4A was originally identified as an N-CoR-interacting protein involved in transcriptional repression of ASCL2 gene (Zhang et al., 2005). It has also been shown to associate with RB and HDACs to repress E2F regulated genes (Gray et al., 2005). JMJD2A is an H3K36me3/me2 and H3K9me3/me2 specific histone demethylase. Overexpression of JMJD2A antagonizes HP1 recruitment to pericentric heterochromatin in an enzymatic activity-dependent manner. Knockdown of JMJD2A increases the level of H3K9me3 at the ASCL2 locus and upregulates the expression of ASCL2, suggesting a role in gene repression through removing histone methylation marks (Klose et al., 2006b). Other family members have been shown to have demethylation activity on histone H3K36me3/me2 and/or H3K9me3/me2 (Whetstine et al., 2006). Overexpression of JMJD2B/KDM4B or JMJD2C/KDM4C leads to decreased level of H3K9me3/me2 and abrogates the recruitment of HP1 to the heterochromatin. (Cloos et al., 2006; Fodor et al., 2006). JMJD2C/KDM4C was originally named GASC1 (gene amplified in squamous cell carcinoma 1) because of its amplification detected in esophageal cancer cell lines (Yang et al., 2000). Knockdown of JMJD2C results in decreased cell proliferation, suggesting its function in cancer development (Cloos et al., 2006). JMJD2C has been shown to interact

with androgen receptor (AR) and LSD1. JMJD2C and LSD1 demethylate H3K9, and stimulate AR-regulated genes cooperatively (Wissmann et al., 2007). Yeast homolog of KDM4, Rph1, has demethylation activity on both H3K9 and K36me3 despite the fact that H3K9 methylation is absent in the budding yeast (Klose et al., 2007a). Deletion of Rph1 failed to show a phenotype in transcription elongation (MPA sensitivity) or telomeric silencing (Klose et al., 2007a). An Rph1 overexpression strain has a growth defect in response to UV-irradiation, and it is slightly resistant to 6-AU and MPA (Kim and Buratowski, 2007; Tu et al., 2007). In addition, Jhd1 or Rph1 deletion decreased the level of RNA polymerase II across actively transcribed genes, *PMA1*, *ADH1* and *YEF3*. It has also been shown that overexpression of Jhd1 and Rph1 suppresses the growth defect in a Bur1 deleted strain, suggesting that H3K36 demethylases are positive regulators of transcription elongation (Kim and Buratowski, 2007).

Here I Identified the KDM4 homologs, dKDM4A and dKDM4B in *Drosophila melanogaster*. I first purified the recombinant dKDM4A and dKDM4B from insect cells and examined the demethylation activity in vitro. I found that dKDM4A can demethylate H3K36me3/me2, while dKDM4B can demethylate both H3K9 and K36me3/me2. The in vivo demethylation activity was examined by overexpressing dKDM4A or dKDM4B in S2 cells. The level of histone methylation was detected by immunofluorescence analysis. The in vivo activity of dKDM4A and dKDM4B is consistent with the result of the in vitro assay. These data suggest that the two KDM4 orthologs in *Drosophila* are both histone demethylases with different specificities.

3.2 Identification of KDM4 Orthologs in *Drosophila melanogaster*

Based on sequence homology, there are two KDM4 orthologs in *Drosophila melanogaster*, dKDM4A (CG15835) and dKDM4B (CG33182). They both contain JmjN and JmjC domains but lack the C-terminal PHD domain, the Tudor domain and the Zinc finger domain found in KDM4 homologs in other species (Figure 3-1A). Alignment of the JmjC domain of KDM4 orthologs reveals that the Fe (II) and α-KG binding sites are conserved in dKDM4A and dKDM4B, suggesting that they could be functional histone demethylases (Figure 3-1B). Alignment of dKDM4A and dDKM4B reveals that two fly KDM4 orthologs are highly conserved at JmjN and JmjC domains, while it shows little similarity at the C-terminus (Figure 3-2).

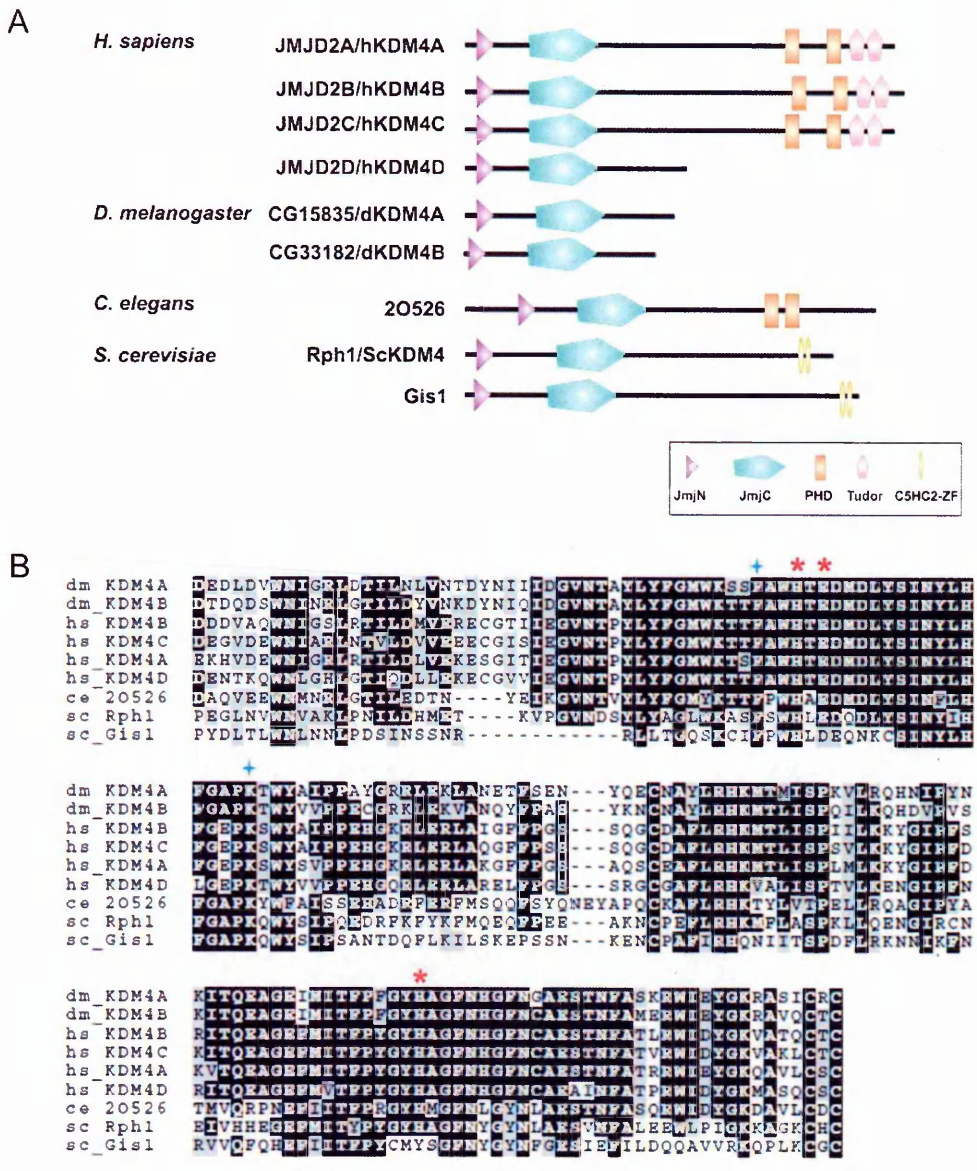

Figure 3-1 The KDM4 family.

(A) Schematic representation of KDM4 family members.
(B) Sequence alignment shows high degree of homology within JmjC domains of KDM4 family. The conserved residues of the Fe (II) binding site and the α-KG binding site are indicated by red asterisks and blue stars respectively.

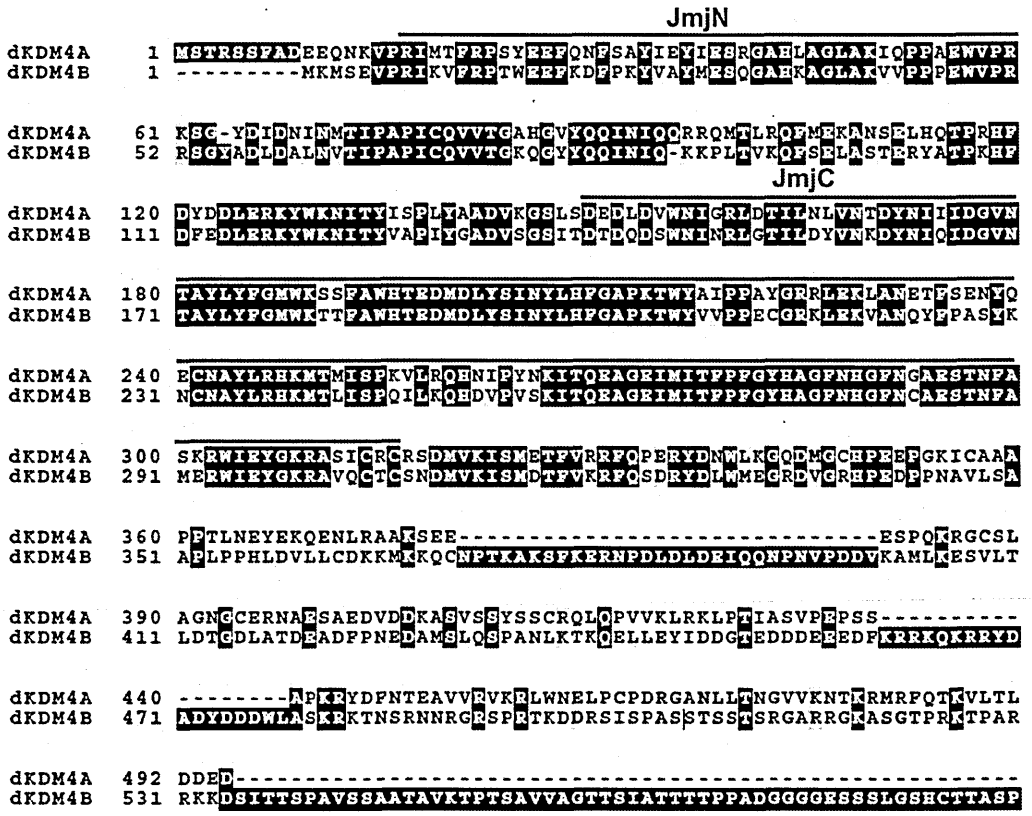

Figure 3-2 dKDM4A and dKDM4B are highly conserved at Jumonji domains.

Sequence alignment of dKDM4A and dKDM4B. JmjN and JmjC domains are marked by blue and green line respectively.

3.3 In vitro Demethylation Activity of KDM4A and KDM4B

To examine whether *Drosophila* KDM4 orthologs have histone demethylation activity, I purified recombinant dKDM4A and dKDM4B from baculovirus-infected Sf21 cells (Figure 3-3A) and tested their activity in an in vitro histone demethylation assay using HeLa core histones as substrates. As shown in Figure 3-3B, dKDM4A specifically demethylates tri- and di-methyl H3K36 of HeLa core histones. Increasing levels of H3K36me1 were also observed, presumably due to accumulation of the end products of the demethylation reaction of di- and tri-methylated histone H3K36. However, the level of histone H3K9 and K4 methylation remained unchanged. In contrast, recombinant

dKDM4B had robust demethylation activity toward both histone H3K9 and K36me3/me2 (Figure 3-3C). To directly test the modification state preference of dKDM4A toward substrates, I utilized methyl-lysine analogs (MLAs) (Simon et al., 2007) to generate recombinant histone H3 containing tri- or mono-methylated K36. Tri- or mono-methylated histone H3 was used as substrates in the demethylation assay (Figure 3-4). dKDM4A displays robust activity towards K36me3 but fails to demethylate K36me1. Like hKDM4A (Klose et al., 2006b), the demethylation reactions mediated by dKDM4A and dKDM4B require Fe (II), α-ketoglutarate and ascorbate as cofactors (Figure 3-5A and B). The slight activity of dKDM4A and dDKM4B in the absence of Fe (II) (Figure 3-5A lane 3) or ascorbate (Figure 3-5B lane 5) is likely caused by co-purification of cofactors with recombinant proteins. To examine the requirement of Fe (II) for the demethylation activity, I purified recombinant dKDM4A and dKDM4B in which a conserved amino acid in the iron binding site is mutated to alanine (Figure 3-3A). The mutant form of dKDM4A and dKDM4B has no demethylation activity on histone H3K36me3, suggesting that Fe (II) is necessary for the catalytic activity (Figure 3-5C and D).

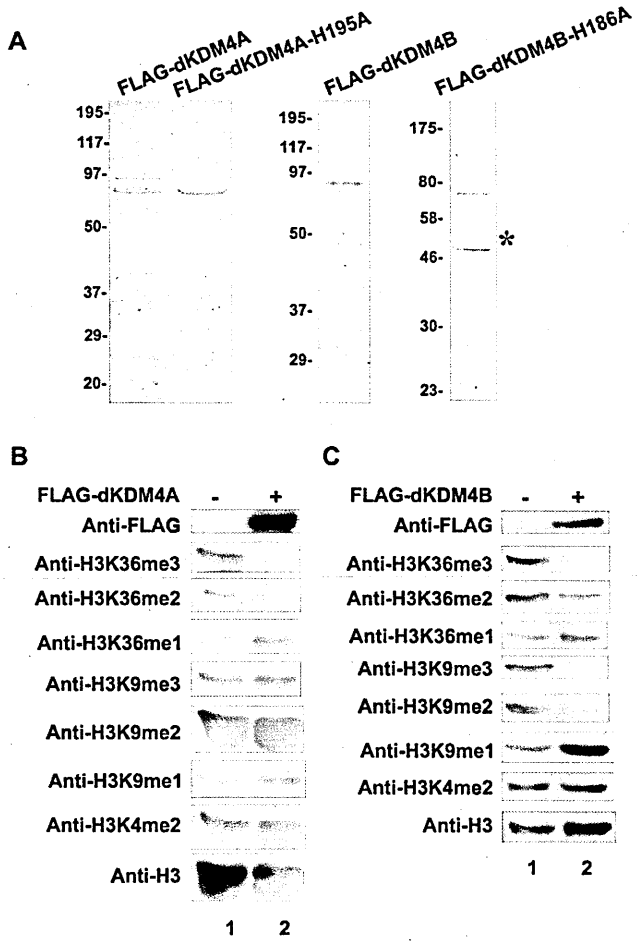

Figure 3-3 dKDM4A and dKDM4B have demethylation activity in vitro.

(A) Purified recombinant dKDM4A, dKDM4B, and their iron-binding mutants dKDM4A-H195A and dKDM4B-H186A from baculovirus-infected Sf21 cells were visualized by Coomassie blue staining. The asterisk indicates the degradation products of recombinant dKDM4B-H186A.
In vitro demethylation assay of dKDM4A (B) or dKDM4B (C) using HeLa core histones as substrates. The reaction mixtures were analyzed by western blot using indicated histone antibodies.

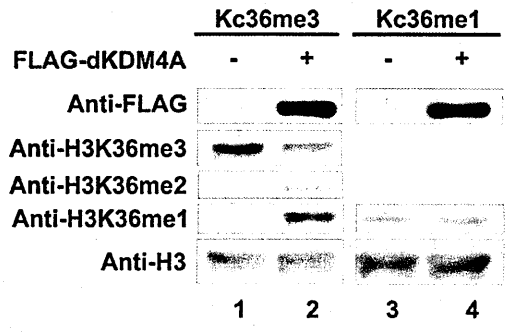

Figure 3-4 The methylation state specificity of dKDM4A.

In vitro demethylation assay using chemically modified recombinant H3 as substrates. Tri-methyl-lysine36 analogs are used in lane 1 and 2; mono-methyl-lysine36 analogs are used in lane3 and 4

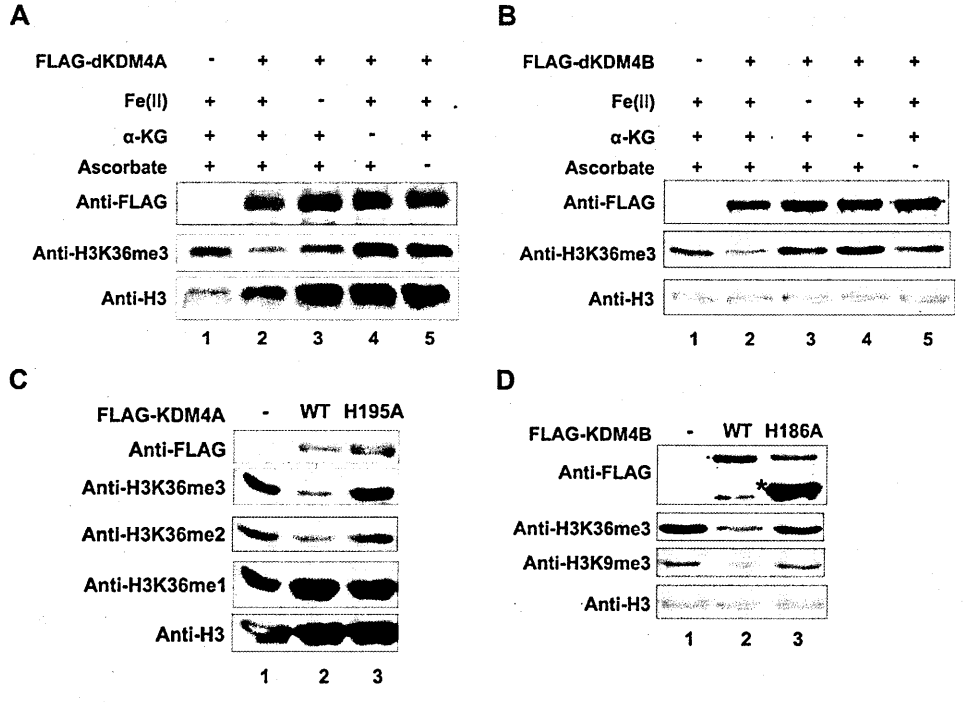

Figure 3-5 Cofactor dependence of dKDM4A and dDKM4B.

(A-B) Each cofactor, Fe (II), α-ketoglutarate and ascorbate was individually excluded from histone demethylation reaction as indicated (lane 3, 4 and 5).
(C) Comparison of histone H3K36 demethylation activity of recombinant dKDM4A (lane 2) and the iron-binding mutant dKDM4A-H195A (lane 3) using HeLa core histones as substrates.
(D) Comparison of histone H3K36 and K9 demethylation activity of recombinant dKDM4B (lane 2) and the iron-binding mutant dKDM4B-H186A (lane 3) using HeLa core histones as substrates. The asterisk indicates the degradation products of recombinant dKDM4B-H186A.

3.4 In vivo Demethylation Activity of KDM4A and KDM4B

To determine whether dKDM4A and dKDM4B function as histone H3K36 demethylases in vivo, I established stable cell lines in which epitope-tagged dKDM4A or dKDM4B is under the control of a copper inducible promoter. The level of histone methylation was then examined by immunofluorescence analysis (Figure 3-6). Cells containing high level of dKDM4A display significantly reduced level of histone H3K36me3 (Figure 3-6A). Overexpression of dKDM4A seems to only lead to demethylation of histone H3K36, since the level of histone H3K9me3 (Figure 3-6B) and K4me2 (Figure 3-6C) remained unchanged. In contrast, overexpression of dKDM4B in S2 cells resulted in decreased level of histone H3K36me3 and H3K9me3, while the level of H3K4me2 was not affected (Figure 3-7). These results are consistent with what I observed in vitro.

To further examine the demethylation activity of dKDM4A in vivo, I knocked down endogenous dKDM4A in S2 cells using double-stranded RNA against dKDM4A. RT-PCR analysis showed that the mRNA level of dKDM4A decreased in S2 cells after 4 days of RNAi treatment (Figure 3-8A). Under these conditions, the level of histone H3K36me3 and me2 increased while the level of histone H3K36me1 decreased (Figure 3-8B). Therefore, dKDM4A is responsible for maintaining proper level of H3K36 methylation in vivo.

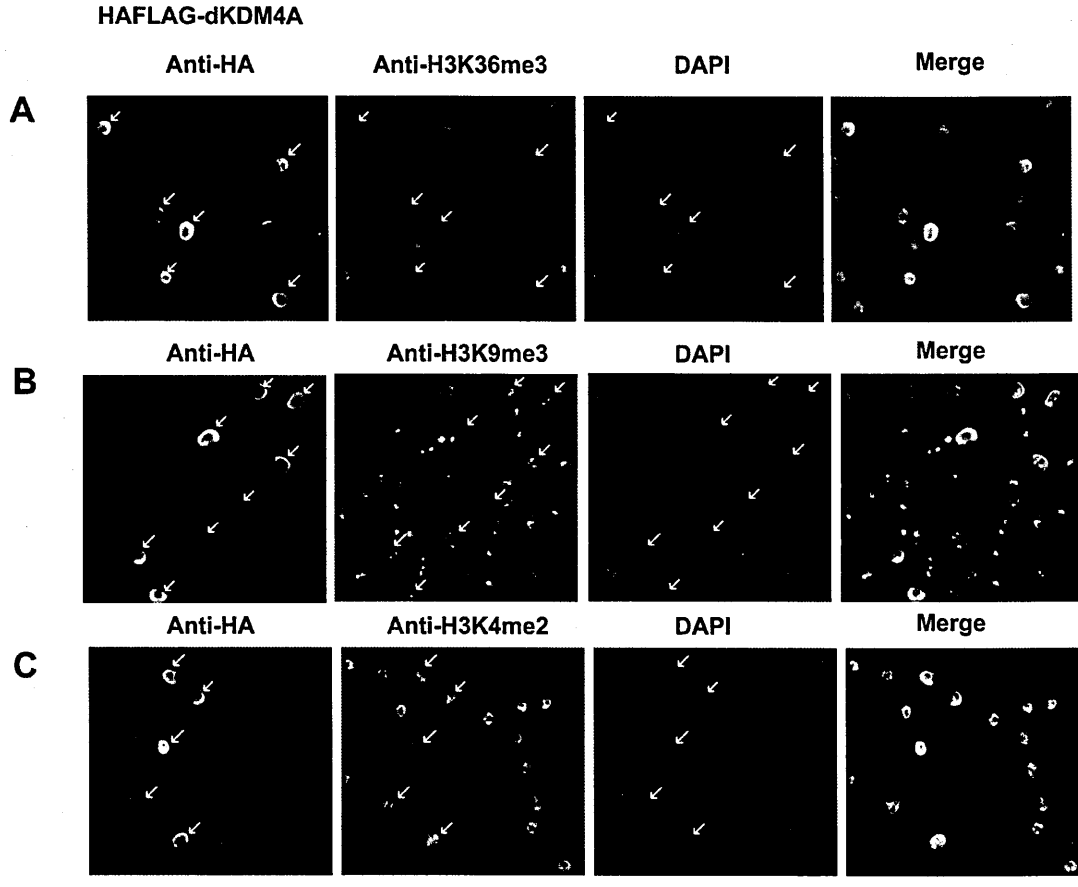

Figure 3-6 dKDM4A has histone H3K36me3 demethylation activity in vivo

Drosophila S2 cells were transfected with FLAG-HA-tagged dKDM4A. The stable cell lines were induced by addition of 100 μM CuSO4 and stained with anti-HA and anti-H3K36me3 (A), anti-H3K9me3 (B) and anti-H3K4me2 (C) antibodies. The green corresponds to anti-HA staining, the red corresponds to anti-histone methylation specific antibodies, and the blue corresponds to DAPI staining. White arrows point to the dKDM4A positive-staining cells.

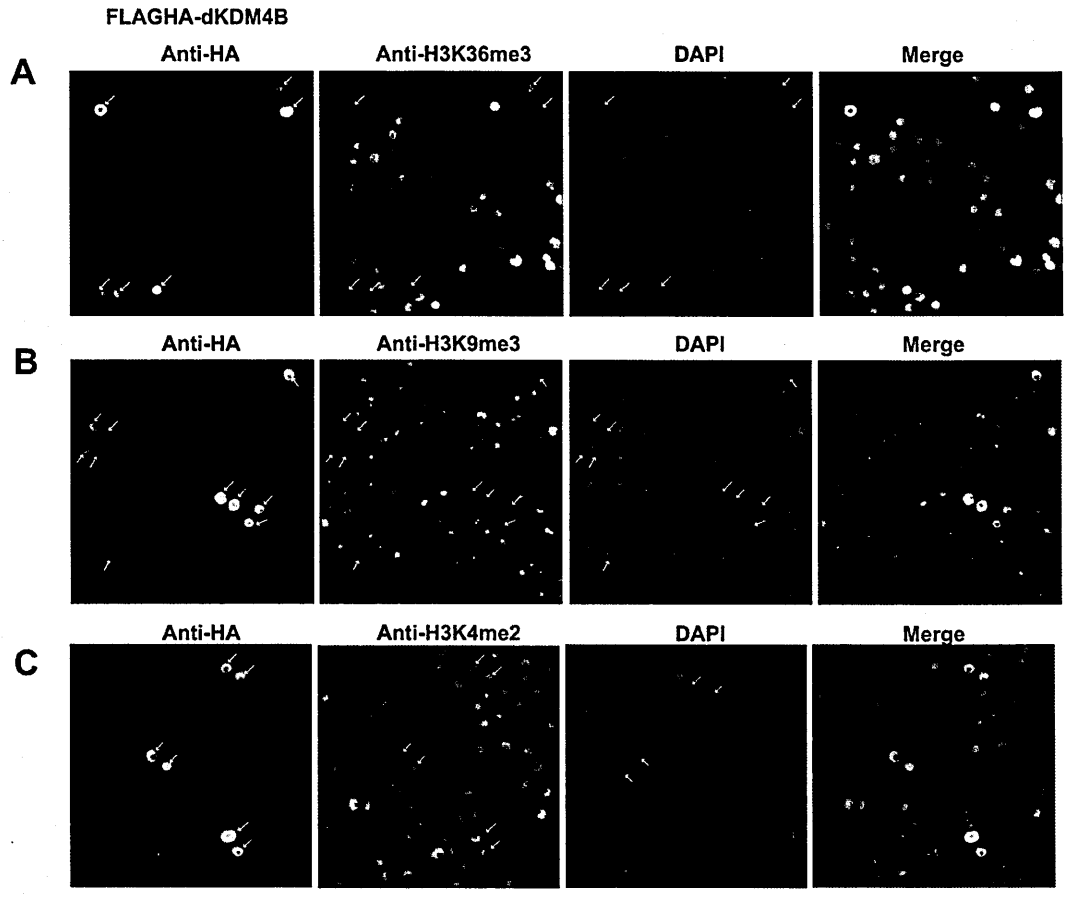

Figure 3-7 dKDM4B has histone H3K36 and K9me3 demethylation activity in vivo.

Drosophila S2 cells were transfected with FLAG-HA-tagged dKDM4B. The stable cell lines were induced by addition of 100 μM $CuSO_4$ and stained with anti-HA and anti-H3K36me3 (A), anti-H3K9me3 (B) and anti-H3K4me2 (C) antibodies. The green corresponds to anti-HA staining, the red corresponds to anti-histone methylation specific antibodies, and the blue corresponds to DAPI staining. White arrows point to the dKDM4B positive-staining cells.

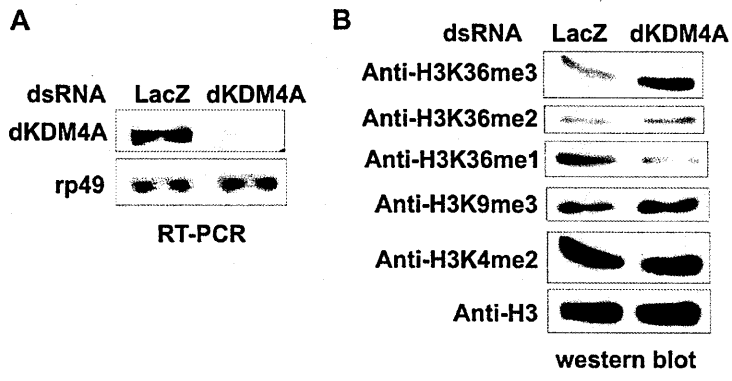

Figure 3-8 Knockdown of dKDM4A in S2 cells leads to increased levels of H3K36me3.

(A) The mRNA level of dKDM4A was examined by RT-PCR with primers specific for dKDM4A and rp49 (internal control).
(B) Acid-extracted bulk histones from dsRNA treated samples were analyzed by western blot using indicated antibodies.

3.5 Discussion

Here I identified JmjC domain-containing KDM4 orthologs in *Drosophila*, dKDM4A and dKDM4B. The in vitro demethylation assay shows that dKDM4A demethylates histone H3K36me3/me2 using an oxidative demethylation mechanism which requires Fe (II), α-ketoglutarate and ascorbate as cofactors, while dKDM4B demethylates histone H3K9 and K36 me3/me2. Overexpression of dKDM4A in *Drosophila* S2 cells reduces the level of histone H3K36me3, whereas knockdown of endogenous dKDM4A increases the level of histone H3K36me3 and me2. Overexpression of dKDM4B in S2 cells results in decreased level of histone H3K36 and K9me3. A recent paper reported that dKDM4A can demethylate both histone H3K36 and K9 when overexpressed in S2 cells (Lloret-Llinares et al., 2008). However, I did not observe a significant decrease of histone H3K9me3 levels in S2 cells overexpressing dKDM4A (Figure 3-6B), and this result is consistent with what I observed in the in vitro assay (Figure 3-3B). Thus, these results together demonstrate that dKDM4A is a bona fide histone H3K36me3/me2 demethylase, and dKDM4B is a histone H3K9 and K36me3/me2 demethylase (Summarized in Table 3-1).

Table 3-1 KDM4 homologs in *Drosophila melanogaster*.

Human Homolog	KDM4/JHDM3/JMJD2	
Fly Homolog	dKDM4A/CG15835	dKDM4B/CG33182
Demethylation Activity of Human KDM4	H3K36me3/me2 H3K9me3/me2	
Demethylation Activity of Fly KDM4	H3K36me3/me2	H3K36me3/me2 H3K9me3/me2
Location on the Chromosome	2R43F2	2R49F7
Size	495 aa	590 aa

Set2-mediated histone H3K36 methylation is an important mark on histone during transcription elongation (Li et al., 2007a). In fungi, such as *S. cerevisiae*, *S. pombe*, and *N. crassa*, a sole histone lysine-methyltransferase Set2 is responsible for all three methylation states of H3K36 (Adhvaryu et al., 2005; Morris et al., 2005; Strahl et al., 2002). In *Drosophila*, histone H3K36 methylation is catalyzed by two enzymes, dSet2 and dMes-4 (Bell et al., 2007; Larschan et al., 2007). Although yeast Set2 is the only histone methyltransferase that catalyzes methylation of histone H3K36, two histone H3K36 demethylases, Jhd1 and Rph1, are responsible for demethylation of histone H3K36 at different modification states in budding yeast (Kim and Buratowski, 2007; Klose et al., 2007a; Tu et al., 2007). There are three histone demethylases that govern demethylation of histone H3K36 in flies. dKDM2 has been identified as a histone H3K36me2 demethylase (Lagarou et al., 2008). I demonstrate here that dKDM4A is a histone H3K36me3 and me2 demethylase, and dKDM4B has demethylation activity on both histone H3K9 and K36me3/me2. Therefore, histone H3K36 methylation in *Drosophila* is likely regulated by highly specific enzymes in both directions. Since both modification and de-modification enzymes possess high modification state specificity, histone H3K36 may be subjected to much more sophisticated regulation in higher eukaryotes than in yeast.

Chapter 4 Identification of Native Drosophila Histone Demethylase Complexes

4.1 Introduction

Like other histone modifying enzymes, many histone demethylases exist as part of a multiprotein complex, and the demethylation activity is regulated by the associated protein factors. For example, KDM5D/JARID1d, a histone H3K4 demethylase, was found to associate with polycomb-like protein Ring6a/MBLR. Ring6a enhances the demethylation activity of JARID1d to regulate the gene expression through demethylation of histone H3K4me3/me2 at the transcription start site of target genes (Lee et al., 2007b). The demethylation activity of LSD1/KDM1 is inhibited by its associated protein BHC80, while the association with CoREST promotes the demethylation activity of LSD1 on nucleosomal substrates (Lee et al., 2005; Shi et al., 2005).

Here I purified native protein complex of dKDM4A and dKDM4B from S2 stable cell lines and used MudPIT analysis to identify the associated proteins in the eluate. While specific binding proteins of dKDM4B were not found, HP1a was identified as a dKDM4A associated protein. A series of biochemical assays were carried out to confirm their interaction and to specify the interacting domains. I found that dKDM4A interacts with the chromoshadow domain of HP1a through a PxVxL motif at the C-terminus of dKDM4A. The physical association of HP1a stimulates the demethylation activity of dKDM4A. I also observed that loss of HP1a leads to an increased level of histone H3K36me3 in vivo. Collectively, these results suggest that HP1a functions in regulation of the demethylation activity of dKDM4A.

4.2 Affinity Purification of dKDM4A and dKDM4B from S2 Cells

To identify protein factors that associate with dKDM4, I established stable cell lines expressing epitope tagged dKDM4A or dKDM4B, and performed affinity purifications (Figure 4-1). Proteins in the eluate were then identified through MudPIT analysis (Washburn et al., 2001).

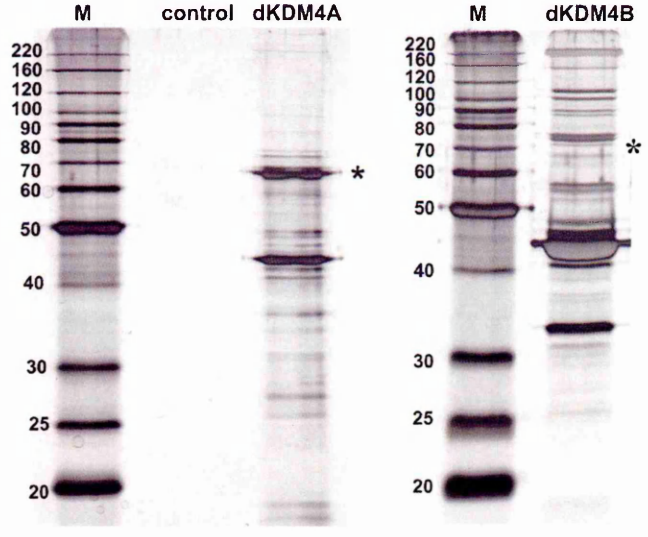

Figure 4-1 Affinity purification of dKDM4A and dKDM4B from S2 stable cell lines.

Silver staining gel showing the native complex purified from HAFLAG-tagged dKDM4A- (A) or dKDM4B-expressing stable cells (B) under 100 μM $CuSO_4$ induction. The asterisk indicates the tagged protein. The eluate of affinity purification from wild-type S2 cells was used as a control.

The MudPIT result of dKDM4A purification shows that the product of *Su(var)2-5*, *Drosophila* HP1a, co-purifies with dKDM4A (Figure 4-2A and Appendix B). HP1a is the second most abundant protein behind the tagged protein dKDM4A, except for some common contaminants. I then performed western blotting analysis using an antibody against HP1a to confirm this interaction. Indeed, HP1a is associated with dKDM4A (Figure 4-2B).

Proteins identified in dKDM4B purification through MudPIT analysis (Appendix C) were more likely to be nonspecific since they are commonly seen in other purifications done in the lab. Thus, I decided to focus on the dKDM4A/HP1a complex.

A

	Unique peptide	Spectra	SC (%)
dKDM4A	36	1086	73.7
HP1a	9	227	58.3

B

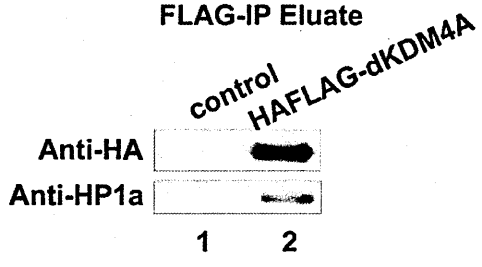

Figure 4-2 HP1a is identified as a dKDM4A associated protein by MudPIT analysis.

(A) The MudPIT analysis of native dKDM4A complex purified from HAFLAG-tagged dKDM4A-expressing stable cells. The table lists the number of non-redundant spectra (unique peptides), total spectra and the amino acid sequence coverage (SC).
(B) The eluate of affinity purification from wild-type S2 cells (control) and dKDM4A-expressing cells was analyzed by western blot using anti-HA and anti-HP1a antibody to detect the tagged dKDM4A and HP1a respectively.

4.3 HP1a Directly Interacts with dKDM4A

To further examine the interaction between dKDM4A and HP1a in another cellular system, I co-infected Sf21 cells with baculovirus encoding FLAG-tagged dKDM4A and HA-tagged or non-tagged HP1a. Anti-FLAG antibody-conjugated agarose beads were used to immunoprecipitate FLAG-dKDM4A. Both Coomassie blue staining (Figure 4-3A) and

western blots (Figure 4-3B) show that HP1a co-purifies with dKDM4A in this system. To test if HP1a directly interacts with dKDM4A, I carried out an in vitro binding assay by incubating recombinant dKDM4A and HP1a, followed by anti-HA immunoprecipitation. The results shown in Figure 4-4A (lane 3) indicate that these two proteins directly bind to each other. This interaction is specific to dKDM4A as dKDM4B failed to be pulled down by HP1a (Figure 4-4A, lane 7). To further demonstrate the specificity of HP1a-dKDM4A interaction, I purified recombinant proteins of the other two isoforms of HP1, HP1b and HP1c. As shown in Fig 4-4B (lane 6 and 7), HP1b and HP1c fail to interact with dKDM4A in the in vitro binding assay, suggesting that dKDM4A only associates with HP1a, but not HP1b or HP1c.

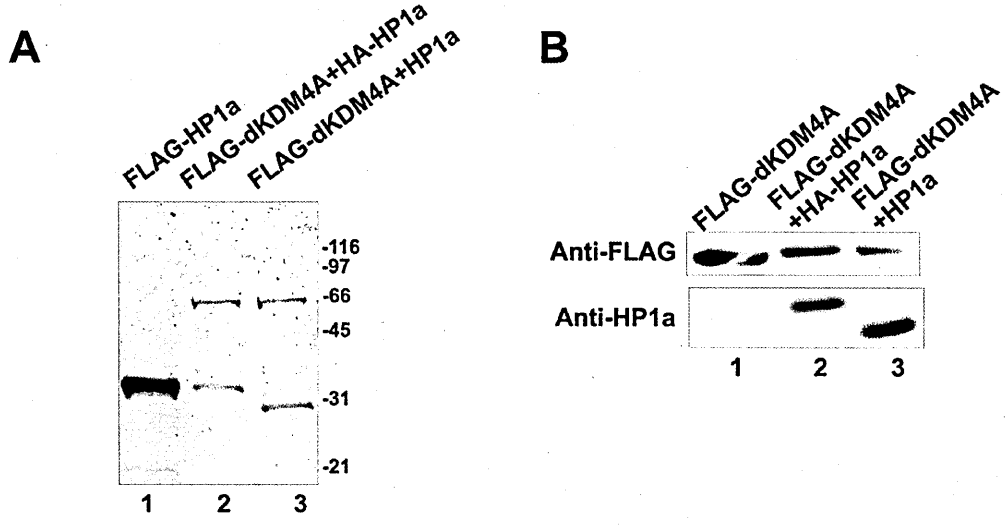

Figure 4-3 Interaction of dKDM4A and HP1a.

(A) FLAG-tagged recombinant proteins were purified from Sf21cells infected with baculovirus encoding FLAG-HP1a (lane 1), or co-infected with baculovirus encoding FLAG-dKDM4A and HA-HP1a (lane 2) or non-tagged HP1a (lane 3). The eluate from anti-FLAG beads was visualized by Coomassie blue staining.
(B) Recombinant dKDM4A (lane 1) and dKDM4A-HP1a complex (lane 2 and 3) purified from Sf21 insect cells were analyzed by western blot.

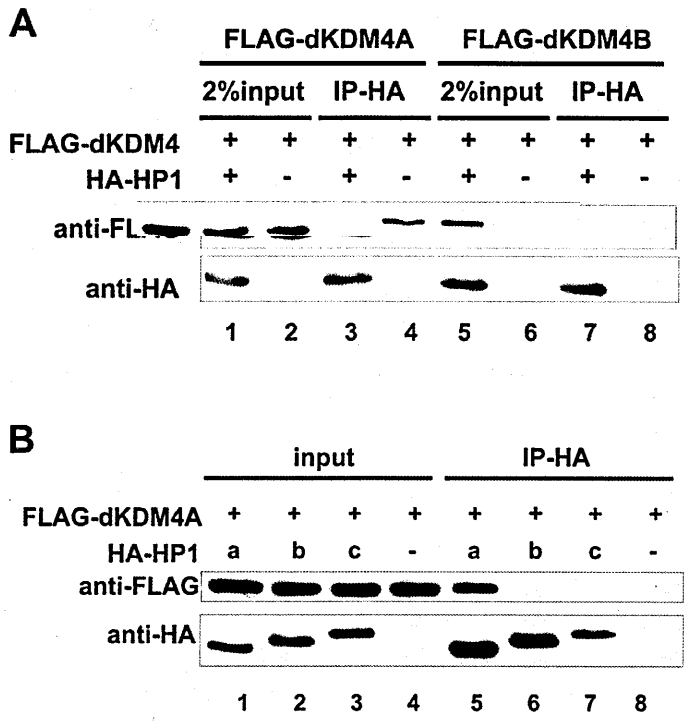

Figure 4-4 dKDM4A specifically interacts with HP1a.

(A) HP1a specifically interacts with dKDM4A but not dKDM4B. Recombinant HP1a and dKDM4A or dKDM4B were mixed with 500 μg of Sf21 cell lysate to reduce background binding. The resulting complexes were immunoprecipitated using anti-HA agarose beads. The entire immunoprecipitated material and 2 % of input were loaded on a gel and analyzed by western blot using anti-FLAG and anti-HA antibodies.
(B) HP1a specifically interacts with HP1a but not HP1b and HP1c. Recombinant dKDM4A and HP1a, HP1b or HP1c were mixed and immunoprecipitated.

4.4 HP1a Cofractionates with dKDM4A

The recombinant complex of dKDM4A and HP1a purified from insect cells was applied to a Superose 6 size exclusion chromatography. The column fractions were analyzed by western blot analysis. The fraction profiles show cofractionation of HP1a and dKDM4A from fractions 17 to 21 (Figure 4-5A). To examine whether HP1a and dKDM4A also exist as a complex in vivo, I applied the eluate of dKDM4A purification from the S2 stable cell line to the Superose 6 size exclusion chromatography. Despite a broader peak of dKDM4A,

the fraction profile of HP1a shows a similar pattern as in the recombinant complex, suggesting that these two proteins form a complex in vivo (Figure 4-5B).

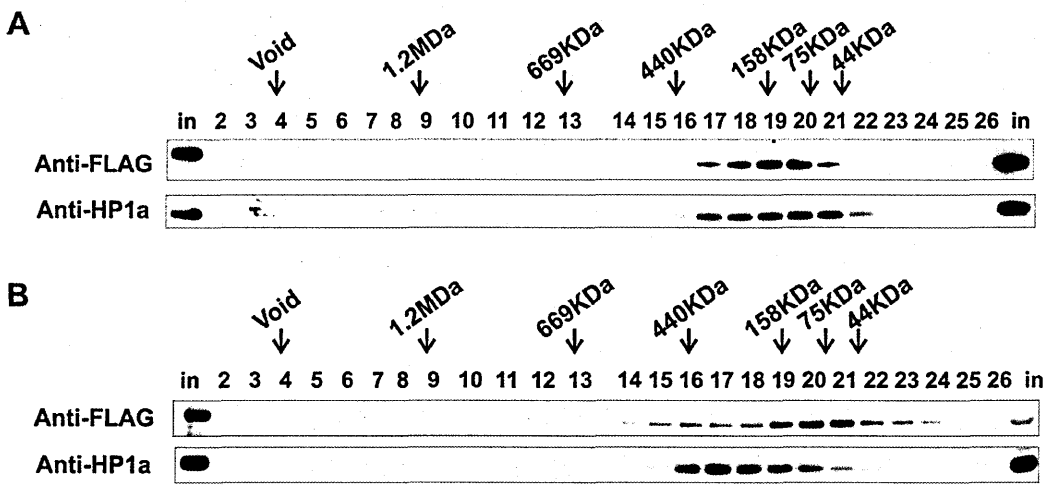

Figure 4-5 HP1a cofractionates with dKDM4A.

The recombinant complex of dKDM4A and HP1a purified from insect cells (A), or the eluate of dKDM4A purification from the S2 stable cell line (B), was loaded onto a Superose 6 gel filtration column. The fraction profiles were examined by western blot using antibodies against FLAG and HP1a. The numbers indicate the fraction number. In, input.

4.5 HP1a Stimulates Demethylation Activity of dKDM4A

While examining the demethylation activity of purified native dKDM4A complex, I noticed that the native complex displays stronger specific activity on histone H3K36me3 compared to recombinant dKDM4A (Figure 4-6A, compare lane 8 with lane 3-5), albeit containing less dKDM4A (anti-FLAG in Figure 4-6A). This result suggests that protein factors associated with dKDM4A may enhance dKDM4A enzymatic activity. Since HP1a binds dKDM4A, I next tested whether HP1a stimulates dKDM4A demethylation activity in vitro. Increasing amounts of HP1a were titrated into a recombinant dKDM4A-mediated demethylation assay. The demethylation activity of dKDM4A on H3K36me3 and me2 is

enhanced in the presence of HP1a (Figure 4-6B). The level of histone H3K9 and K4 methylation remains unchanged in the same reaction, and HP1a alone does not affect histone methylation levels (Figure 4-6B, lane6). Furthermore, no enhancement of dKDM4A activity was observed when HP1b and HP1c were added to the demethylation reactions (Figure 4-6C). This suggests that the stimulation of dKDM4A demethylation activity is specific to HP1a.

Since HP1 is known to recognize methylated H3K9 through its chromo domain (Bannister et al., 2001; Lachner et al., 2001), I wondered whether the chromo domain is important for HP1a to stimulate dKDM4A demethylation activity. To this end, I generated recombinant protein with a mutation in the HP1a CD (V26M) that has been shown previously to abolish HP1a binding to histone H3K9me (Jacobs et al., 2001). As shown in Figure 4-7A (lane1-5), this mutant fails to enhance the demethylation activity of dKDM4A on histone H3K36me3. It is likely that this defect is due to a reduced interaction of HP1a with histone H3 because its interaction with dKDM4A was unaffected by the mutation (Figure 4-7B).

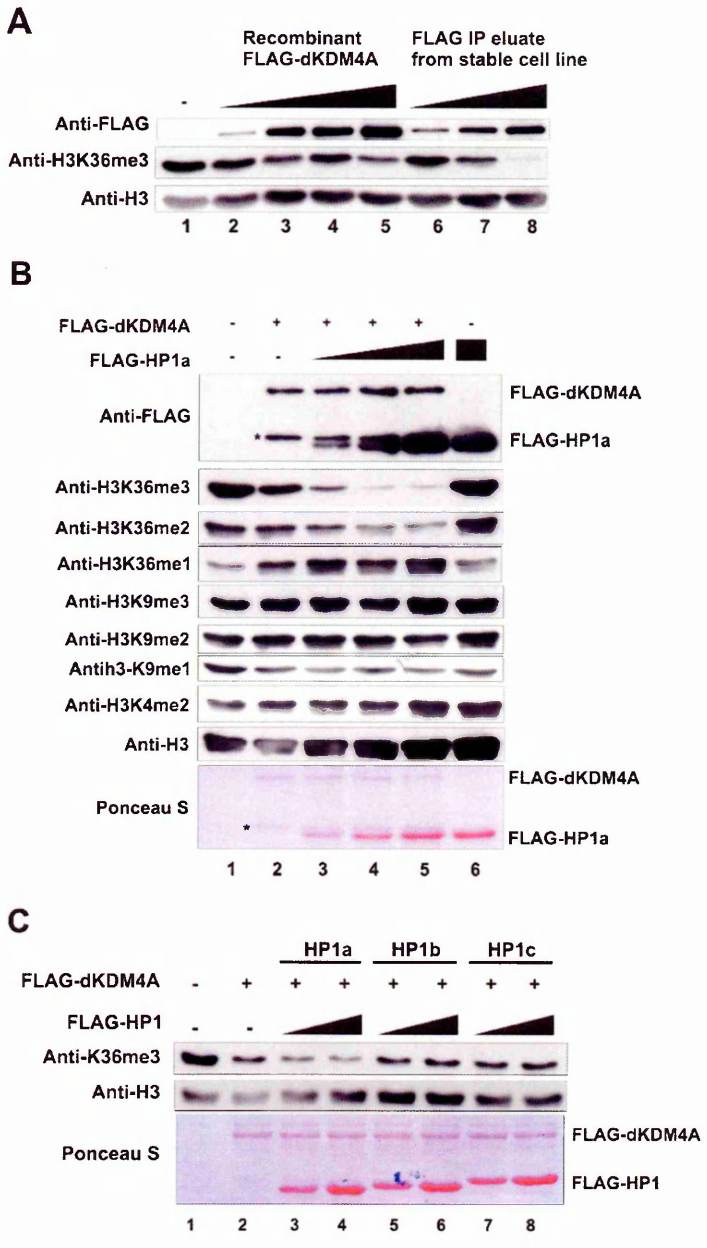

Figure 4-6 HP1a stimulates the histone demethylation activity of dKDM4A.

(A) In vitro demethylation assay using recombinant dKDM4A or the dKDM4A complex that were purified from HAFLAG-dKDM4A-expressing stable cells. HeLa core histones were used as substrates, and the reactions were analyzed by western blot.
(B) In vitro demethylation assay using recombinant dKDM4A with addition of HP1a. HeLa core histones were used as substrates, and the reactions were analyzed by western blot. The molar ratio of dKDM4A and HP1a is 1:1, 1:2 and 1:4 in lane 3, 4 and 5. HP1a was added to the reaction without dKDM4a as a control in lane 6. Asterisks indicate the degradation products of recombinant dKDM4A.
(C) In vitro demethylation assay using recombinant dKDM4A with addition of HP1a, HP1b or HP1c. The molar ratio of dKDM4A and HP1 is 1:1 in lane 3, 5 and 7 and 1:2 in lane 4, 6, and 8.

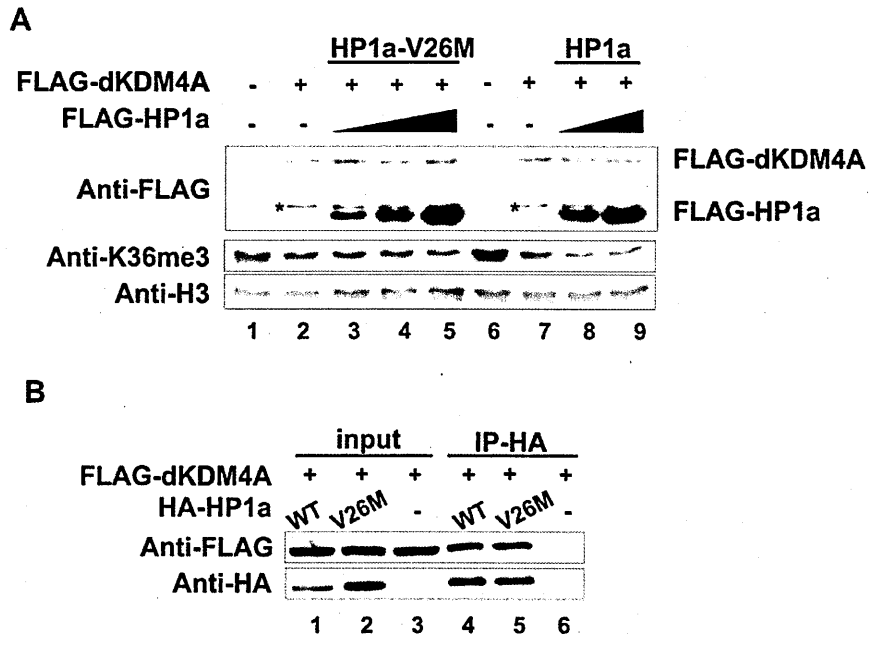

Figure 4-7 Stimulation of the demethylation activity of dKDM4A depends on the CD of HP1a.

(A) In vitro demethylation assay using recombinant dKDM4A with addition of HP1a or HP1a-V26M mutant. HeLa core histones were used as substrates. The molar ratio of dKDM4A and HP1a is 1:1, 1:2 and 1:4 in lane 3, 4 and 5; 1:2 and 1:4 in lane 8 and 9. Asterisks indicate the degradation products of recombinant dKDM4A.
(B) Recombinant dKDM4A and HP1a or HP1a-V26M were mixed with 500μg of Sf21 cell lysate and immunoprecipitated using anti-HA agarose beads. The entire immunoprecipitated material and 2 % of input were analyzed by western blot using anti-FLAG and anti-HA antibodies.

4.6 The CSD of HP1a and a Consensus HP1-interacting PxVxL Motif in dKDM4A are Responsible for the HP1a-dKDM4A Interaction

To map the domain of HP1a that mediates the direct interaction with dKDM4A, I purified truncated forms of HP1a that contain either the CD or the CSD alone (Figure 4-8A) and tested them in the in vitro binding assay. As shown in Figure 4-8B, the CSD is sufficient for the binding of HP1a to dKDM4A, while the CD does not interact with dKDM4A under the same conditions.

To dissect the interaction between dKDM4A and HP1a CSD further, I introduced two point mutations at conserved residues within CSD, I191E and W200A. These mutations

have been shown to disrupt the dimerization of CSD and its interaction with HP1 binding proteins (Brasher et al., 2000; Thiru et al., 2004). As expected, recombinant HP1a-I191E and W200A both fail to interact with dKDM4A (Figure 4-8C), suggesting that an intact CSD dimerization interface is required for the HP1-dKDM4A interaction.

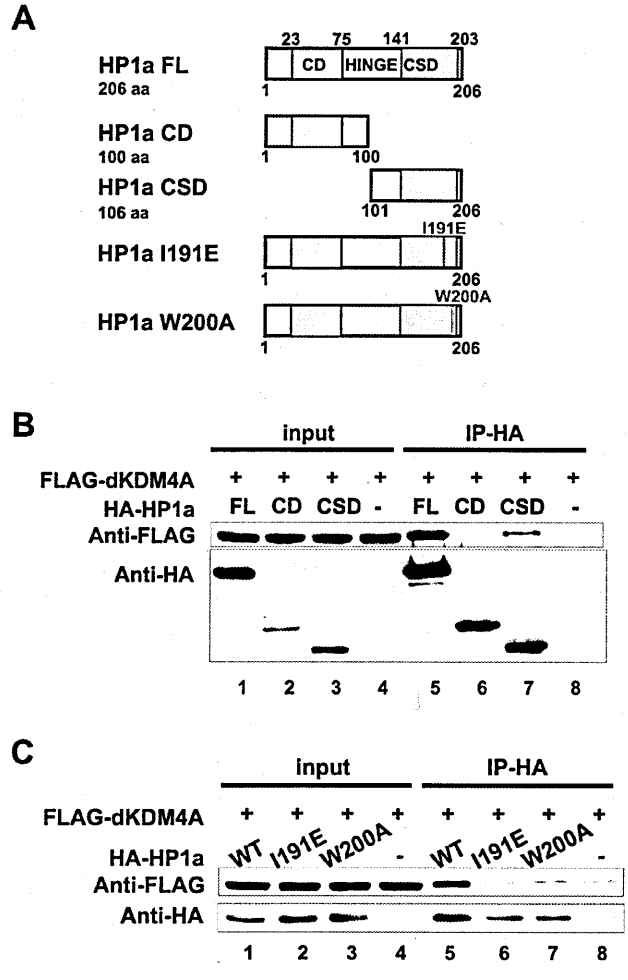

Figure 4-8 An intact CSD dimerization interface of HP1a is required for its interaction with dKDM4A.

(A) Schematic representation of HP1a truncation mutants (CD and CSD) and two critical residues that are predicted to disrupt either its dimerization (I191E) or its target-binding interface (W200A). Full-length HP1a (FL) contains a chromo domain (CD), a hinge domain and a chromoshadow domain (CSD).
(B) HP1a CSD but not CD binds to dKDM4A. Recombinant dKDM4A and full-length HP1a (FL), truncation mutants HP1a CD, or HP1a CSD were mixed with 500 μg of Sf21 cell lysate and immunoprecipitated using anti-HA agarose beads. The entire immunoprecipitated material and 2 % of input were analyzed by western blot using anti-FLAG and anti-HA antibodies.
(C) HP1a mutants I191E and W200A fail to interact with dKDM4A.

The CSD of HP1 recognizes a consensus peptide pentamer, PxVx [M /L/V], in most HP1-interacting proteins (Smothers and Henikoff, 2000; Thiru et al., 2004). I found that the C-terminal region of dKDM4A contains a PxVxL motif, PVVKL (amino acid 421 to 425) (Figure 4-9A). To examine whether HP1a associates with dKDM4A through this motif, I generated a mutant in which the critical valine 423 was mutated to alanine. Recombinant dKDM4A-V423A protein was purified from baculovirus-infected Sf21 cells (Figure 4-9B). This mutant protein could no longer stably associate with HP1a (Figure 4-9C, lane 5-8). Thus, HP1a associates with dKDM4A through the conserved PxVxL motif.

To examine whether the stimulation of dKDM4A activity by HP1a relies on their physical association, recombinant dKDM4A-V423A protein, which fails to bind HP1a, was used in the in vitro demethylation assay. This mutation has minimal effect on intrinsic enzymatic activity of dKDM4A (compare lane2 and lane7 in Figure 4-9D). When increasing amounts of HP1a were titrated into the reaction, I did not observe the stimulation of the demethylation activity of the dKDM4A-V423A mutant (Figure 4-9D, lane 3-5). Taken together, these results indicate that the association of HP1a with dKDM4A regulates the histone H3K36 demethylation activity of dKDM4A.

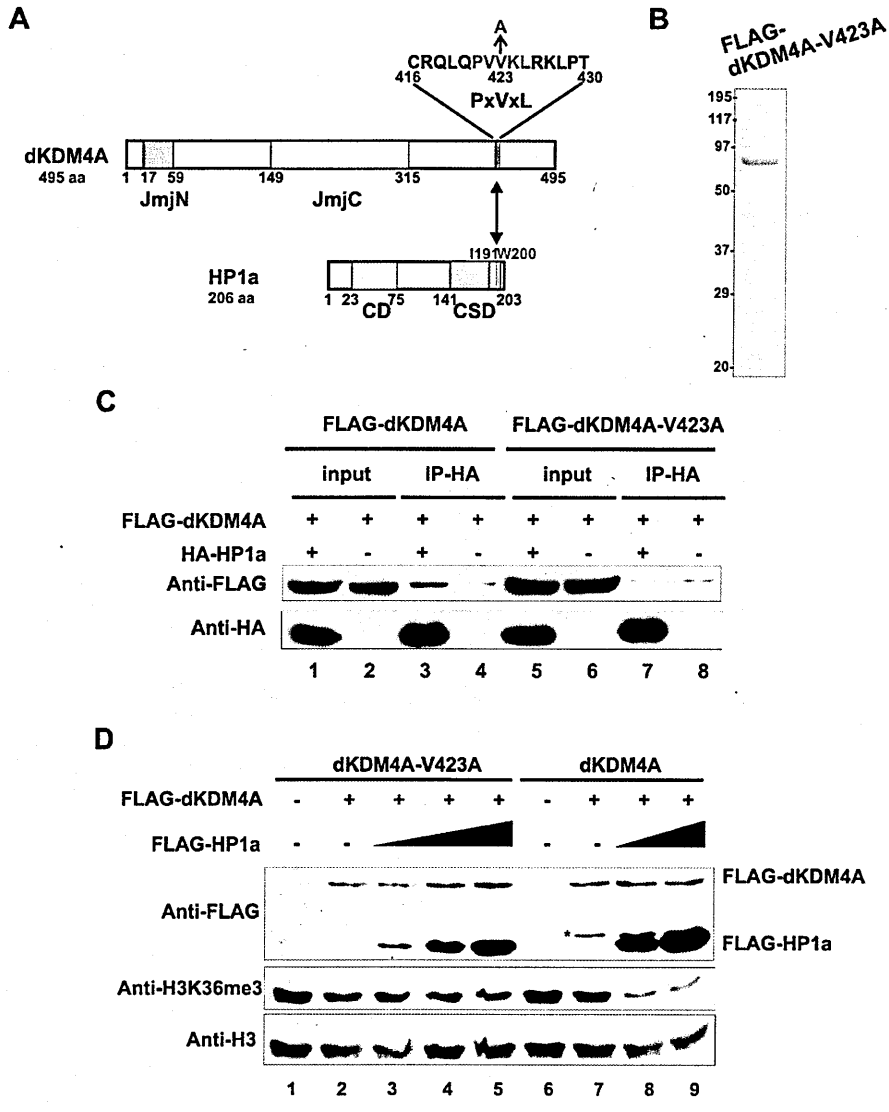

Figure 4-9 dKDM4A interacts with HP1a through a conserved HP1a-binding PxVxL motif.

(A) Schematic representation of consensus HP1a binding motif within dKDM4A. The amino acid sequence from 421 to 425 of dKDM4A contains an HP1a binding PxVxL motif, which is colored red. The critical residue (V423) was mutated into alanine as indicated.
(B) Recombinant dKDM4A-V423A was purified from baculovirus-infected Sf21 cells and visualized by Coomassie blue staining.
(C) HP1a directly associates with dKDM4A through a consensus HP1 binding motif. Recombinant HP1a and dKDM4A or V423A mutant were mixed and immunoprecipitated using anti-HA agarose beads.
(D) In vitro demethylation assay using recombinant dKDM4A-V423A or wild-type dKDM4A in the presence of HP1a. HeLa core histones were used as substrates. The molar ratio of dKDM4A and HP1a is 1:1, 1:2 and 1:4 in lane 3, 4 and 5; 1:2 and 1:4 in lane 8 and 9. Asterisk indicates the degradation of recombinant dKDM4A.

4.7 The Biological Function of dKDM4A-HP1a Interaction

To explore the biological function of HP1a-dKDM4A interaction, I crossed transgenic flies, UAS-*Kdm4A-HA$_1$FLAG$_2$* or UAS-*Kdm4A-V423A-HA$_1$FLAG$_2$*, with Sgs3-GAL4 to overexpress dKDM4A in salivary glands. I first performed immunofluorescence analysis of polytene chromosomes from the larvae overexpressing wild type dKDMA4A in salivary glands. Salivary glands from wild type (OreR) and dKDM4A-overexpressing larvae were squashed on the same slide to minimize any procedural variation. Indeed, I found that overexpression of dKDM4A induces HP1a to spread into chromosome arms (Figure 4-10A). This pattern is in contrast to that of HP1a in wild type flies, in which it is mainly located at the chromocenter. This result is in agreement with a recent paper using a similar system (Lloret-Llinares et al., 2008). I then tested if the spreading of HP1a is directly related to its interaction with dKDM4A using transgenic larvae that overexpress dKDM4A mutant (V423A) in salivary glands. A very similar staining pattern of the mutant dKDM4A was observed (Figure 4-10B, anti-HA), compared to the wild type dKDM4A (Figure 4-10A, anti-HA). However, consistent with the fact that dKDM4A-V423A does not bind to HP1a in vitro, the spreading of HP1a was significantly reduced in the larvae overexpressing dKDM4A-V423A (Figure 4-10B). This result supports the notion that the binding of HP1a to chromosome arms is helped through its interaction with overexpressed dKDM4A.

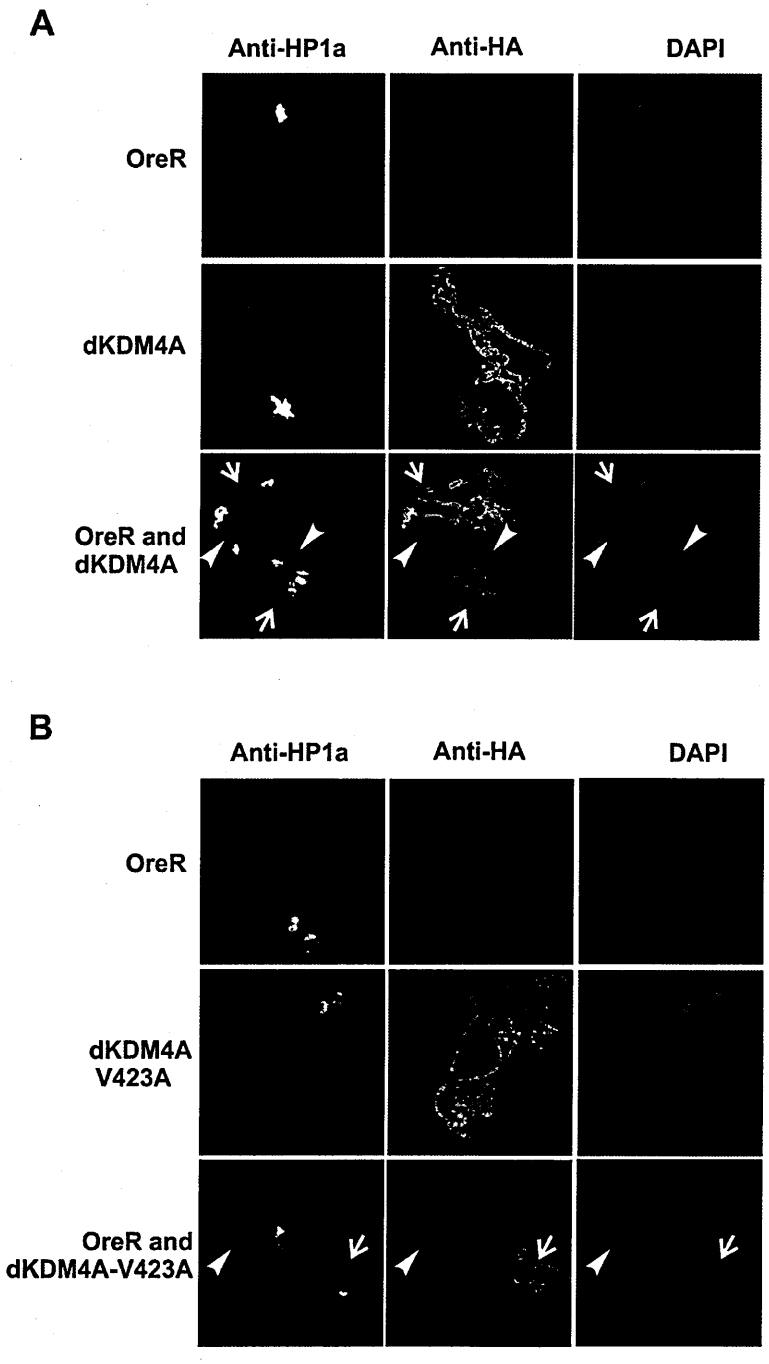

Figure 4-10 Overexpression of dKDM4A induces HP1a spreading into euchromatin.

Salivary glands from wild type were placed on the same slide as those prepared from either the dKDM4A-HAFLAG overexpressing line (A) or the dKDM4A-V423A-HAFLAG-overexperssing line (B). Each combination of glands were squashed together, and resulting polytene chromosomes were stained with antibodies against HP1a and HA. Images from each slide were taken on a confocal laser scanning microscope using the exact same setting. The red corresponds to anti-HP1a staining, the green corresponds to anti-HA staining of dKDM4A-HAFLAG, which was used to distinguish between OreR or dKDM4A overexpressing chromosomes, and the blue corresponds to DAPI staining. Arrowheads indicate polytene chromosomes from wild type larvae, and arrows indicate polytene chromosomes from dKDM4A or dKDM4A-V423A-overexpressing larvae.

4.8 HP1a Regulates Histone H3K36 Methylation in Drosophila Larvae

The biochemical data suggest that HP1a collaborates with dKDM4A to regulate the level of H3K36me. Thus, I wondered whether mutations disrupting HP1a or dKDM4A expression might share a similar phenotype. To this end, I obtained a fly stock containing the P-element KG04636 inserted within the coding region of dKDM4A (Figure 4-11A). This insertion abrogated the expression of dKDM4A as detected by real-time RT-PCR (Figure 4-11B) and western blot (Figure 4-11C). Although the mutant is homozygous viable, the P-element insertion elevates the bulk level of histone H3K36me3 in mutant embryos (Figure 4-11C). A rescue experiment was done by precisely hopping out the P element. The precise excision restored the expression level of dKDM4A, and the level of H3K36me3 was also rescued (Figure 4-11B and C). A previous study showed that chromatin bound HP1a was not detectable in the *Su(var)2-5*^{04}*/Su(var)2-5*^{05} mutant larvae (Fanti et al., 1998). To test if loss of HP1a gives rise to similar changes in the histone methylation, I examined the level of histone H3K36me3 in third instar larvae of this mutant. As shown in Figure 4-11D (upper panel), HP1a was not detected in nuclear extracts from *Su(var)2-5*^{04}*/Su(var)2-5*^{05} larvae. However, the level of histone H3K36me3 increased significantly compared to that of wild type (Figure 4-11D, lower panel). This result supports the notion that HP1a is required for the demethylation of H3K36 mediated by dKDM4A in vivo.

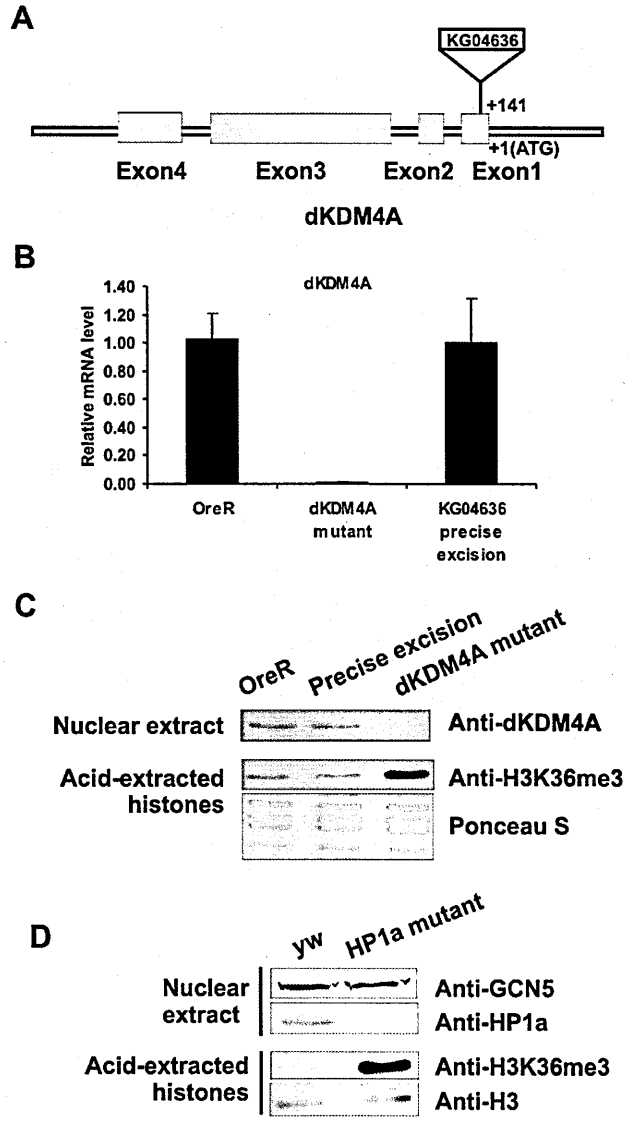

Figure 4-11 HP1a regulates histone H3K36me3 methylation in Drosophila larvae.

(A) Schematic representation of the insertion site of P element KG04636.
P element insertion abrogates the expression of dKDM4A in mRNA level (B) and protein level (C), and elevates the bulk level of H3K36me3. Precise excision of P element rescued the expression of dKDM4A and the levels of H3K36me3. RNA was extracted from embryos of OreR, dKDM4A mutants (KG04636) and mutants rescued by precise excision of the P element. The mRNA level of dKDM4A was determined by real-time RT-PCR and normalized to rp49. The result was shown as relative dKDM4A expression level compared to OreR. The error bars represent standard deviation from 3 biological repeats. Nuclear extracts and acid-extracted histones from embryos were analyzed by western blot using indicated antibodies.
(D) Loss of HP1a significantly increases the level of histone H3K36me3 in *Drosophila* larvae. Nuclear extracts (upper panel) or acid-extracted histones (lower panel) from third instar larvae of *yw* and the HP1a null mutant (*Su(var)2-5*^{04}*/Su(var)2-5*^{05}) were subjected to western blot using indicated antibodies. The levels of GCN5 and histone H3 were used as loading controls.

4.9 Discussion

Purification of the dKDM4A complex from S2 cells revealed a specific association of HP1a with dKDM4A. Three of the HP1-like chromatin proteins (HP1a, HP1b, HP1c) in *Drosophila* share high amino acid sequence similarity. Both HP1a and HP1b localize to the euchromatin and heterochromatin, while HP1c is found only in the euchromatin (Smothers and Henikoff, 2001). It is unclear whether these HP1-like chromatin proteins have specific or redundant functions in transcription regulation. However, I demonstrate here that dKDM4A specifically interacts with HP1a, but not HP1b and HP1c. Furthermore, HP1b and HP1c cannot stimulate dKDM4A demethylation activity in vitro.

A previous study showed that the yeast homolog of KDM4, Rph1 (ScKDM4), did not stably associate with any other protein (Klose et al., 2007a). It was speculated that the C-terminal ZF domain of Rph1, which can potentially bind to DNA, allows Rph1 to function without associated factors (Klose et al., 2007a). Unlike other proteins in the KDM4 family, which commonly contain PHD, tudor or ZF domains (Figure 3-1), dKDM4A only has JmjN and JmjC domains. Here I found that HP1a stably associates with dKDM4A and stimulates its demethylation activity. Since the H3K9 binding motif is required for this stimulation, the CD of HP1a might contribute to target dKDM4A to specific loci, particularly to H3K9me enriched regions, to regulate gene expression.

In *S. pombe*, the HP1 homolog, Swi6, recruits a JmjC domain-containing protein Epe1 to heterochromatin loci where they function together to counteract repressive chromatin (Zofall and Grewal, 2006). Here I show that HP1a directly interacts with dKDM4A through a consensus binding motif PxVxL. Most importantly, the presence of HP1a stimulates histone demethylation activity of dKDM4A in vitro, and HP1a is required for maintaining normal level of H3K36me3 in vivo as well. Since Epe1 on its own seems to have no histone demethylation activity (Tsukada et al., 2006), it would be interesting to see

whether a similar scenario also occurs in *S. pombe*, in which Swi6 may stimulate enzymatic activity of Epe1 towards other non-histone substrates.

HP1 has been reported to associate with actively transcribed euchromatin regions (Cryderman et al., 2005; de Wit et al., 2007; Piacentini et al., 2003; Vakoc et al., 2005). Mammalian HP1γ and histone H3K9 methylation are enriched at the coding region of active genes, implying that they may play a role during transcription elongation (Vakoc et al., 2005). In yeast, histone H3K36me3 appears to be a repressive mark at coding region of actively transcribed genes (Li et al., 2007a). In higher eukaryotes, histone H3K9 methylation, which is absent in the budding yeast, might replace the role of K36 methylation in the coding regions of transcribed genes (Berger, 2007). However, the mechanism by which HP1 functions in active transcription is largely unknown. Our findings here suggest a possible role of HP1a in recruitment of the histone H3K36me3/me2 demethylase dKDM4A to transcribed regions to remove histone H3K36 methylation. The formation of the HP1a-dKDM4A complex may help to release HP1a from heterochromatin regions, thus targeting it to specific gene loci. It is also possible that dKDM4A, which targets histone modification marks within the 3' ORF of actively transcribed genes, recruits HP1a to euchromatic regions. We currently favor a model in which HP1a facilitates recruitment of dKDM4A, because the HP1a CD mutant, V26M, fails to stimulate dKDM4A activity. This result suggests that HP1a binding to histone H3 is required for the enhancement of dKDM4A demethylation activity. HP1a-mediated histone demethylation may serve as a regulatory mechanism to control chromatin states during active transcription elongation. Alternatively, a similar mechanism might also apply to maintaining silenced states of heterochromatin.

Chapter 5 Identification of KDM4A Target Genes

5.1 Introduction

I have demonstrated that dKDM4A is a functional histone H3K36me3/me2 demethylase, and the association of HP1a stimulates the demethylation activity of dKDM4A. I next sought to explore the biological function of dKDM4A and the HP1a-dKDM4A complex. There are many questions to be addressed regarding to the role of dKDM4A in vivo. Does dKDM4A directly regulate gene expressions through demethylation of H3K36me3? What genes are targeted by dKDM4A? Where does the HP1-dKDM4A complex function in the genome?

Previous studies have revealed a possible role of KDM4 family proteins in gene transcription. Human KDM4A/JMJD2A was found to bind to the promoter of ASCL2 gene and function as an N-CoR-associated corepressor (Zhang et al., 2005). Knockdown of JMJD2A results in upregulation of ASCL2 and increased H3K9me3 levels, while there are only subtle changes in the level of H3K36me3 (Gray et al., 2005). Human KDM4B/JMJD2B was found to be a co-regulator in ER signaling. The induction of a subset of ER-target genes was reduced in JMJD2B-depleted cells, resulting in defective proliferation. JMJD2B binds to the ER binding site of those genes and mediates demethylation of H3K9me3 to facilitate gene induction (Kawazu et al., 2011). Human KDM4 homologs have demethylation activity on histone H3K36 and/or K9 methylation, while *Drosophila* KDM4A only shows demethylation activity towards H3K36me3/me2, suggesting that dKDM4A might have different functions as a histone H3K36 demethylase.

The yeast KDM4 homolog, Rph1, was found to regulate H3K36 methylation at actively transcribed regions and play a positive role in transcription elongation (Kim and

Buratowski, 2007). A recent study shows that Rph1 is associated with the promoter of PHR1 gene through zinc finger domains and regulates the level of H3K36me3, resulting in repression of PHR expression (Liang et al., 2011).

However, the genome-wide distribution of KDM4 homologs remains unknown. As shown in Figure 3-1A, *Drosophila* homologs of KDM4 lack PHD, tudor and zinc finger domains that are found in other KDM4 homologs in humans, worms and yeast. Thus, the mechanism of targeting KDM4 might be diverse between different homologs. Here I performed genome-wide analysis, including RNA-seq and ChIP-chip analysis to examine the role of dKDM4A in gene transcription and to identify candidate target genes of dKDM4A, as well as common target genes of HP1a and dKDM4A.

5.2 Gene Expression Profiles of dKDM4A Mutant

To examine whether loss of dKDM4A affects gene expression, I performed mRNA-seq analysis with RNA extracted from early embryos (2-4 hours) of P element inserted-dKDM4A mutant flies and flies rescued by precise excision of the P element. The differential gene expression between dKDM4A mutants and the rescued fly lines were examined. Genes were filtered by FPKM $\geq$ 3 to exclude the lowly expressed genes. Of the 175 genes affected in the dKDM4A mutants, 126 genes were upregulated in the absence of dKDM4A, while 49 genes were downregulated (Figure 5-1A and Appendix D). GO term analysis revealed that genes upregulated in the dKDM4A mutant are associated with several metabolic processes (Figure 5-1B and Table 5-1); genes downregulated in the dKDM4A mutant are associated with oxidation/reduction, gene translation and mRNA metabolic processes (Figure 5-1C and Table 5-2).

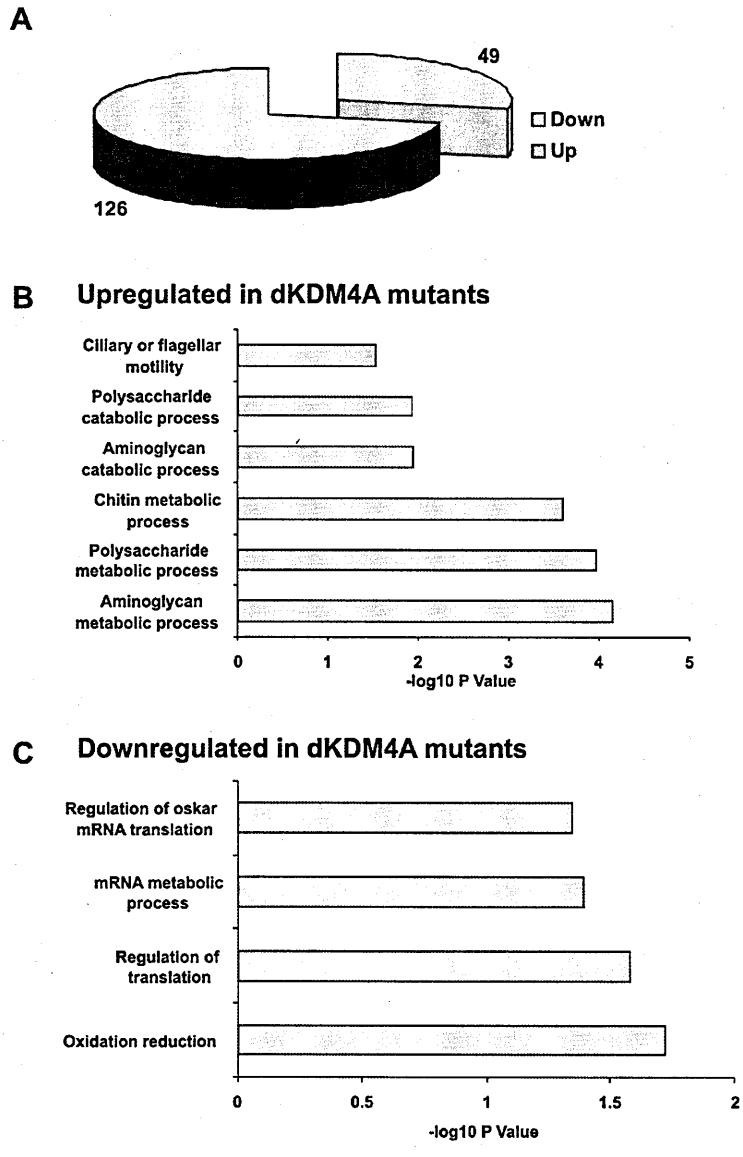

Figure 5-1 Loss of dKDM4A in early embryos leads to changes in gene expression in a small subset of genes.

(A) The differential gene expression was analyzed by RNA-seq analysis of 2-4 hours embryos of P element inserted-dKDM4A mutant flies and flies rescued by precise excision of the P element. 126 genes were upregulated in the absence of dKDM4A, while 49 genes were downregulated. (FPKM $\geq$ 3, fold change $\geq$2)
(B-C) GO term analysis of genes up- (B) or down-regulated (C) in dKDM4A mutants. (P value <0.05)

Table 5-1 GO terms analysis of genes upregulated in dKDM4A mutant embryos

GO Term	P Value	Gene
GO:0006022 Aminoglycan metabolic process	6.86E-05	Gasp, Idgf3,Idgf2, CG7298, Muc26B, obst-E, Pmi
GO:0005976 Polysaccharide metabolic process	1.04E-04	Gasp, Idgf3,Idgf2, CG7298, Muc26B, obst-E, Pmi
GO:0006030 Chitin metabolic process	2.47E-04	Gasp, Idgf3,Idgf2, CG7298, Muc26B, obst-E
GO:0006026 Aminoglycan catabolic process	1.12E-02	Idgf3,Idgf2, Pmi
GO:0000272 Polysaccharide catabolic process	1.18E-02	Idgf3,Idgf2, Pmi
GO:0001539 Ciliary or flagellar motility	2.99E-02	TpnC4, TpnC73F

P value <0.05, a minimum of 2 gene products

Table 5-2 GO terms analysis of genes downregulated in dKDM4A mutant embryos

GO Term	P Value	Gene
GO:0055114 Oxidation reduction	1.89E-02	Nos, Kdm4A, CG11200, Adh, CG8503, CG6463, P5cr
GO:0006417 Regulation of translation	2.63E-02	CG14425, aret, osk
GO:0016071 mRNA metabolic process	4.09E-02	CG9344, CG14425, aret, osk
GO:0046011 Regulation of oskar mRNA translation	4.49E-02	aret, osk

P value <0.05, a minimum of 2 gene products

5.3 Identification of dKDM4A Target Genes by H3K36me3 ChIP-chip Analysis

Previously I observed an increased level of bulk histone H3K36me3 resulting from the loss of dKDM4A in mutant embryos (Figure 4-11C). To examine the increase of H3K36me3 levels genome-wide and to identify target genes of dKDM4A, I performed chromatin immunoprecipitation using an antibody against histone H3K36me3 in early embryos (2-4 hours) followed by microarray analysis (ChIP-chip). Immunoprecipitated DNA from dKDM4A mutant and wild type (mutants rescued by P precise excision of the P element) fly lines were labeled and hybridized along with input DNA on high-density genomic tiling microarrays. When comparing the level of H3K36me3 in dKDM4A

mutants to that in the wild type, there are 834 positive H3K36me3 peaks indicating increased H3K36me3 levels in dKDM4A mutants. These 834 peaks are matched to 658 genes, which represent putative target genes of dKDM4A (Appendix E). I examined the ratio of genes with increased H3K36me3 levels (mt/WT) on each chromosome region. The pericentric heterochromatin regions (e.g. 2Lh and 2LHet) are defined based on the Release 5 of the *D. melanogaster* genome sequence (Hoskins et al., 2007; Smith et al., 2007) and epigenomic euchromatin-heterochromatin borders, which is determined by sharp transitions of H3K9me2 (Riddle et al., 2011). Interestingly, genes with increased H3K36me3 levels are found to be over-represented at heterochromatic regions compared to euchromatin arms (Figure 5-2A and B). There are 68 genes at pericentric heterochromatin showing increased levels of H3K36me3 in the dKDM4A mutant (Figure 5-2C). These results suggest that dKDM4A might be important in regulation of H3K36me3 levels at heterochromatic regions.

A

	Genes with H3K36me3 peaks (mt/WT)	Total genes of the chromosome	%
Chr2L	95	2573	3.69
Chr2Lh	4	21	19.05
Chr2LHet	1	7	14.29
Chr2R	157	2703	5.81
Chr2Rh	8	40	20.00
Chr2RHet	18	68	26.47
Chr3L	115	2668	4.31
Chr3Lh	5	23	21.74
Chr3LHet	12	57	21.05
Chr3R	138	3348	4.12
Chr3RHet	12	53	22.64
Chr4	6	83	7.23
ChrX	76	2194	3.46
ChrXHet	1	12	8.33
ChrYHet	1	8	12.50
ChrU	9	187	4.81

C

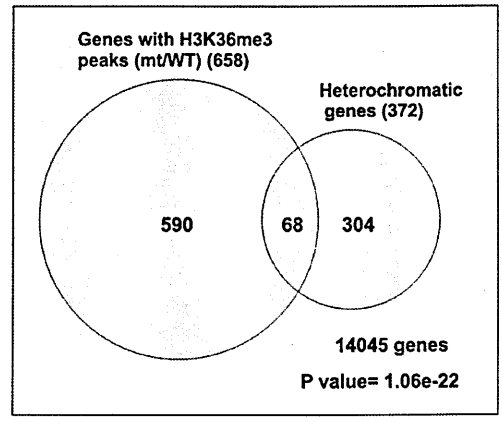

B

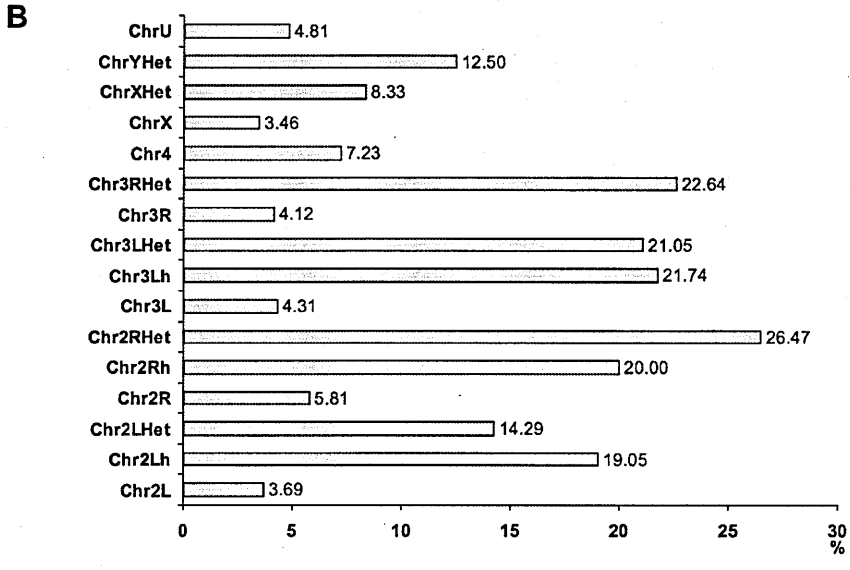

Figure 5-2 Genes with increased H3K36me3 levels in dKDM4A mutants are over-represented at heterochromatic regions.

(A-B) The numbers and ratio of genes with increased H3K36me3 levels (mt/WT) on each chromosome. (C) The Venn diagram analysis of genes with increased H3K36me3 levels in the dKDM4A mutant and heterochromatic genes. The P value is obtained from the hypergeometric test.

5.4 Genes with Differential Expression Levels Show Little Correlation with Increased H3K36me3 Levels in the dKDM4A Mutant

To examine whether genes which are up- or down-regulated in the dKDM4A mutant are direct targets of dKDM4A, I compared genes showing differential expression levels in the dKDM4A mutant with putative target genes of dKDM4A identified by H3K36me3 ChIP-chip analysis. The Venn diagram analysis shows that only 18 out of 126 genes upregulated in the dKDM4A mutant (Figure 5-3A) and 5 out of 49 genes downregulated in the dKDM4A mutant (Figure 5-3B) show increased levels of H3K36me3 in the absence of dKDM4A. It suggests that the differential gene expression in the dDKM4A mutant has little correlation with increased levels of H3K36me3.

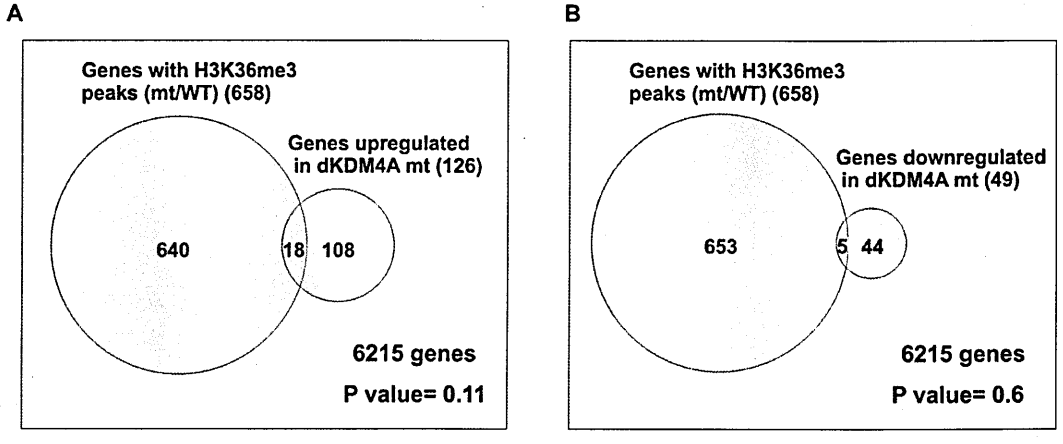

Figure 5-3 Genes with differential expression levels show little correlation with increased H3K36me3 levels in the dKDM4A mutant

The Venn diagram analysis of genes with increased H3K36me3 levels in the dKDM4A mutant and genes that are up- (A) or down-regulated (B) in the dKDM4A mutant demonstrates little overlap between two datasets. The total number of genes (6215) in RNA-seq analysis is used as the universal set.

5.5 Identification of Common Target Genes of dKDM4A and HP1a

I have previously identified the direct interaction between HP1a and dKDM4A, and the association of HP1a stimulates the H3K36me3 demethylation activity of dKDM4A. To examine whether there are common target genes of dKDM4A and HP1a, I compared the peak regions of increased H3K36me3 levels in the dKDM4A mutant to HP1a binding sites. The list of HP1a binding sites were generated by the modENCODE project, and the binding sites were identified by ChIP-chip analysis using an antibody against HP1a in early embryos (2-4 hours) of the wild-type Oregon R flies (Roy et al., 2010). The overlapped peaks between two datasets were extracted. If multiple neighboring peaks of HP1a binding sites overlap to a single H3K36me3 peak, I combined the HP1a binding sites into one peak, and vice versa. There are 147 peaks that show both enrichment of HP1a in wild type embryos and increased levels of H3K36me3 in dKDM4A mutants. These 147 peaks are matched to 69 genes, which are candidate common target genes of HP1a and dKDM4A (Figure 5-4A and Table 5-3). Among the 69 genes, 55 genes are located at heterochromatic regions, including 4 genes at the 4th chromosome (Figure 5-4B and C), while 7 genes are located at euchromatic regions (Figure 5-4B and D). There are 7 genes assigned to the chromosome U, which contains unmapped heterochromatic sequences (Hoskins et al., 2007) (Figure 5-4B). These data suggest that dKDM4A-HP1a complex may function in regulation of the level of H3K36me3 at heterochromatin.

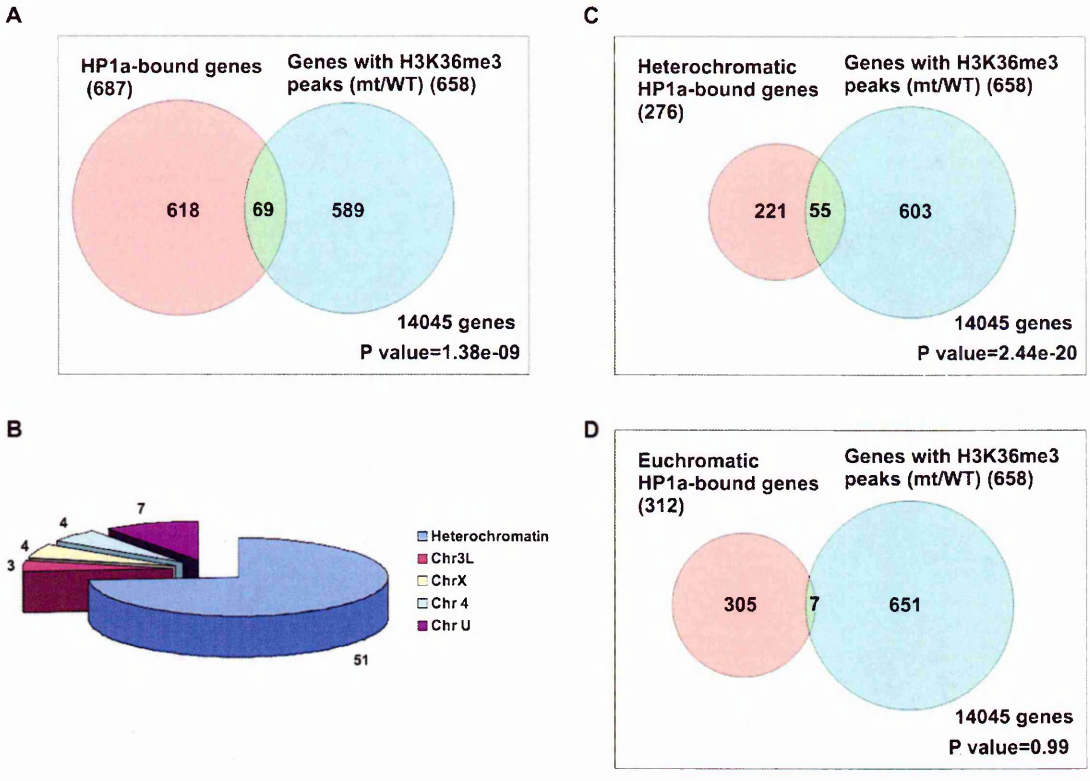

Figure 5-4 Identification of Common Target Genes of dKDM4A and HP1a.

(A) The Venn diagram analysis of genes bound by HP1a and genes with increased H3K36me3 levels in the dKDM4A mutant. (B) The localization of HP1a and dKDM4A common target genes. (C-D) The Venn diagram analysis of heterochromatic genes (C) or euchromatic genes (D) bound by HP1a and genes with increased H3K36me3 levels in the dKDM4A mutant. Genes assigned to the chromosome U are not included in the analysis.

Table 5-3 Candidate common target genes of dKDM4A and HP1a.

Gene	chr	mt1	mt2	wt1	wt2	fc (mt/WT)	log2 fc
CG17490	chr2Lh	30.86	26.82	33.08	28.21	0.94	-0.09
cta	chr2Lh	23.51	23.79	20.50	21.25	1.13	0.18
lt	chr2Lh	36.23	43.73	42.22	36.77	1.01	0.02
Cht3	chr2Lh	0.89	1.07	0.71	0.64	1.45	0.53 *
CG40006	chr2Lh	8.70	7.07	8.08	7.19	1.03	0.05
CG40040	chr2LHet						
CG10396	chr2Rh	0.78	0.28	0.50	1.10	0.67	-0.59 *
CG17508	chr2Rh	57.64	48.77	64.05	55.22	0.89	-0.16
d4	chr2Rh	225.76	202.03	221.95	193.90	1.03	0.04
CG30438	chr2Rh	1.01	0.88	1.13	1.18	0.82	-0.29 *
CG30440	chr2Rh	10.74	9.57	13.89	11.10	0.81	-0.30
Nipped-A	chr2Rh	20.42	20.01	19.05	17.12	1.12	0.16
Gprk1	chr2Rh	15.45	13.96	21.75	17.25	0.75	-0.41
CG12552	chr2RHet						
Scp1	chr2RHet	2.22	1.89	0.49	0.50	4.17	2.06 *
CG17514	chr2RHet	46.64	42.72	38.01	33.81	1.24	0.32
Haspin	chr2RHet	56.73	49.71	61.90	50.86	0.94	-0.08
CG40084	chr2RHet						
CG40085	chr2RHet						
CG40211	chr2RHet						
CG40212	chr2RHet						
CG40263	chr2RHet	1.70	1.83	2.59	2.13	0.75	-0.42 *
CG40270	chr2RHet						
CG40461	chr2RHet						
CG40498	chr2RHet	0.73	0.39	0.43	0.48	1.24	0.31 *
CG41233	chr2RHet						
CG41265	chr2RHet	1.70	1.52	1.06	1.15	1.45	0.54 *
CG41323	chr2RHet						
CG41595	chr2RHet						
Aplip1	chr3L	0.15	0.23	0.08	0.11	2.01	1.01 *
nAcRalpha	chr3Lh	8.82	8.29	10.80	10.76	0.79	-0.33
nvd	chr3Lh	0.91	0.72	2.84	2.14	0.33	-1.61 *
CG40053	chr3Lh	0.42	0.28	0.18	0.40	1.22	0.29 *
Snap25	chr3Lh	1.35	1.18	1.24	0.13	1.84	0.88 *
Lsp1gamma	chr3L	0.65	0.69	0.82	0.75	0.85	-0.24 *
CG9149	chr3L	1.72	2.12	2.16	2.11	0.90	-0.16 *
Dbp80	chr3LHet	83.60	69.28	95.19	76.48	0.89	-0.17
CG17374	chr3LHet	1.28	1.30	1.75	1.37	0.83	-0.27 *
CG40178	chr3LHet	5.54	5.00	9.12	7.59	0.63	-0.66
CG40337	chr3LHet						
CG40413	chr3LHet						
CG41050	chr3LHet						
CG41283	chr3LHet						
CG41348	chr3LHet						
CG15831	chr3RHet	NA	0.04	0.08	0.08	0.49	-1.02 *
CG40158	chr3RHet						
CG40368	chr3RHet						
CG41075	chr3RHet						
CG41133	chr3RHet						
CG41249	chr3RHet						
CG41286	chr3RHet						
CG41300	chr3RHet						
CG41335	chr3RHet						
Pur-alpha	chr4	10.74	9.49	12.98	11.63	0.82	-0.28

bt	chr4	1.04	0.83	0.62	0.37	1.89	0.91 *
CG33521	chr4	0.90	0.92	0.75	0.83	1.15	0.20 *
Caps	chr4	2.70	2.38	4.11	3.33	0.68	-0.55
CG17626	chrU						
CG40091	chrU						
CG40195	chrU						
CG40378	chrU	0.26	0.09	0.13	0.04	1.97	0.98 *
CG41087	chrU						
CG41327	chrU						
CG41520	chrU	0.51	0.57	0.47	0.55	1.07	0.10 *
Flo-2	chrX	26.98	27.42	24.37	22.33	1.16	0.22
drd	chrX	0.64	0.73	0.47	0.27	1.85	0.89 *
wupA	chrX	18.62	13.92	8.79	7.65	1.98	0.98
CG9518	chrX						
kl-5	chrYHet						

- mt1, mt2, WT1 and WT2 represent FPKM value of RNA-seq analysis from two biological repeats of dKDM4A mutant and wild-type embryos.
- Asterisks indicate FPKM ≤ 3. These genes were excluded from the differential gene expression analysis.
- fc: fold change, average FPKM mt/WT

5.6 Regulation of H3K36me3 Levels at Specific Heterochromatic Genes by dKDM4A

The ChIP profile of increased H3K36me3 (mt/WT) is highly correlated with the distribution of HP1a at heterochromatic genes (Figure 5-5). To ensure the results we observed is not due to a second mutation or additional insertions of the P element within the genome, I carried out another rescue experiment, in which FLAG-tagged dKDM4A is expressed under the control of its endogenous promoter in the dKDM4A mutant fly line (Figure 5-6A). In the FLAG-dKDM4A rescued fly line, the expression of dKDM4A is restored to the endogenous level as examined by real-time RT-PCR and western blot analysis (Figure 5-6B and C, upper panel). The level of histone H3K36me3 is also recued in the FLAG-dKDM4A expressing fly line (Figure 5-6C, lower panel).

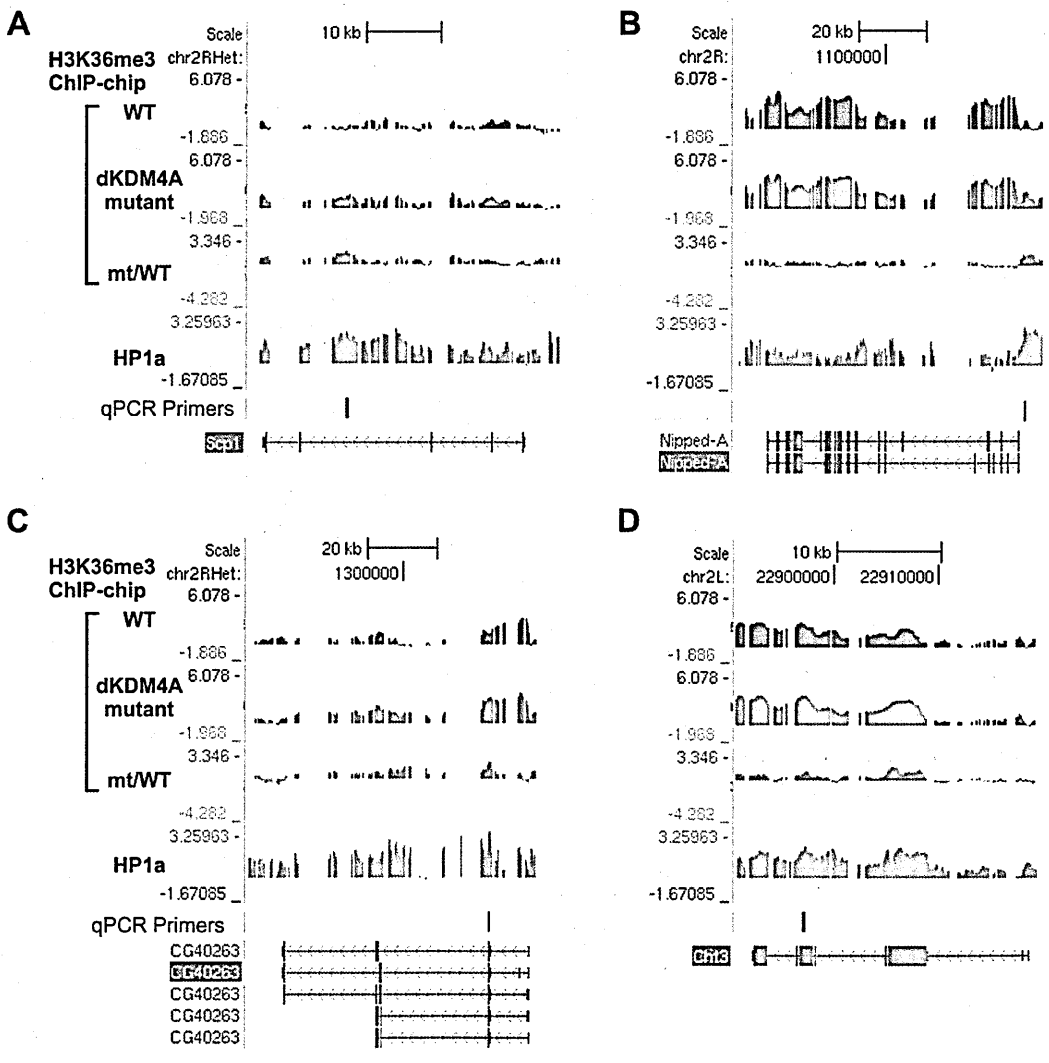

Figure 5-5 HP1a-bound heterochromatic genes show increased H3K36me3 levels in the dKDM4A mutant.

H3K36me3 ChIP-chip profiles of four HP1a-bound genes, Scp1 (A), Nipped-A (B), CG40263 (C) and cht3 (D). The profile of H3K36me3 ChIP in wild type is shown in blue and the profile of H3K36me3 ChIP in the dKDM4A mutant is shown in red. The profile of increased H3K36me3 levels (mt/WT) is shown in green. The enrichment of HP1a is shown in brown. The location of primers used in Figure 5-7 are indicated in the panel of qPCR primers.

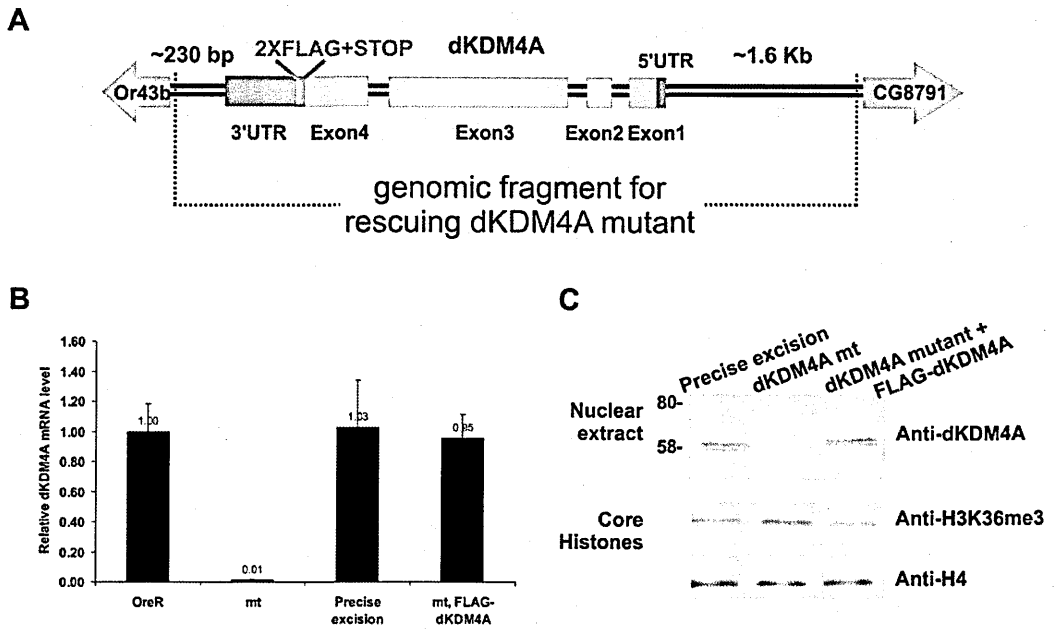

Figure 5-6 Rescue of the dKDM4A mutant by expressing FLAG-dDM4A in mutant flies.

(A) Schematic representation of the genomic fragment used for rescuing the dKDM4A mutant.
(B) Relative mRNA levels of dKDM4A in embryos of OreR, dKDM4A mutants, precise excision- and FLAG-dKDM4A-rescued fly lines. The mRNA level of dKDM4A was determined by real-time RT-PCR and normalized to rp49. The result was shown as relative dKDM4A expression level compared to OreR. The error bars represent standard deviation from 3 biological repeats.
(C) Nuclear extracts and acid-extracted histones from embryos of dKDM4A mutants, precise excision- and FLAG-dKDM4A-rescued fly lines were analyzed by western blot using indicated antibodies.

To examine the regulation of H3K36me3 levels by dKDM4A at heterochromatic genes, I performed ChIP-qPCR of H3K36me3 at putative common target genes of dKDM4A and HP1a in early embryos of yw67c23, dKDM4A mutant and the rescued fly lines. At heterochromatic genes (Scp1, Nipped-A, CG40263 and Cht3), there is an increase of H3K36me3 levels in the absence of dKDM4A. The increased H3K36me3 levels were rescued by expressing FLAG-dKDM4A in mutant embryos. In contrast, the differences of H3K36me3 levels at an intergenic region within chromosome 2L are minimal (Figure 5-

7A). These results suggest that dKDM4A regulates the level of H3K36me3 at HP1a-enriched heterochromatic genes.

I further examined whether the level of HP1a at Scp1, Nipped-A and CG40263 is affected in the absence of dKDM4A. I performed ChIP-qPCR analysis using an antibody against HP1a in early embryos of dKDM4A mutant flies and flies rescued by precise excision of the P element. As shown in Figure 5-7B, there is a slight decrease of HP1a at Scp1 and CG40263 in dKDM4A mutant embryos, and a marginal difference at Nipped-A gene, suggesting that loss of dKDM4A does not affect the recruitment of HP1a to the heterochromatic genes.

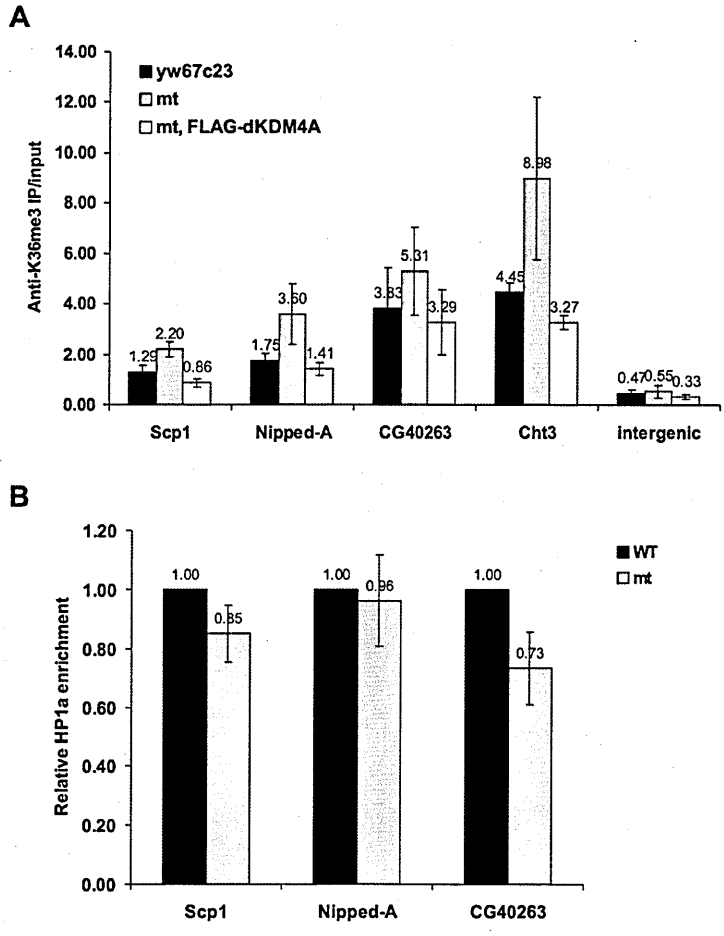

Figure 5-7 The increase of H3K36me3 levels at specific heterochromatic genes can be rescued by expressing FLAG-dKDM4A in the mutants

(A) The increase of H3K36me3 levels at four HP1a-bound heterochromatic genes in dKDM4A mutant embryos was observed by ChIP-qPCR. Expressing FLAG-dKDM4A in the mutant rescued the levels of H3K36me3. The primer set amplifying an intergenic region at chromosome 2L was used as a negative control. The error bars represent standard deviation from 3 biological repeats.
(B) The enrichment of HP1a at Scp1, Nipped-A and CG40263 was examined by HP1a ChIP-qPCR in wild-type and dDKM4A mutant embryos. The result was shown as relative HP1a enrichment compared to the wild type.

5.7 Discussion

In this chapter, I examined the effect of dKDM4A depletion on gene expression in early embryos by RNA-seq analysis. The differential gene expression analysis showed that a small subset of genes display changes in expression levels in the dKDM4A mutant. A recent study of the function of dKDM4A in adult males reveals that the dKDM4A mutant flies has a reduction of life span in males and a male-specific wing twitching phenotype, which is observed in male-male courtship behaviors (Lorbeck et al., 2010). They also found that a longevity-associated *Hsp22* gene and a male-male courtship-related gene, *fruitless (fru),* are downregulated in adult males of the dKDM4A mutant. However, it is not clear whether the expression of *Hsp22* and *fru* is directly regulated by dKDM4A through modulating the level of H3K36me3.

To identify candidate target genes of dKDM4A, I performed K36me3 ChIP-chip in early embryos of dKDM4A mutant and wild type flies. Genes with increased levels of H3K36me3 in the dKDM4A mutants are likely targeted by dKDM4A. Most of these dKDM4A target genes do not show changes in gene expression levels in the absence of dKDM4A in the RNA-seq analysis (Figure5-3). In fact, the role of histone H3K36me3 in regulation of gene transcription levels is not well specified. It was shown that increased H3K36me3 levels cause delayed induction of the HIS4 gene in budding yeast (Nelson et al., 2006). In contrast, loss of H3K36me3 in a mammalian cell line does not affect the kinetics of gene induction or the expression levels of constitutively active genes (Edmunds et al., 2008). They also failed to observe any increased H3 or H4 acetylation, Pol II occupancy, or intragenic transcription at active genes in Setd2-depleted cells. It suggests that H3K36me3 may not be involved in regulation of gene expression, and it may function in different pathways in yeast and in higher eukaryotes.

Through biochemistry approaches, I identified the association of HP1a and dKDM4A. Here I identified the candidate gene targets of the HP1a-dKDM4A complex by comparing

the H3K36me3 ChIP-chip result with the HP1a ChIP-chip data generated by the modENCODE project. I found that among all putative common targets, about 80% of the genes are heterochromatic genes, suggesting that the HP1a-dKDM4A complex may function in heterochromatin. Loss of dKDM4A does not affect the recruitment of HP1a to heterochromatic genes (Figure 5-7B), suggesting that dKDM4A is recruited to heterochromatin by HP1a through a direct interaction. It is also supported by my previous observation, in that a mutant form of HP1a containing a point mutation (V26M) within its chromo domain failed to stimulate the demethylation activity of dKDM4A (Figure 4-7), suggesting that the binding of HP1a to the heterochromatic histone mark, H3K9me2/3, is required for stimulation of dKDM4A demethylation activity. In addition, loss of HP1a in *Drosophila* larvae resulted in increased H3K36me3 levels (Figure 4-11D). Taken together, HP1a may function in recruiting dKDM4A to heterochromatin and regulate the level of H3K36me3 there.

At this point, the function of the HP1a-dKDM4A complex at heterochromatin remains unclear. HP1a was known to be involved in both gene silencing and active transcription. However, the expression levels of most heterochromatic genes targeted by the HP1a-dKDM4A complex were not affected by the loss of dKDM4A. In fact, several heterochromatic loci targeted by the HP1a-dKDM4A complex reside at intergenic regions, suggesting that regulation of H3K36me3 levels may contribute to the structure of the heterochromatin instead of gene transcription. In addition, HP1a was also found to be involved in DNA repair of double-strand breaks (DSBs) at heterochromatin (Dinant and Luijsterburg, 2009; Luijsterburg et al., 2009). A recent study shows that DSBs occurred at heterochromatin are repaired by homologous recombination. An interesting finding is that heterochromatic DSBs move outside of the heterochromatin domain to complete DNA repair mediated by Rad51, preventing recombination among repetitive sequences within heterochromatin. HP1a is required to recruit Smc5/6 complex, which prevents formation of

Rad51 foci within heterochromatin domain (Chiolo et al., 2011). It is possible that the regulation of H3K36me3 levels by the HP1a-dKDM4A complex also contributes to the DNA repair process in heterochromatin.

Chapter 6 Summary and Future Directions

Since the first discovery of the histone demethylase a few years ago, numerous studies have been carried out to explore biochemical and biological functions of dynamic regulation of histone methylation (reviewed in (Cloos et al., 2008; Mosammaparast and Shi, 2010)). Histone demethylases have been found to be involved in cellular differentiation, development, and are linked to several human diseases, suggesting that regulation of histone methylation is critical for cellular processes.

In this thesis, I identified two KDM4 homologs in *Drosophila*, dKDM4A and dKDM4B. Results from both in vitro and in vivo assays showed that dKDM4A is a histone demethylase specific to histone H3K36me3/me2, whereas dKDM4B has histone demethylation activity on both histone H3K9 and K36me3/me2. Through affinity purification of dKDM4A from S2 cells followed by MudPIT analysis, HP1a was identified as a dKDM4A associated protein. I further confirmed that HP1a directly binds to dKDM4A through the CSD of HP1a and the PxVxL motif within dKDM4A. Interestingly, HP1a association stimulates the demethylation activity of dKDM4A. A mutant form of HP1a containing a point mutation (V26M) within the CD, which was known to abolish the binding of HP1a to H3K9me2/3, failed to stimulate the demethylation activity of dKDM4A, suggesting that HP1 binding to histone H3 is required for the enhancement of dKDM4A activity. Loss of HP1a in *Drosophila* larvae resulted in increased levels of H3K36me3, supporting the notion that HP1a is required for dKDM4A-mediated demethylation of H3K36me3.

To examine if loss of dKDM4A affects gene expression, I performed RNA-seq analysis in early embryos of dKDM4A mutant (P element insertion) and wild type (precise excision of P element) fly lines. There is only a small subset of genes showing changes in gene

expression levels. To identify target genes of dKDM4A, I performed H3K36me3 ChIP-chip analysis in early embryos of dKDM4A mutant and wild type fly lines. By comparing the result of H3K36me3 ChIP-chip with RNA-seq analysis, I found that the majority of genes which show changes in gene expression levels in the dKDM4A mutant have no increases in H3K36me3 levels. It suggests that demethylation of H3K36me3 by dKDM4A may not contribute directly to regulation of the genes whose expression was affected. Since I found that HP1a associates with dKDM4A, I next sought to identify common target genes of HP1a and dKDM4A. I found that most of the candidate target genes of HP1a-dKDM4A complex are at heterochromatin. The increase of H3K36me3 levels of these heterochromatic genes in dKDM4A mutants can be rescued by expressing FLAG tagged dKDM4A at the endogenous level. Loss of dKDM4A did not affect the recruitment of HP1a to heterochromatic genes, suggesting that HP1a functions in recruiting dKDM4A to heterochromatin.

Although a global increase of H3K36me3 levels was observed in the dKDM4A mutant, it does not cause any severe phenotype as dKDM4A mutant flies are homozygous viable. It is possible that dKDM4B, a histone H3K9 and K36me2/me3 demethylase, compensates the demethylation of H3K36me3 in the dKDM4A mutant. At this point, the biological functions of dKDM4A and dKDM4A-HP1a complex remain unclear as I will discuss below with future directions of this project.

6.1 The Recruitment of dKDM4A to Heterochromatin by HP1a

Several lines of evidence from my in vitro and in vivo results support the notion that HP1a functions in recruiting dKDM4A to H3K9me2/me3-enriched heterochromatin through direct interaction. The physical association of HP1a stimulates the demethylation activity of dKDM4A. To further support this model, I can test if loss of H3K9 methylation in the Su(var)3-9 mutant results in an increase of H3K36me3 levels. Su(var)3-9 is the

histone methyltransferase which mediates histone H3K9 methylation at heterochromatin (Schotta et al., 2002). Since a H3K9 methyl binding mutant form of HP1a failed to stimulate the demethylation of dKDM4A, H3K9 methylation mediated by Su(var)3-9 may act upstream of regulation of K36me3 levels by dKDM4A-HP1a complex.

The result of H3K36me3 ChIP-chip and ChIP-qPCR showed increased levels of H3K36me3 at heterochromatic genes. Expressing a FLAG-tagged dKDMA in dKDM4A mutant embryos restored the H3K36me3 levels to that in wild-type embryos. To further confirm that the rescue of H3K36me3 levels is resulted from the recruitment of dKDM4A to heterochromatin by HP1a, a mutant form (V423A) of dKDM4A which failed to bind to HP1a can be expressed in the dKDM4A mutant embryos. If the heterochromatic genes are direct targets of dKDM4A-HP1a complex, expressing the mutant form of dKDM4A (V423A) will fail to rescue the increased levels of H3K36me at these genes. I can also perform FLAG ChIP-qPCR at heterochromatic genes in FLAG-dKDM4A or FLAG-dKDM4-V423A expressing embryos. If enrichment of FLAG at heterochromatic genes is lost due to the mutation within PxVxL motif of dKDM4A, it further supports that HP1a is required for recruiting dKDM4A to heterochromatin.

6.2 The Function of HP1a-dKDM4A Complex at Heterochromatin

Despite the fact that there are a subset of HP1a bound heterochromatic genes which show increased levels of H3K36me3 in the dKDM4A mutant, based on RNA-seq analysis, most of the genes bound by HP1 did not show differences in gene expression levels in the dKDM4A mutant compared to the wild type. A few genes, *Scp1*, *nvd* and *wupA*, showed changes in gene expression levels by 1.6 to 2 fold, but were excluded from the differential gene expression analysis due to the cutoff threshold (FPKM $\geq$ 3, fold change >2). At this point, I can not conclude if changes in expression levels of these genes are direct effects of dKDM4A depletion. Since the expression of most heterochromatic genes remains

unchanged in the absence of dKDM4A, it is possible that dKDM4A-HP1a complex functions in other cellular processes. In addition to gene silencing and establishment of heterochromatic structure, HP1a has also been found to function in regulation of DNA replication and DNA repair at heterochromatin (reviewed in (Kwon and Workman, 2011)). A genome-wide study of the role of HP1a in modulating replication timing showed that knockdown of HP1a resulted in delayed replication timing at HP1a target regions, including the 4th chromosome and pericentric regions (Schwaiger et al., 2010). The regulation of H3K36me3 levels by dKDM4A-HP1a complex may contribute to modulate the replication timing at heterochromatin. Interestingly, histone H3K36 methylation has been shown to function as a regulator of the timing of Cdc45 association with replication origins in budding yeast (Pryde et al., 2009). High levels of H3K36me3 were found to be correlated with late replication origins, suggesting a negative role of H3K36 methylation in Cdc45 binding to replication origin. Furthermore, an increase in H3K36me1 and a decrease in H3K36me3 levels at replication origins were observed at the time of Cdc45 binding. It raises a possibility that histone H3K36 demethylases may be involved in activation of replication origins. To test if dKDM4A-HP1a complex is involved in regulation of replication timing at heterochromatin, I can knockdown dKDM4A or HP1a by dsRNA in *Drosophila* cell lines and examine if that results in the same effect on replication timing of heterochromatic genes. Since the levels of H3K36me3 may have a more global effect on replication timing, I can examine if the distribution of dKDM4A (see below) coincides with ORC binding sites which has been identified by modENCODE project (Roy et al., 2010). I can also test if loss of dKDM4A affects the binding of replication factors to replication origins, or results in replication timing defects.

6.3 Identification of Direct Targets of dKDM4A by FLAG ChIP-seq Analysis

In this thesis, I performed H3K36me3 ChIP-chip analysis to identify candidate target genes of dKDM4A. However, it is not the most direct way to identify dKDM4A target sites since there might be a demethylation activity-independent role, or non-histone targets of dKDM4A. To identify dKDM4A target sites, I performed ChIP with antibodies against endogenous dKDM4A. However, the antibodies we generated did not work efficiently in ChIP assays. Alternatively, a FLAG ChIP can be carried out in the rescued dDKM4A mutant embryos in which FLAG-tagged dKDM4A is expressed at endogenous levels (Figure 5-6). This genome-wide dKDM4A distribution revealed by FLAG ChIP-seq analysis can then compare to the H3K36me3 or HP1a ChIP-chip result. It will also be interesting to examine if dKDM4A is present at replication origins as I discussed in the previous section.

REFERENCES

Aagaard, L., Laible, G., Selenko, P., Schmid, M., Dorn, R., Schotta, G., Kuhfittig, S., Wolf, A., Lebersorger, A., Singh, P.B., *et al.* (1999). Functional mammalian homologues of the Drosophila PEV-modifier Su(var)3-9 encode centromere-associated proteins which complex with the heterochromatin component M31. The EMBO journal *18*, 1923-1938.

Aasland, R., and Stewart, A.F. (1995). The chromo shadow domain, a second chromo domain in heterochromatin-binding protein 1, HP1. Nucleic acids research *23*, 3168-3173.

Adhvaryu, K.K., Morris, S.A., Strahl, B.D., and Selker, E.U. (2005). Methylation of histone H3 lysine 36 is required for normal development in Neurospora crassa. Eukaryotic cell *4*, 1455-1464.

Agger, K., Christensen, J., Cloos, P.A., and Helin, K. (2008). The emerging functions of histone demethylases. Current opinion in genetics & development *18*, 159-168.

Agger, K., Cloos, P.A., Christensen, J., Pasini, D., Rose, S., Rappsilber, J., Issaeva, I., Canaani, E., Salcini, A.E., and Helin, K. (2007). UTX and JMJD3 are histone H3K27 demethylases involved in HOX gene regulation and development. Nature *449*, 731-734.

Agger, K., Cloos, P.A., Rudkjaer, L., Williams, K., Andersen, G., Christensen, J., and Helin, K. (2009). The H3K27me3 demethylase JMJD3 contributes to the activation of the INK4A-ARF locus in response to oncogene- and stress-induced senescence. Genes & development *23*, 1171-1176.

Allan, J., Staynov, D.Z., and Gould, H. (1980). Reversible dissociation of linker histone from chromatin with preservation of internucleosomal repeat. Proceedings of the National Academy of Sciences of the United States of America *77*, 885-889.

Allfrey, V.G., Faulkner, R., and Mirsky, A.E. (1964). Acetylation and Methylation of Histones and Their Possible Role in the Regulation of Rna Synthesis. Proceedings of the National Academy of Sciences of the United States of America *51*, 786-794.

Andersson, R., Enroth, S., Rada-Iglesias, A., Wadelius, C., and Komorowski, J. (2009). Nucleosomes are well positioned in exons and carry characteristic histone modifications. Genome Res *19*, 1732-1741.

Aravind, L., and Iyer, L.M. (2002). The SWIRM domain: a conserved module found in chromosomal proteins points to novel chromatin-modifying activities. Genome Biol *3*, RESEARCH0039.

Arents, G., Burlingame, R.W., Wang, B.C., Love, W.E., and Moudrianakis, E.N. (1991). The nucleosomal core histone octamer at 3.1 A resolution: a tripartite protein assembly and a left-handed superhelix. Proceedings of the National Academy of Sciences of the United States of America *88*, 10148-10152.

Arents, G., and Moudrianakis, E.N. (1995). The histone fold: a ubiquitous architectural motif utilized in DNA compaction and protein dimerization. Proceedings of the National Academy of Sciences of the United States of America *92*, 11170-11174.

Ausio, J., and van Holde, K.E. (1986). Histone hyperacetylation: its effects on nucleosome conformation and stability. Biochemistry *25*, 1421-1428.

Badugu, R., Yoo, Y., Singh, P.B., and Kellum, R. (2005). Mutations in the heterochromatin protein 1 (HP1) hinge domain affect HP1 protein interactions and chromosomal distribution. Chromosoma *113*, 370-384.

Balciunas, D., and Ronne, H. (2000). Evidence of domain swapping within the jumonji family of transcription factors. Trends Biochem Sci *25*, 274-276.

Bannister, A.J., Schneider, R., and Kouzarides, T. (2002). Histone methylation: dynamic or static? Cell *109*, 801-806.

Bannister, A.J., Schneider, R., Myers, F.A., Thorne, A.W., Crane-Robinson, C., and Kouzarides, T. (2005). Spatial distribution of di- and tri-methyl lysine 36 of histone H3 at active genes. The Journal of biological chemistry *280*, 17732-17736.

Bannister, A.J., Zegerman, P., Partridge, J.F., Miska, E.A., Thomas, J.O., Allshire, R.C., and Kouzarides, T. (2001). Selective recognition of methylated lysine 9 on histone H3 by the HP1 chromo domain. Nature *410*, 120-124.

Barradas, M., Anderton, E., Acosta, J.C., Li, S., Banito, A., Rodriguez-Niedenfuhr, M., Maertens, G., Banck, M., Zhou, M.M., Walsh, M.J., *et al.* (2009). Histone demethylase JMJD3 contributes to epigenetic control of INK4a/ARF by oncogenic RAS. Genes & development *23*, 1177-1182.

Bell, O., Conrad, T., Kind, J., Wirbelauer, C., Akhtar, A., and Schubeler, D. (2008). Transcription-coupled methylation of histone H3 at lysine 36 regulates dosage compensation by enhancing recruitment of the MSL complex in Drosophila melanogaster. Molecular and cellular biology *28*, 3401-3409.

Bell, O., Wirbelauer, C., Hild, M., Scharf, A.N., Schwaiger, M., MacAlpine, D.M., Zilbermann, F., van Leeuwen, F., Bell, S.P., Imhof, A., *et al.* (2007). Localized H3K36 methylation states define histone H4K16 acetylation during transcriptional elongation in Drosophila. The EMBO journal *26*, 4974-4984.

Belmont, A.S., Sedat, J.W., and Agard, D.A. (1987). A three-dimensional approach to mitotic chromosome structure: evidence for a complex hierarchical organization. The Journal of cell biology *105*, 77-92.

Benevolenskaya, E.V., Murray, H.L., Branton, P., Young, R.A., and Kaelin, W.G., Jr. (2005). Binding of pRB to the PHD protein RBP2 promotes cellular differentiation. Molecular cell *18*, 623-635.

Benjamini, Y., Hochberg, Y. (1995) Controlling the false discovery rate: a practical and powerful approach to multiple testing. Journal of the Royal Statistical Society, Series B, 57, 289-300.

Berger, S.L. (2007). The complex language of chromatin regulation during transcription. Nature *447*, 407-412.

Blackledge, N.P., Zhou, J.C., Tolstorukov, M.Y., Farcas, A.M., Park, P.J., and Klose, R.J. (2010). CpG islands recruit a histone H3 lysine 36 demethylase. Molecular cell *38*, 179-190.

Blatch, G.L., and Lassle, M. (1999). The tetratricopeptide repeat: a structural motif mediating protein-protein interactions. Bioessays *21*, 932-939.

Borun, T.W., Pearson, D., and Paik, W.K. (1972). Studies of histone methylation during the HeLa S-3 cell cycle. The Journal of biological chemistry *247*, 4288-4298.

Bose, J., Gruber, A.D., Helming, L., Schiebe, S., Wegener, I., Hafner, M., Beales, M., Kontgen, F., and Lengeling, A. (2004). The phosphatidylserine receptor has essential functions during embryogenesis but not in apoptotic cell removal. J Biol *3*, 15.

Brand, A.H., and Perrimon, N. (1993). Targeted gene expression as a means of altering cell fates and generating dominant phenotypes. Development (Cambridge, England) *118*, 401-415.

Brasher, S.V., Smith, B.O., Fogh, R.H., Nietlispach, D., Thiru, A., Nielsen, P.R., Broadhurst, R.W., Ball, L.J., Murzina, N.V., and Laue, E.D. (2000). The structure of mouse HP1 suggests a unique mode of single peptide recognition by the shadow chromo domain dimer. The EMBO journal *19*, 1587-1597.

Brownell, J.E., and Allis, C.D. (1996). Special HATs for special occasions: linking histone acetylation to chromatin assembly and gene activation. Current opinion in genetics & development *6*, 176-184.

Brownell, J.E., Zhou, J., Ranalli, T., Kobayashi, R., Edmondson, D.G., Roth, S.Y., and Allis, C.D. (1996). Tetrahymena histone acetyltransferase A: a homolog to yeast Gcn5p linking histone acetylation to gene activation. Cell *84*, 843-851.

Burlingame, R.W., Love, W.E., Wang, B.C., Hamlin, R., Nguyen, H.X., and Moudrianakis, E.N. (1985). Crystallographic structure of the octameric histone core of the nucleosome at a resolution of 3.3 A. Science (New York, N.Y *228*, 546-553.

Byvoet, P. (1972). In vivo turnover and distribution of radio-N-methyl in arginine-rich histones from rat tissues. Arch Biochem Biophys *152*, 887-888.

Cao, R., Tsukada, Y., and Zhang, Y. (2005). Role of Bmi-1 and Ring1A in H2A ubiquitylation and Hox gene silencing. Molecular cell *20*, 845-854.

Cao, R., Wang, L., Wang, H., Xia, L., Erdjument-Bromage, H., Tempst, P., Jones, R.S., and Zhang, Y. (2002). Role of histone H3 lysine 27 methylation in Polycomb-group silencing. Science (New York, N.Y *298*, 1039-1043.

Cao, R., and Zhang, Y. (2004). The functions of E(Z)/EZH2-mediated methylation of lysine 27 in histone H3. Current opinion in genetics & development *14*, 155-164.

Carrozza, M.J., Li, B., Florens, L., Suganuma, T., Swanson, S.K., Lee, K.K., Shia, W.J., Anderson, S., Yates, J., Washburn, M.P., and Workman, J.L. (2005). Histone H3 methylation by Set2 directs deacetylation of coding regions by Rpd3S to suppress spurious intragenic transcription. Cell *123*, 581-592.

Carrozza, M.J., Utley, R.T., Workman, J.L., and Cote, J. (2003). The diverse functions of histone acetyltransferase complexes. Trends Genet *19*, 321-329.

Carruthers, L.M., Bednar, J., Woodcock, C.L., and Hansen, J.C. (1998). Linker histones stabilize the intrinsic salt-dependent folding of nucleosomal arrays: mechanistic ramifications for higher-order chromatin folding. Biochemistry *37*, 14776-14787.

Carruthers, L.M., and Hansen, J.C. (2000). The core histone N termini function independently of linker histones during chromatin condensation. The Journal of biological chemistry *275*, 37285-37290.

Celeste, A., Petersen, S., Romanienko, P.J., Fernandez-Capetillo, O., Chen, H.T., Sedelnikova, O.A., Reina-San-Martin, B., Coppola, V., Meffre, E., Difilippantonio, M.J., *et al.* (2002). Genomic instability in mice lacking histone H2AX. Science (New York, N.Y *296*, 922-927.

Cenciarelli, C., Chiaur, D.S., Guardavaccaro, D., Parks, W., Vidal, M., and Pagano, M. (1999). Identification of a family of human F-box proteins. Curr Biol *9*, 1177-1179.

Chang, B., Chen, Y., Zhao, Y., and Bruick, R.K. (2007). JMJD6 is a histone arginine demethylase. Science (New York, N.Y *318*, 444-447.

Chen, H.Y., Sun, J.M., Zhang, Y., Davie, J.R., and Meistrich, M.L. (1998). Ubiquitination of histone H3 in elongating spermatids of rat testes. The Journal of biological chemistry *273*, 13165-13169.

Chiolo, I., Minoda, A., Colmenares, S.U., Polyzos, A., Costes, S.V., and Karpen, G.H. (2011). Double-Strand Breaks in Heterochromatin Move Outside of a Dynamic HP1a Domain to Complete Recombinational Repair. Cell *144*, 732-744.

Cho, Y.W., Hong, T., Hong, S., Guo, H., Yu, H., Kim, D., Guszczynski, T., Dressler, G.R., Copeland, T.D., Kalkum, M., and Ge, K. (2007). PTIP associates with MLL3- and MLL4-containing histone H3 lysine 4 methyltransferase complex. The Journal of biological chemistry *282*, 20395-20406.

Christensen, J., Agger, K., Cloos, P.A., Pasini, D., Rose, S., Sennels, L., Rappsilber, J., Hansen, K.H., Salcini, A.E., and Helin, K. (2007). RBP2 belongs to a family of demethylases, specific for tri-and dimethylated lysine 4 on histone 3. Cell *128*, 1063-1076.

Clissold, P.M., and Ponting, C.P. (2001). JmjC: cupin metalloenzyme-like domains in jumonji, hairless and phospholipase A2beta. Trends Biochem Sci *26*, 7-9.

Cloos, P.A., Christensen, J., Agger, K., and Helin, K. (2008). Erasing the methyl mark: histone demethylases at the center of cellular differentiation and disease. Genes & development *22*, 1115-1140.

Cloos, P.A., Christensen, J., Agger, K., Maiolica, A., Rappsilber, J., Antal, T., Hansen, K.H., and Helin, K. (2006). The putative oncogene GASC1 demethylates tri- and dimethylated lysine 9 on histone H3. Nature *442*, 307-311.

Cowieson, N.P., Partridge, J.F., Allshire, R.C., and McLaughlin, P.J. (2000). Dimerisation of a chromo shadow domain and distinctions from the chromodomain as revealed by structural analysis. Curr Biol *10*, 517-525.

Cryderman, D.E., Grade, S.K., Li, Y., Fanti, L., Pimpinelli, S., and Wallrath, L.L. (2005). Role of Drosophila HP1 in euchromatic gene expression. Dev Dyn *232*, 767-774.

Cryderman, D.E., Tang, H., Bell, C., Gilmour, D.S., and Wallrath, L.L. (1999). Heterochromatic silencing of Drosophila heat shock genes acts at the level of promoter potentiation. Nucleic acids research *27*, 3364-3370.

Czermin, B., Melfi, R., McCabe, D., Seitz, V., Imhof, A., and Pirrotta, V. (2002). Drosophila enhancer of Zeste/ESC complexes have a histone H3 methyltransferase activity that marks chromosomal Polycomb sites. Cell *111*, 185-196.

Czermin, B., Schotta, G., Hulsmann, B.B., Brehm, A., Becker, P.B., Reuter, G., and Imhof, A. (2001). Physical and functional association of SU(VAR)3-9 and HDAC1 in Drosophila. EMBO Rep *2*, 915-919.

Danzer, J.R., and Wallrath, L.L. (2004). Mechanisms of HP1-mediated gene silencing in Drosophila. Development (Cambridge, England) *131*, 3571-3580.

De Lucia, F., Ni, J.Q., Vaillant, C., and Sun, F.L. (2005). HP1 modulates the transcription of cell-cycle regulators in Drosophila melanogaster. Nucleic acids research *33*, 2852-2858.

De Santa, F., Totaro, M.G., Prosperini, E., Notarbartolo, S., Testa, G., and Natoli, G. (2007). The histone H3 lysine-27 demethylase Jmjd3 links inflammation to inhibition of polycomb-mediated gene silencing. Cell *130*, 1083-1094.

de Wit, E., Greil, F., and van Steensel, B. (2007). High-resolution mapping reveals links of HP1 with active and inactive chromatin components. PLoS Genet *3*, e38.

Defeo-Jones, D., Huang, P.S., Jones, R.E., Haskell, K.M., Vuocolo, G.A., Hanobik, M.G., Huber, H.E., and Oliff, A. (1991). Cloning of cDNAs for cellular proteins that bind to the retinoblastoma gene product. Nature *352*, 251-254.

Dhami, P., Saffrey, P., Bruce, A.W., Dillon, S.C., Chiang, K., Bonhoure, N., Koch, C.M., Bye, J., James, K., Foad, N.S., *et al.* (2010). Complex exon-intron marking by histone modifications is not determined solely by nucleosome distribution. PLoS One *5*, e12339.

Dinant, C., and Luijsterburg, M.S. (2009). The emerging role of HP1 in the DNA damage response. Molecular and cellular biology *29*, 6335-6340.

Dou, Y., Bowen, J., Liu, Y., and Gorovsky, M.A. (2002). Phosphorylation and an ATP-dependent process increase the dynamic exchange of H1 in chromatin. The Journal of cell biology *158*, 1161-1170.

Dou, Y., and Gorovsky, M.A. (2002). Regulation of transcription by H1 phosphorylation in Tetrahymena is position independent and requires clustered sites. Proceedings of the National Academy of Sciences of the United States of America *99*, 6142-6146.

Downs, J.A., Lowndes, N.F., and Jackson, S.P. (2000). A role for Saccharomyces cerevisiae histone H2A in DNA repair. Nature *408*, 1001-1004.

Drouin, S., Laramee, L., Jacques, P.E., Forest, A., Bergeron, M., and Robert, F. (2010). DSIF and RNA polymerase II CTD phosphorylation coordinate the recruitment of Rpd3S to actively transcribed genes. PLoS Genet *6*, e1001173.

Edmondson, D.G., Davie, J.K., Zhou, J., Mirnikjoo, B., Tatchell, K., and Dent, S.Y. (2002). Site-specific loss of acetylation upon phosphorylation of histone H3. The Journal of biological chemistry *277*, 29496-29502.

Edmunds, J.W., Mahadevan, L.C., and Clayton, A.L. (2008). Dynamic histone H3 methylation during gene induction: HYPB/Setd2 mediates all H3K36 trimethylation. The EMBO journal *27*, 406-420.

Eissenberg, J.C., James, T.C., Foster-Hartnett, D.M., Hartnett, T., Ngan, V., and Elgin, S.C. (1990). Mutation in a heterochromatin-specific chromosomal protein is associated with suppression of position-effect variegation in Drosophila melanogaster. Proceedings of the National Academy of Sciences of the United States of America *87*, 9923-9927.

Fang, J., Feng, Q., Ketel, C.S., Wang, H., Cao, R., Xia, L., Erdjument-Bromage, H., Tempst, P., Simon, J.A., and Zhang, Y. (2002). Purification and functional characterization of SET8, a nucleosomal histone H4-lysine 20-specific methyltransferase. Curr Biol *12*, 1086-1099.

Fang, J., Hogan, G.J., Liang, G., Lieb, J.D., and Zhang, Y. (2007). The Saccharomyces cerevisiae histone demethylase Jhd1 fine-tunes the distribution of H3K36me2. Molecular and cellular biology *27*, 5055-5065.

Fanti, L., Berloco, M., Piacentini, L., and Pimpinelli, S. (2003). Chromosomal distribution of heterochromatin protein 1 (HP1) in Drosophila: a cytological map of euchromatic HP1 binding sites. Genetica *117*, 135-147.

Fanti, L., Giovinazzo, G., Berloco, M., and Pimpinelli, S. (1998). The heterochromatin protein 1 prevents telomere fusions in Drosophila. Molecular cell *2*, 527-538.

Feng, Q., Wang, H., Ng, H.H., Erdjument-Bromage, H., Tempst, P., Struhl, K., and Zhang, Y. (2002). Methylation of H3-lysine 79 is mediated by a new family of HMTases without a SET domain. Curr Biol *12*, 1052-1058.

Fischle, W., Tseng, B.S., Dormann, H.L., Ueberheide, B.M., Garcia, B.A., Shabanowitz, J., Hunt, D.F., Funabiki, H., and Allis, C.D. (2005). Regulation of HP1-chromatin binding by histone H3 methylation and phosphorylation. Nature *438*, 1116-1122.

Fodor, B.D., Kubicek, S., Yonezawa, M., O'Sullivan, R.J., Sengupta, R., Perez-Burgos, L., Opravil, S., Mechtler, K., Schotta, G., and Jenuwein, T. (2006). Jmjd2b antagonizes H3K9 trimethylation at pericentric heterochromatin in mammalian cells. Genes & development *20*, 1557-1562.

Frescas, D., Guardavaccaro, D., Bassermann, F., Koyama-Nasu, R., and Pagano, M. (2007). JHDM1B/FBXL10 is a nucleolar protein that represses transcription of ribosomal RNA genes. Nature *450*, 309-313.

Goldknopf, I.L., Taylor, C.W., Baum, R.M., Yeoman, L.C., Olson, M.O., Prestayko, A.W., and Busch, H. (1975). Isolation and characterization of protein A24, a "histone-like" non-histone chromosomal protein. The Journal of biological chemistry *250*, 7182-7187.

Goto, H., Tomono, Y., Ajiro, K., Kosako, H., Fujita, M., Sakurai, M., Okawa, K., Iwamatsu, A., Okigaki, T., Takahashi, T., and Inagaki, M. (1999). Identification of a novel phosphorylation site on histone H3 coupled with mitotic chromosome condensation. The Journal of biological chemistry *274*, 25543-25549.

Govind, C.K., Qiu, H., Ginsburg, D.S., Ruan, C., Hofmeyer, K., Hu, C., Swaminathan, V., Workman, J.L., Li, B., and Hinnebusch, A.G. (2010). Phosphorylated Pol II CTD recruits multiple HDACs, including Rpd3C(S), for methylation-dependent deacetylation of ORF nucleosomes. Molecular cell *39*, 234-246.

Gray, S.G., Iglesias, A.H., Lizcano, F., Villanueva, R., Camelo, S., Jingu, H., Teh, B.T., Koibuchi, N., Chin, W.W., Kokkotou, E., and Dangond, F. (2005). Functional characterization of JMJD2A, a histone deacetylase- and retinoblastoma-binding protein. The Journal of biological chemistry *280*, 28507-28518.

Guelman, S., Suganuma, T., Florens, L., Swanson, S.K., Kiesecker, C.L., Kusch, T., Anderson, S., Yates, J.R., 3rd, Washburn, M.P., Abmayr, S.M., and Workman, J.L. (2006a). Host cell factor and an uncharacterized SANT domain protein are stable components of ATAC, a novel dAda2A/dGcn5-containing histone acetyltransferase complex in Drosophila. Molecular and cellular biology *26*, 871-882.

Guelman, S., Suganuma, T., Florens, L., Weake, V., Swanson, S.K., Washburn, M.P., Abmayr, S.M., and Workman, J.L. (2006b). The essential gene wda encodes a WD40 repeat subunit of Drosophila SAGA required for histone H3 acetylation. Molecular and cellular biology *26*, 7178-7189.

Hakimi, M.A., Bochar, D.A., Chenoweth, J., Lane, W.S., Mandel, G., and Shiekhattar, R. (2002). A core-BRAF35 complex containing histone deacetylase mediates repression of neuronal-specific genes. Proceedings of the National Academy of Sciences of the United States of America *99*, 7420-7425.

Hayes, J.J., Pruss, D., and Wolffe, A.P. (1994). Contacts of the globular domain of histone H5 and core histones with DNA in a "chromatosome". Proceedings of the National Academy of Sciences of the United States of America *91*, 7817-7821.

He, J., Kallin, E.M., Tsukada, Y., and Zhang, Y. (2008). The H3K36 demethylase Jhdm1b/Kdm2b regulates cell proliferation and senescence through p15(Ink4b). Nature structural & molecular biology *15*, 1169-1175.

Hebbes, T.R., Clayton, A.L., Thorne, A.W., and Crane-Robinson, C. (1994). Core histone hyperacetylation co-maps with generalized DNase I sensitivity in the chicken beta-globin chromosomal domain. The EMBO journal *13*, 1823-1830.

Hebbes, T.R., Thorne, A.W., and Crane-Robinson, C. (1988). A direct link between core histone acetylation and transcriptionally active chromatin. The EMBO journal *7*, 1395-1402.

Hicke, L. (2001). Protein regulation by monoubiquitin. Nature reviews *2*, 195-201.

Hochstrasser, M. (1996). Ubiquitin-dependent protein degradation. Annu Rev Genet *30*, 405-439.

Hon, G., Wang, W., and Ren, B. (2009). Discovery and annotation of functional chromatin signatures in the human genome. PLoS Comput Biol *5*, e1000566.

Hong, L., Schroth, G.P., Matthews, H.R., Yau, P., and Bradbury, E.M. (1993). Studies of the DNA binding properties of histone H4 amino terminus. Thermal denaturation studies reveal that acetylation markedly reduces the binding constant of the H4 "tail" to DNA. The Journal of biological chemistry *268*, 305-314.

Hoog, C., Schalling, M., Grunder-Brundell, E., and Daneholt, B. (1991). Analysis of a murine male germ cell-specific transcript that encodes a putative zinc finger protein. Mol Reprod Dev *30*, 173-181.

Horn, P.J., and Peterson, C.L. (2002). Molecular biology. Chromatin higher order folding--wrapping up transcription. Science (New York, N.Y *297*, 1824-1827.

Hoskins, R.A., Carlson, J.W., Kennedy, C., Acevedo, D., Evans-Holm, M., Frise, E., Wan, K.H., Park, S., Mendez-Lago, M., Rossi, F., *et al.* (2007). Sequence finishing and mapping of Drosophila melanogaster heterochromatin. Science (New York, N.Y *316*, 1625-1628.

Hsia, D.A., Tepper, C.G., Pochampalli, M.R., Hsia, E.Y., Izumiya, C., Huerta, S.B., Wright, M.E., Chen, H.W., Kung, H.J., and Izumiya, Y. (2010). KDM8, a H3K36me2 histone demethylase that acts in the cyclin A1 coding region to regulate cancer cell proliferation. Proceedings of the National Academy of Sciences of the United States of America *107*, 9671-9676.

Huang da, W., Sherman, B.T., and Lempicki, R.A. (2009). Systematic and integrative analysis of large gene lists using DAVID bioinformatics resources. Nature protocols *4*, 44-57.

Huyen, Y., Zgheib, O., Ditullio, R.A., Jr., Gorgoulis, V.G., Zacharatos, P., Petty, T.J., Sheston, E.A., Mellert, H.S., Stavridi, E.S., and Halazonetis, T.D. (2004). Methylated lysine 79 of histone H3 targets 53BP1 to DNA double-strand breaks. Nature *432*, 406-411.

Hwang, W.W., Venkatasubrahmanyam, S., Ianculescu, A.G., Tong, A., Boone, C., and Madhani, H.D. (2003). A conserved RING finger protein required for histone H2B monoubiquitination and cell size control. Molecular cell *11*, 261-266.

Iizuka, M., and Smith, M.M. (2003). Functional consequences of histone modifications. Current opinion in genetics & development *13*, 154-160.

Issaeva, I., Zonis, Y., Rozovskaia, T., Orlovsky, K., Croce, C.M., Nakamura, T., Mazo, A., Eisenbach, L., and Canaani, E. (2007). Knockdown of ALR (MLL2) reveals ALR target genes and leads to alterations in cell adhesion and growth. Molecular and cellular biology *27*, 1889-1903.

Iwase, S., Lan, F., Bayliss, P., de la Torre-Ubieta, L., Huarte, M., Qi, H.H., Whetstine, J.R., Bonni, A., Roberts, T.M., and Shi, Y. (2007). The X-linked mental retardation gene

SMCX/JARID1C defines a family of histone H3 lysine 4 demethylases. Cell *128*, 1077-1088.

Jacobs, S.A., and Khorasanizadeh, S. (2002). Structure of HP1 chromodomain bound to a lysine 9-methylated histone H3 tail. Science (New York, N.Y *295*, 2080-2083.

Jacobs, S.A., Taverna, S.D., Zhang, Y., Briggs, S.D., Li, J., Eissenberg, J.C., Allis, C.D., and Khorasanizadeh, S. (2001). Specificity of the HP1 chromo domain for the methylated N-terminus of histone H3. The EMBO journal *20*, 5232-5241.

James, T.C., Eissenberg, J.C., Craig, C., Dietrich, V., Hobson, A., and Elgin, S.C. (1989). Distribution patterns of HP1, a heterochromatin-associated nonhistone chromosomal protein of Drosophila. European journal of cell biology *50*, 170-180.

Jensen, L.R., Amende, M., Gurok, U., Moser, B., Gimmel, V., Tzschach, A., Janecke, A.R., Tariverdian, G., Chelly, J., Fryns, J.P., *et al.* (2005). Mutations in the JARID1C gene, which is involved in transcriptional regulation and chromatin remodeling, cause X-linked mental retardation. Am J Hum Genet *76*, 227-236.

Jenuwein, T., and Allis, C.D. (2001). Translating the histone code. Science (New York, N.Y *293*, 1074-1080.

Joshi, A.A., and Struhl, K. (2005). Eaf3 chromodomain interaction with methylated H3-K36 links histone deacetylation to Pol II elongation. Molecular cell *20*, 971-978.

Karachentsev, D., Sarma, K., Reinberg, D., and Steward, R. (2005). PR-Set7-dependent methylation of histone H4 Lys 20 functions in repression of gene expression and is essential for mitosis. Genes & development *19*, 431-435.

Kawazu, M., Saso, K., Tong, K.I., McQuire, T., Goto, K., Son, D.O., Wakeham, A., Miyagishi, M., Mak, T.W., and Okada, H. (2011). Histone Demethylase JMJD2B Functions as a Co-Factor of Estrogen Receptor in Breast Cancer Proliferation and Mammary Gland Development. PLoS One *6*, e17830.

Keogh, M.C., Kurdistani, S.K., Morris, S.A., Ahn, S.H., Podolny, V., Collins, S.R., Schuldiner, M., Chin, K., Punna, T., Thompson, N.J., *et al.* (2005). Cotranscriptional set2 methylation of histone H3 lysine 36 recruits a repressive Rpd3 complex. Cell *123*, 593-605.

Kim, T., and Buratowski, S. (2007). Two Saccharomyces cerevisiae JmjC domain proteins demethylate histone H3 Lys36 in transcribed regions to promote elongation. The Journal of biological chemistry *282*, 20827-20835.

Kleine-Kohlbrecher, D., Christensen, J., Vandamme, J., Abarrategui, I., Bak, M., Tommerup, N., Shi, X., Gozani, O., Rappsilber, J., Salcini, A.E., and Helin, K. (2010). A functional link between the histone demethylase PHF8 and the transcription factor ZNF711 in X-linked mental retardation. Molecular cell *38*, 165-178.

Klose, R.J., Gardner, K.E., Liang, G., Erdjument-Bromage, H., Tempst, P., and Zhang, Y. (2007a). Demethylation of histone H3K36 and H3K9 by Rph1: a vestige of an H3K9 methylation system in Saccharomyces cerevisiae? Molecular and cellular biology *27*, 3951-3961.

Klose, R.J., Kallin, E.M., and Zhang, Y. (2006a). JmjC-domain-containing proteins and histone demethylation. Nat Rev Genet *7*, 715-727.

Klose, R.J., Yamane, K., Bae, Y., Zhang, D., Erdjument-Bromage, H., Tempst, P., Wong, J., and Zhang, Y. (2006b). The transcriptional repressor JHDM3A demethylates trimethyl histone H3 lysine 9 and lysine 36. Nature *442*, 312-316.

Klose, R.J., Yan, Q., Tothova, Z., Yamane, K., Erdjument-Bromage, H., Tempst, P., Gilliland, D.G., Zhang, Y., and Kaelin, W.G., Jr. (2007b). The retinoblastoma binding protein RBP2 is an H3K4 demethylase. Cell *128*, 889-900.

Klug, A., Rhodes, D., Smith, J., Finch, J.T., and Thomas, J.O. (1980). A low resolution structure for the histone core of the nucleosome. Nature *287*, 509-516.

Kolasinska-Zwierz, P., Down, T., Latorre, I., Liu, T., Liu, X.S., and Ahringer, J. (2009). Differential chromatin marking of introns and expressed exons by H3K36me3. Nature genetics *41*, 376-381.

Kornberg, R.D., and Lorch, Y. (1999). Twenty-five years of the nucleosome, fundamental particle of the eukaryote chromosome. Cell *98*, 285-294.

Kouzarides, T. (2007). Chromatin modifications and their function. Cell *128*, 693-705.

Krogan, N.J., Kim, M., Tong, A., Golshani, A., Cagney, G., Canadien, V., Richards, D.P., Beattie, B.K., Emili, A., Boone, C., *et al.* (2003). Methylation of histone H3 by Set2 in Saccharomyces cerevisiae is linked to transcriptional elongation by RNA polymerase II. Molecular and cellular biology *23*, 4207-4218.

Kuzmichev, A., Nishioka, K., Erdjument-Bromage, H., Tempst, P., and Reinberg, D. (2002). Histone methyltransferase activity associated with a human multiprotein complex containing the Enhancer of Zeste protein. Genes & development *16*, 2893-2905.

Kwon, S.H., and Workman, J.L. (2011). The changing faces of HP1: From heterochromatin formation and gene silencing to euchromatic gene expression: HP1 acts as a positive regulator of transcription. Bioessays *33*, 280-289.

Lachner, M., O'Carroll, D., Rea, S., Mechtler, K., and Jenuwein, T. (2001). Methylation of histone H3 lysine 9 creates a binding site for HP1 proteins. Nature *410*, 116-120.

Lagarou, A., Mohd-Sarip, A., Moshkin, Y.M., Chalkley, G.E., Bezstarosti, K., Demmers, J.A., and Verrijzer, C.P. (2008). dKDM2 couples histone H2A ubiquitylation to histone H3 demethylation during Polycomb group silencing. Genes & development *22*, 2799-2810.

Lan, F., Bayliss, P.E., Rinn, J.L., Whetstine, J.R., Wang, J.K., Chen, S., Iwase, S., Alpatov, R., Issaeva, I., Canaani, E., *et al.* (2007). A histone H3 lysine 27 demethylase regulates animal posterior development. Nature *449*, 689-694.

Larschan, E., Alekseyenko, A.A., Gortchakov, A.A., Peng, S., Li, B., Yang, P., Workman, J.L., Park, P.J., and Kuroda, M.I. (2007). MSL complex is attracted to genes marked by H3K36 trimethylation using a sequence-independent mechanism. Molecular cell *28*, 121-133.

Latham, J.A., and Dent, S.Y. (2007). Cross-regulation of histone modifications. Nature structural & molecular biology *14*, 1017-1024.

Laumonnier, F., Holbert, S., Ronce, N., Faravelli, F., Lenzner, S., Schwartz, C.E., Lespinasse, J., Van Esch, H., Lacombe, D., Goizet, C., *et al.* (2005). Mutations in PHF8 are associated with X linked mental retardation and cleft lip/cleft palate. J Med Genet *42*, 780-786.

Lee, J.S., Shukla, A., Schneider, J., Swanson, S.K., Washburn, M.P., Florens, L., Bhaumik, S.R., and Shilatifard, A. (2007a). Histone crosstalk between H2B monoubiquitination and H3 methylation mediated by COMPASS. Cell *131*, 1084-1096.

Lee, M.G., Norman, J., Shilatifard, A., and Shiekhattar, R. (2007b). Physical and functional association of a trimethyl H3K4 demethylase and Ring6a/MBLR, a polycomb-like protein. Cell *128*, 877-887.

Lee, M.G., Villa, R., Trojer, P., Norman, J., Yan, K.P., Reinberg, D., Di Croce, L., and Shiekhattar, R. (2007c). Demethylation of H3K27 regulates polycomb recruitment and H2A ubiquitination. Science (New York, N.Y *318*, 447-450.

Lee, M.G., Wynder, C., Cooch, N., and Shiekhattar, R. (2005). An essential role for CoREST in nucleosomal histone 3 lysine 4 demethylation. Nature *437*, 432-435.

Lee, T.I., Johnstone, S.E., and Young, R.A. (2006). Chromatin immunoprecipitation and microarray-based analysis of protein location. Nature protocols *1*, 729-748.

Li, B., Carey, M., and Workman, J.L. (2007a). The role of chromatin during transcription. Cell *128*, 707-719.

Li, B., Gogol, M., Carey, M., Lee, D., Seidel, C., and Workman, J.L. (2007b). Combined action of PHD and chromo domains directs the Rpd3S HDAC to transcribed chromatin. Science (New York, N.Y *316*, 1050-1054.

Li, B., Howe, L., Anderson, S., Yates, J.R., 3rd, and Workman, J.L. (2003). The Set2 histone methyltransferase functions through the phosphorylated carboxyl-terminal domain of RNA polymerase II. The Journal of biological chemistry *278*, 8897-8903.

Li, B., Pattenden, S.G., Lee, D., Gutierrez, J., Chen, J., Seidel, C., Gerton, J., and Workman, J.L. (2005). Preferential occupancy of histone variant H2AZ at inactive promoters influences local histone modifications and chromatin remodeling. Proceedings of the National Academy of Sciences of the United States of America *102*, 18385-18390.

Li, H., Ilin, S., Wang, W., Duncan, E.M., Wysocka, J., Allis, C.D., and Patel, D.J. (2006). Molecular basis for site-specific read-out of histone H3K4me3 by the BPTF PHD finger of NURF. Nature *442*, 91-95.

Li, Y., Kirschmann, D.A., and Wallrath, L.L. (2002). Does heterochromatin protein 1 always follow code? Proceedings of the National Academy of Sciences of the United States of America *99 Suppl 4*, 16462-16469.

Li, Y., Trojer, P., Xu, C.F., Cheung, P., Kuo, A., Drury, W.J., 3rd, Qiao, Q., Neubert, T.A., Xu, R.M., Gozani, O., and Reinberg, D. (2009). The target of the NSD family of histone

lysine methyltransferases depends on the nature of the substrate. The Journal of biological chemistry *284*, 34283-34295.

Liang, C.Y., Hsu, P.H., Chou, D.F., Pan, C.Y., Wang, L.C., Huang, W.C., Tsai, M.D., and Lo, W.S. (2011). The histone H3K36 demethylase Rph1/KDM4 regulates the expression of the photoreactivation gene PHR1. Nucleic acids research.

Liu, G., Bollig-Fischer, A., Kreike, B., van de Vijver, M.J., Abrams, J., Ethier, S.P., and Yang, Z.Q. (2009). Genomic amplification and oncogenic properties of the GASC1 histone demethylase gene in breast cancer. Oncogene *28*, 4491-4500.

Liu, L.P., Ni, J.Q., Shi, Y.D., Oakeley, E.J., and Sun, F.L. (2005). Sex-specific role of Drosophila melanogaster HP1 in regulating chromatin structure and gene transcription. Nature genetics *37*, 1361-1366.

Liu, W., Tanasa, B., Tyurina, O.V., Zhou, T.Y., Gassmann, R., Liu, W.T., Ohgi, K.A., Benner, C., Garcia-Bassets, I., Aggarwal, A.K., *et al.* (2010). PHF8 mediates histone H4 lysine 20 demethylation events involved in cell cycle progression. Nature *466*, 508-512.

Lloret-Llinares, M., Carre, C., Vaquero, A., de Olano, N., and Azorin, F. (2008). Characterization of Drosophila melanogaster JmjC+N histone demethylases. Nucleic acids research *36*, 2852-2863.

Lo, W.S., Duggan, L., Emre, N.C., Belotserkovskya, R., Lane, W.S., Shiekhattar, R., and Berger, S.L. (2001). Snf1--a histone kinase that works in concert with the histone acetyltransferase Gcn5 to regulate transcription. Science (New York, N.Y *293*, 1142-1146.

Lo, W.S., Trievel, R.C., Rojas, J.R., Duggan, L., Hsu, J.Y., Allis, C.D., Marmorstein, R., and Berger, S.L. (2000). Phosphorylation of serine 10 in histone H3 is functionally linked in vitro and in vivo to Gcn5-mediated acetylation at lysine 14. Molecular cell *5*, 917-926.

Loh, Y.H., Zhang, W., Chen, X., George, J., and Ng, H.H. (2007). Jmjd1a and Jmjd2c histone H3 Lys 9 demethylases regulate self-renewal in embryonic stem cells. Genes & development *21*, 2545-2557.

Lomberk, G., Bensi, D., Fernandez-Zapico, M.E., and Urrutia, R. (2006). Evidence for the existence of an HP1-mediated subcode within the histone code. Nat Cell Biol *8*, 407-415.

Lorbeck, M.T., Singh, N., Zervos, A., Dhatta, M., Lapchenko, M., Yang, C., and Elefant, F. (2010). The histone demethylase Dmel\Kdm4A controls genes required for life span and male-specific sex determination in Drosophila. Gene *450*, 8-17.

Lu, B.Y., Emtage, P.C., Duyf, B.J., Hilliker, A.J., and Eissenberg, J.C. (2000). Heterochromatin protein 1 is required for the normal expression of two heterochromatin genes in Drosophila. Genetics *155*, 699-708.

Lu, P.J., Sundquist, K., Baeckstrom, D., Poulsom, R., Hanby, A., Meier-Ewert, S., Jones, T., Mitchell, M., Pitha-Rowe, P., Freemont, P., and Taylor-Papadimitriou, J. (1999). A novel gene (PLU-1) containing highly conserved putative DNA/chromatin binding motifs is specifically up-regulated in breast cancer. The Journal of biological chemistry *274*, 15633-15645.

Lucio-Eterovic, A.K., Singh, M.M., Gardner, J.E., Veerappan, C.S., Rice, J.C., and Carpenter, P.B. (2010). Role for the nuclear receptor-binding SET domain protein 1 (NSD1) methyltransferase in coordinating lysine 36 methylation at histone 3 with RNA polymerase II function. Proceedings of the National Academy of Sciences of the United States of America *107*, 16952-16957.

Luco, R.F., Pan, Q., Tominaga, K., Blencowe, B.J., Pereira-Smith, O.M., and Misteli, T. (2010). Regulation of alternative splicing by histone modifications. Science (New York, N.Y *327*, 996-1000.

Luger, K., Mader, A.W., Richmond, R.K., Sargent, D.F., and Richmond, T.J. (1997). Crystal structure of the nucleosome core particle at 2.8 A resolution. Nature *389*, 251-260.

Luijsterburg, M.S., Dinant, C., Lans, H., Stap, J., Wiernasz, E., Lagerwerf, S., Warmerdam, D.O., Lindh, M., Brink, M.C., Dobrucki, J.W., *et al.* (2009). Heterochromatin protein 1 is recruited to various types of DNA damage. The Journal of cell biology *185*, 577-586.

Madigan, J.P., Chotkowski, H.L., and Glaser, R.L. (2002). DNA double-strand break-induced phosphorylation of Drosophila histone variant H2Av helps prevent radiation-induced apoptosis. Nucleic acids research *30*, 3698-3705.

Mahadevan, L.C., Willis, A.C., and Barratt, M.J. (1991). Rapid histone H3 phosphorylation in response to growth factors, phorbol esters, okadaic acid, and protein synthesis inhibitors. Cell *65*, 775-783.

Maison, C., Bailly, D., Roche, D., de Oca, R.M., Probst, A.V., Vassias, I., Dingli, F., Lombard, B., Loew, D., Quivy, J.P., and Almouzni, G. (2011). SUMOylation promotes de novo targeting of HP1alpha to pericentric heterochromatin. Nature genetics.

Markstein, M., Pitsouli, C., Villalta, C., Celniker, S.E., and Perrimon, N. (2008). Exploiting position effects and the gypsy retrovirus insulator to engineer precisely expressed transgenes. Nature genetics *40*, 476-483.

Martin, C., and Zhang, Y. (2005). The diverse functions of histone lysine methylation. Nature reviews *6*, 838-849.

Metzger, E., Wissmann, M., Yin, N., Muller, J.M., Schneider, R., Peters, A.H., Gunther, T., Buettner, R., and Schule, R. (2005). LSD1 demethylates repressive histone marks to promote androgen-receptor-dependent transcription. Nature *437*, 436-439.

Min, J., Zhang, Y., and Xu, R.M. (2003). Structural basis for specific binding of Polycomb chromodomain to histone H3 methylated at Lys 27. Genes & development *17*, 1823-1828.

Morris, S.A., Shibata, Y., Noma, K., Tsukamoto, Y., Warren, E., Temple, B., Grewal, S.I., and Strahl, B.D. (2005). Histone H3 K36 methylation is associated with transcription elongation in Schizosaccharomyces pombe. Eukaryotic cell *4*, 1446-1454.

Mosammaparast, N., and Shi, Y. (2010). Reversal of histone methylation: biochemical and molecular mechanisms of histone demethylases. Annu Rev Biochem *79*, 155-179.

Muchardt, C., Guilleme, M., Seeler, J.S., Trouche, D., Dejean, A., and Yaniv, M. (2002). Coordinated methyl and RNA binding is required for heterochromatin localization of mammalian HP1alpha. EMBO Rep *3*, 975-981.

Muller, J., Hart, C.M., Francis, N.J., Vargas, M.L., Sengupta, A., Wild, B., Miller, E.L., O'Connor, M.B., Kingston, R.E., and Simon, J.A. (2002). Histone methyltransferase activity of a Drosophila Polycomb group repressor complex. Cell *111*, 197-208.

Nelson, C.J., Santos-Rosa, H., and Kouzarides, T. (2006). Proline isomerization of histone H3 regulates lysine methylation and gene expression. Cell *126*, 905-916.

Ng, H.H., Ciccone, D.N., Morshead, K.B., Oettinger, M.A., and Struhl, K. (2003). Lysine-79 of histone H3 is hypomethylated at silenced loci in yeast and mammalian cells: a potential mechanism for position-effect variegation. Proceedings of the National Academy of Sciences of the United States of America *100*, 1820-1825.

Nielsen, A.L., Oulad-Abdelghani, M., Ortiz, J.A., Remboutsika, E., Chambon, P., and Losson, R. (2001). Heterochromatin formation in mammalian cells: interaction between histones and HP1 proteins. Molecular cell *7*, 729-739.

Nielsen, P.R., Nietlispach, D., Mott, H.R., Callaghan, J., Bannister, A., Kouzarides, T., Murzin, A.G., Murzina, N.V., and Laue, E.D. (2002). Structure of the HP1 chromodomain bound to histone H3 methylated at lysine 9. Nature *416*, 103-107.

Nishioka, K., Rice, J.C., Sarma, K., Erdjument-Bromage, H., Werner, J., Wang, Y., Chuikov, S., Valenzuela, P., Tempst, P., Steward, R., *et al.* (2002). PR-Set7 is a nucleosome-specific methyltransferase that modifies lysine 20 of histone H4 and is associated with silent chromatin. Molecular cell *9*, 1201-1213.

Noll, M., and Kornberg, R.D. (1977). Action of micrococcal nuclease on chromatin and the location of histone H1. J Mol Biol *109*, 393-404.

Northcott, P.A., Nakahara, Y., Wu, X., Feuk, L., Ellison, D.W., Croul, S., Mack, S., Kongkham, P.N., Peacock, J., Dubuc, A., *et al.* (2009). Multiple recurrent genetic events converge on control of histone lysine methylation in medulloblastoma. Nature genetics *41*, 465-472.

Nowak, S.J., and Corces, V.G. (2004). Phosphorylation of histone H3: a balancing act between chromosome condensation and transcriptional activation. Trends Genet *20*, 214-220.

Okada, Y., Scott, G., Ray, M.K., Mishina, Y., and Zhang, Y. (2007). Histone demethylase JHDM2A is critical for Tnp1 and Prm1 transcription and spermatogenesis. Nature *450*, 119-123.

Paro, R., and Hogness, D.S. (1991). The Polycomb protein shares a homologous domain with a heterochromatin-associated protein of Drosophila. Proceedings of the National Academy of Sciences of the United States of America *88*, 263-267.

Parthun, M.R., Widom, J., and Gottschling, D.E. (1996). The major cytoplasmic histone acetyltransferase in yeast: links to chromatin replication and histone metabolism. Cell *87*, 85-94.

Pedersen, M.T., and Helin, K. (2010). Histone demethylases in development and disease. Trends Cell Biol *20*, 662-671.

Pena, P.V., Davrazou, F., Shi, X., Walter, K.L., Verkhusha, V.V., Gozani, O., Zhao, R., and Kutateladze, T.G. (2006). Molecular mechanism of histone H3K4me3 recognition by plant homeodomain of ING2. Nature *442*, 100-103.

Perrini, B., Piacentini, L., Fanti, L., Altieri, F., Chichiarelli, S., Berloco, M., Turano, C., Ferraro, A., and Pimpinelli, S. (2004). HP1 controls telomere capping, telomere elongation, and telomere silencing by two different mechanisms in Drosophila. Molecular cell *15*, 467-476.

Pham, A.D., and Sauer, F. (2000). Ubiquitin-activating/conjugating activity of TAFII250, a mediator of activation of gene expression in Drosophila. Science (New York, N.Y *289*, 2357-2360.

Piacentini, L., Fanti, L., Berloco, M., Perrini, B., and Pimpinelli, S. (2003). Heterochromatin protein 1 (HP1) is associated with induced gene expression in Drosophila euchromatin. The Journal of cell biology *161*, 707-714.

Pokholok, D.K., Harbison, C.T., Levine, S., Cole, M., Hannett, N.M., Lee, T.I., Bell, G.W., Walker, K., Rolfe, P.A., Herbolsheimer, E., *et al.* (2005). Genome-wide map of nucleosome acetylation and methylation in yeast. Cell *122*, 517-527.

Pryde, F., Jain, D., Kerr, A., Curley, R., Mariotti, F.R., and Vogelauer, M. (2009). H3 k36 methylation helps determine the timing of cdc45 association with replication origins. PLoS One *4*, e5882.

Qi, H.H., Sarkissian, M., Hu, G.Q., Wang, Z., Bhattacharjee, A., Gordon, D.B., Gonzales, M., Lan, F., Ongusaha, P.P., Huarte, M., *et al.* (2010). Histone H4K20/H3K9 demethylase PHF8 regulates zebrafish brain and craniofacial development. Nature *466*, 503-507.

Rea, S., Eisenhaber, F., O'Carroll, D., Strahl, B.D., Sun, Z.W., Schmid, M., Opravil, S., Mechtler, K., Ponting, C.P., Allis, C.D., and Jenuwein, T. (2000). Regulation of chromatin structure by site-specific histone H3 methyltransferases. Nature *406*, 593-599.

Rice, J.C., Briggs, S.D., Ueberheide, B., Barber, C.M., Shabanowitz, J., Hunt, D.F., Shinkai, Y., and Allis, C.D. (2003). Histone methyltransferases direct different degrees of methylation to define distinct chromatin domains. Molecular cell *12*, 1591-1598.

Richmond, T.J., Finch, J.T., Rushton, B., Rhodes, D., and Klug, A. (1984). Structure of the nucleosome core particle at 7 A resolution. Nature *311*, 532-537.

Riddle, N.C., Minoda, A., Kharchenko, P.V., Alekseyenko, A.A., Schwartz, Y.B., Tolstorukov, M.Y., Gorchakov, A.A., Jaffe, J.D., Kennedy, C., Linder-Basso, D., *et al.* (2011). Plasticity in patterns of histone modifications and chromosomal proteins in Drosophila heterochromatin. Genome Res *21*, 147-163.

Robzyk, K., Recht, J., and Osley, M.A. (2000). Rad6-dependent ubiquitination of histone H2B in yeast. Science (New York, N.Y *287*, 501-504.

Roy, S., Ernst, J., Kharchenko, P.V., Kheradpour, P., Negre, N., Eaton, M.L., Landolin, J.M., Bristow, C.A., Ma, L., Lin, M.F., *et al.* (2010). Identification of functional elements and regulatory circuits by Drosophila modENCODE. Science (New York, N.Y *330*, 1787-1797.

Sandmann, T., Jakobsen, J.S., and Furlong, E.E. (2006). ChIP-on-chip protocol for genome-wide analysis of transcription factor binding in Drosophila melanogaster embryos. Nature protocols *1*, 2839-2855.

Schaft, D., Roguev, A., Kotovic, K.M., Shevchenko, A., Sarov, M., Shevchenko, A., Neugebauer, K.M., and Stewart, A.F. (2003). The histone 3 lysine 36 methyltransferase, SET2, is involved in transcriptional elongation. Nucleic acids research *31*, 2475-2482.

Schneider, J.E., Bose, J., Bamforth, S.D., Gruber, A.D., Broadbent, C., Clarke, K., Neubauer, S., Lengeling, A., and Bhattacharya, S. (2004). Identification of cardiac malformations in mice lacking Ptdsr using a novel high-throughput magnetic resonance imaging technique. BMC Dev Biol *4*, 16.

Schotta, G., Ebert, A., Krauss, V., Fischer, A., Hoffmann, J., Rea, S., Jenuwein, T., Dorn, R., and Reuter, G. (2002). Central role of Drosophila SU(VAR)3-9 in histone H3-K9 methylation and heterochromatic gene silencing. The EMBO journal *21*, 1121-1131.

Schotta, G., Lachner, M., Sarma, K., Ebert, A., Sengupta, R., Reuter, G., Reinberg, D., and Jenuwein, T. (2004). A silencing pathway to induce H3-K9 and H4-K20 trimethylation at constitutive heterochromatin. Genes & development *18*, 1251-1262.

Schultz, D.C., Ayyanathan, K., Negorev, D., Maul, G.G., and Rauscher, F.J., 3rd (2002). SETDB1: a novel KAP-1-associated histone H3, lysine 9-specific methyltransferase that contributes to HP1-mediated silencing of euchromatic genes by KRAB zinc-finger proteins. Genes & development *16*, 919-932.

Schwaiger, M., Kohler, H., Oakeley, E.J., Stadler, M.B., and Schubeler, D. (2010). Heterochromatin protein 1 (HP1) modulates replication timing of the Drosophila genome. Genome Res *20*, 771-780.

Sen, G.L., Webster, D.E., Barragan, D.I., Chang, H.Y., and Khavari, P.A. (2008). Control of differentiation in a self-renewing mammalian tissue by the histone demethylase JMJD3. Genes & development *22*, 1865-1870.

Shi, X., Hong, T., Walter, K.L., Ewalt, M., Michishita, E., Hung, T., Carney, D., Pena, P., Lan, F., Kaadige, M.R., *et al.* (2006). ING2 PHD domain links histone H3 lysine 4 methylation to active gene repression. Nature *442*, 96-99.

Shi, Y., Lan, F., Matson, C., Mulligan, P., Whetstine, J.R., Cole, P.A., Casero, R.A., and Shi, Y. (2004). Histone demethylation mediated by the nuclear amine oxidase homolog LSD1. Cell *119*, 941-953.

Shi, Y., Sawada, J., Sui, G., Affar el, B., Whetstine, J.R., Lan, F., Ogawa, H., Luke, M.P., and Nakatani, Y. (2003). Coordinated histone modifications mediated by a CtBP co-repressor complex. Nature *422*, 735-738.

Shi, Y.J., Matson, C., Lan, F., Iwase, S., Baba, T., and Shi, Y. (2005). Regulation of LSD1 histone demethylase activity by its associated factors. Molecular cell *19*, 857-864.

Shilatifard, A. (2006). Chromatin modifications by methylation and ubiquitination: implications in the regulation of gene expression. Annu Rev Biochem *75*, 243-269.

Simon, M.D., Chu, F., Racki, L.R., de la Cruz, C.C., Burlingame, A.L., Panning, B., Narlikar, G.J., and Shokat, K.M. (2007). The site-specific installation of methyl-lysine analogs into recombinant histones. Cell *128*, 1003-1012.

Simpson, R.T. (1978). Structure of the chromatosome, a chromatin particle containing 160 base pairs of DNA and all the histones. Biochemistry *17*, 5524-5531.

Smith, C.D., Shu, S., Mungall, C.J., and Karpen, G.H. (2007). The Release 5.1 annotation of Drosophila melanogaster heterochromatin. Science (New York, N.Y *316*, 1586-1591.

Smothers, J.F., and Henikoff, S. (2000). The HP1 chromo shadow domain binds a consensus peptide pentamer. Curr Biol *10*, 27-30.

Smothers, J.F., and Henikoff, S. (2001). The hinge and chromo shadow domain impart distinct targeting of HP1-like proteins. Molecular and cellular biology *21*, 2555-2569.

Spierer, A., Seum, C., Delattre, M., and Spierer, P. (2005). Loss of the modifiers of variegation Su(var)3-7 or HP1 impacts male X polytene chromosome morphology and dosage compensation. Journal of cell science *118*, 5047-5057.

Stewart, M.D., Li, J., and Wong, J. (2005). Relationship between histone H3 lysine 9 methylation, transcription repression, and heterochromatin protein 1 recruitment. Molecular and cellular biology *25*, 2525-2538.

Strahl, B.D., Grant, P.A., Briggs, S.D., Sun, Z.W., Bone, J.R., Caldwell, J.A., Mollah, S., Cook, R.G., Shabanowitz, J., Hunt, D.F., and Allis, C.D. (2002). Set2 is a nucleosomal histone H3-selective methyltransferase that mediates transcriptional repression. Molecular and cellular biology *22*, 1298-1306.

Straub, T., and Becker, P.B. (2007). Dosage compensation: the beginning and end of generalization. Nat Rev Genet *8*, 47-57.

Suganuma, T., Gutierrez, J.L., Li, B., Florens, L., Swanson, S.K., Washburn, M.P., Abmayr, S.M., and Workman, J.L. (2008). ATAC is a double histone acetyltransferase complex that stimulates nucleosome sliding. Nature structural & molecular biology *15*, 364-372.

Sun, X.J., Wei, J., Wu, X.Y., Hu, M., Wang, L., Wang, H.H., Zhang, Q.H., Chen, S.J., Huang, Q.H., and Chen, Z. (2005). Identification and characterization of a novel human histone H3 lysine 36-specific methyltransferase. The Journal of biological chemistry *280*, 35261-35271.

Sural, T.H., Peng, S., Li, B., Workman, J.L., Park, P.J., and Kuroda, M.I. (2008). The MSL3 chromodomain directs a key targeting step for dosage compensation of the Drosophila melanogaster X chromosome. Nature structural & molecular biology *15*, 1318-1325.

Syntichaki, P., Topalidou, I., and Thireos, G. (2000). The Gcn5 bromodomain co-ordinates nucleosome remodelling. Nature *404*, 414-417.

Tahiliani, M., Mei, P., Fang, R., Leonor, T., Rutenberg, M., Shimizu, F., Li, J., Rao, A., and Shi, Y. (2007). The histone H3K4 demethylase SMCX links REST target genes to X-linked mental retardation. Nature *447*, 601-605.

Takeuchi, T., Yamazaki, Y., Katoh-Fukui, Y., Tsuchiya, R., Kondo, S., Motoyama, J., and Higashinakagawa, T. (1995). Gene trap capture of a novel mouse gene, jumonji, required for neural tube formation. Genes & development *9*, 1211-1222.

Tanaka, Y., Okamoto, K., Teye, K., Umata, T., Yamagiwa, N., Suto, Y., Zhang, Y., and Tsuneoka, M. (2010). JmjC enzyme KDM2A is a regulator of rRNA transcription in response to starvation. The EMBO journal *29*, 1510-1522.

Thiru, A., Nietlispach, D., Mott, H.R., Okuwaki, M., Lyon, D., Nielsen, P.R., Hirshberg, M., Verreault, A., Murzina, N.V., and Laue, E.D. (2004). Structural basis of HP1/PXVXL motif peptide interactions and HP1 localisation to heterochromatin. The EMBO journal *23*, 489-499.

Thoma, F., Koller, T., and Klug, A. (1979). Involvement of histone H1 in the organization of the nucleosome and of the salt-dependent superstructures of chromatin. The Journal of cell biology *83*, 403-427.

Thomas, J.O., Rees, C., and Finch, J.T. (1992). Cooperative binding of the globular domains of histones H1 and H5 to DNA. Nucleic acids research *20*, 187-194.

Thompson, J.D., Gibson, T.J., Plewniak, F., Jeanmougin, F., and Higgins, D.G. (1997). The CLUSTAL_X windows interface: flexible strategies for multiple sequence alignment aided by quality analysis tools. Nucleic acids research *25*, 4876-4882.

Thorne, A.W., Sautiere, P., Briand, G., and Crane-Robinson, C. (1987). The structure of ubiquitinated histone H2B. The EMBO journal *6*, 1005-1010.

Tong, J.K., Hassig, C.A., Schnitzler, G.R., Kingston, R.E., and Schreiber, S.L. (1998). Chromatin deacetylation by an ATP-dependent nucleosome remodelling complex. Nature *395*, 917-921.

Trapnell, C., Pachter, L., and Salzberg, S.L. (2009). TopHat: discovering splice junctions with RNA-Seq. Bioinformatics *25*, 1105-1111.

Trapnell, C., Williams, B.A., Pertea, G., Mortazavi, A., Kwan, G., van Baren, M.J., Salzberg, S.L., Wold, B.J., and Pachter, L. (2010). Transcript assembly and quantification by RNA-Seq reveals unannotated transcripts and isoform switching during cell differentiation. Nature biotechnology *28*, 511-515.

Trewick, S.C., McLaughlin, P.J., and Allshire, R.C. (2005). Methylation: lost in hydroxylation? EMBO Rep *6*, 315-320.

Trojer, P., Zhang, J., Yonezawa, M., Schmidt, A., Zheng, H., Jenuwein, T., and Reinberg, D. (2009). Dynamic Histone H1 Isotype 4 Methylation and Demethylation by Histone

Lysine Methyltransferase G9a/KMT1C and the Jumonji Domain-containing JMJD2/KDM4 Proteins. The Journal of biological chemistry *284*, 8395-8405.

Tsukada, Y., Fang, J., Erdjument-Bromage, H., Warren, M.E., Borchers, C.H., Tempst, P., and Zhang, Y. (2006). Histone demethylation by a family of JmjC domain-containing proteins. Nature *439*, 811-816.

Tsukada, Y., Ishitani, T., and Nakayama, K.I. (2010). KDM7 is a dual demethylase for histone H3 Lys 9 and Lys 27 and functions in brain development. Genes & development *24*, 432-437.

Tu, S., Bulloch, E.M., Yang, L., Ren, C., Huang, W.C., Hsu, P.H., Chen, C.H., Liao, C.L., Yu, H.M., Lo, W.S., *et al.* (2007). Identification of histone demethylases in Saccharomyces cerevisiae. The Journal of biological chemistry *282*, 14262-14271.

Vakoc, C.R., Mandat, S.A., Olenchock, B.A., and Blobel, G.A. (2005). Histone H3 lysine 9 methylation and HP1gamma are associated with transcription elongation through mammalian chromatin. Molecular cell *19*, 381-391.

van Holde, K., and Zlatanova, J. (2007). Chromatin fiber structure: Where is the problem now? Seminars in cell & developmental biology *18*, 651-658.

van Leeuwen, F., Gafken, P.R., and Gottschling, D.E. (2002). Dot1p modulates silencing in yeast by methylation of the nucleosome core. Cell *109*, 745-756.

Wakimoto, B.T., and Hearn, M.G. (1990). The effects of chromosome rearrangements on the expression of heterochromatic genes in chromosome 2L of Drosophila melanogaster. Genetics *125*, 141-154.

Wallrath, L.L., and Elgin, S.C. (1995). Position effect variegation in Drosophila is associated with an altered chromatin structure. Genes & development *9*, 1263-1277.

Wang, H., Wang, L., Erdjument-Bromage, H., Vidal, M., Tempst, P., Jones, R.S., and Zhang, Y. (2004). Role of histone H2A ubiquitination in Polycomb silencing. Nature *431*, 873-878.

Washburn, M.P., Wolters, D., and Yates, J.R., 3rd (2001). Large-scale analysis of the yeast proteome by multidimensional protein identification technology. Nature biotechnology *19*, 242-247.

Webby, C.J., Wolf, A., Gromak, N., Dreger, M., Kramer, H., Kessler, B., Nielsen, M.L., Schmitz, C., Butler, D.S., Yates, J.R., 3rd, *et al.* (2009). Jmjd6 catalyses lysyl-hydroxylation of U2AF65, a protein associated with RNA splicing. Science (New York, N.Y *325*, 90-93.

Wei, Y., Yu, L., Bowen, J., Gorovsky, M.A., and Allis, C.D. (1999). Phosphorylation of histone H3 is required for proper chromosome condensation and segregation. Cell *97*, 99-109.

Weiler, K.S., and Wakimoto, B.T. (1995). Heterochromatin and gene expression in Drosophila. Annu Rev Genet *29*, 577-605.

Whetstine, J.R., Nottke, A., Lan, F., Huarte, M., Smolikov, S., Chen, Z., Spooner, E., Li, E., Zhang, G., Colaiacovo, M., and Shi, Y. (2006). Reversal of histone lysine trimethylation by the JMJD2 family of histone demethylases. Cell *125*, 467-481.

Winston, J.T., Koepp, D.M., Zhu, C., Elledge, S.J., and Harper, J.W. (1999). A family of mammalian F-box proteins. Curr Biol *9*, 1180-1182.

Wissmann, M., Yin, N., Muller, J.M., Greschik, H., Fodor, B.D., Jenuwein, T., Vogler, C., Schneider, R., Gunther, T., Buettner, R., *et al.* (2007). Cooperative demethylation by JMJD2C and LSD1 promotes androgen receptor-dependent gene expression. Nat Cell Biol *9*, 347-353.

Wood, A., Krogan, N.J., Dover, J., Schneider, J., Heidt, J., Boateng, M.A., Dean, K., Golshani, A., Zhang, Y., Greenblatt, J.F., *et al.* (2003). Bre1, an E3 ubiquitin ligase required for recruitment and substrate selection of Rad6 at a promoter. Molecular cell *11*, 267-274.

Wysocka, J., Swigut, T., Milne, T.A., Dou, Y., Zhang, X., Burlingame, A.L., Roeder, R.G., Brivanlou, A.H., and Allis, C.D. (2005). WDR5 associates with histone H3 methylated at K4 and is essential for H3 K4 methylation and vertebrate development. Cell *121*, 859-872.

Xiang, Y., Zhu, Z., Han, G., Ye, X., Xu, B., Peng, Z., Ma, Y., Yu, Y., Lin, H., Chen, A.P., and Chen, C.D. (2007). JARID1B is a histone H3 lysine 4 demethylase up-regulated in prostate cancer. Proceedings of the National Academy of Sciences of the United States of America *104*, 19226-19231.

Xiao, T., Hall, H., Kizer, K.O., Shibata, Y., Hall, M.C., Borchers, C.H., and Strahl, B.D. (2003). Phosphorylation of RNA polymerase II CTD regulates H3 methylation in yeast. Genes & development *17*, 654-663.

Yamane, K., Tateishi, K., Klose, R.J., Fang, J., Fabrizio, L.A., Erdjument-Bromage, H., Taylor-Papadimitriou, J., Tempst, P., and Zhang, Y. (2007). PLU-1 is an H3K4 demethylase involved in transcriptional repression and breast cancer cell proliferation. Molecular cell *25*, 801-812.

Yamane, K., Toumazou, C., Tsukada, Y., Erdjument-Bromage, H., Tempst, P., Wong, J., and Zhang, Y. (2006). JHDM2A, a JmjC-containing H3K9 demethylase, facilitates transcription activation by androgen receptor. Cell *125*, 483-495.

Yang, Z.Q., Imoto, I., Fukuda, Y., Pimkhaokham, A., Shimada, Y., Imamura, M., Sugano, S., Nakamura, Y., and Inazawa, J. (2000). Identification of a novel gene, GASC1, within an amplicon at 9p23-24 frequently detected in esophageal cancer cell lines. Cancer Res *60*, 4735-4739.

Yang, Z.Q., Imoto, I., Pimkhaokham, A., Shimada, Y., Sasaki, K., Oka, M., and Inazawa, J. (2001). A novel amplicon at 9p23 - 24 in squamous cell carcinoma of the esophagus that lies proximal to GASC1 and harbors NFIB. Jpn J Cancer Res *92*, 423-428.

You, A., Tong, J.K., Grozinger, C.M., and Schreiber, S.L. (2001). CoREST is an integral component of the CoREST- human histone deacetylase complex. Proceedings of the National Academy of Sciences of the United States of America *98*, 1454-1458.

Zhang, D., Yoon, H.G., and Wong, J. (2005). JMJD2A is a novel N-CoR-interacting protein and is involved in repression of the human transcription factor achaete scute-like homologue 2 (ASCL2/Hash2). Molecular and cellular biology *25*, 6404-6414.

Zhao, T., Heyduk, T., and Eissenberg, J.C. (2001). Phosphorylation site mutations in heterochromatin protein 1 (HP1) reduce or eliminate silencing activity. The Journal of biological chemistry *276*, 9512-9518.

Zhou, W., Zhu, P., Wang, J., Pascual, G., Ohgi, K.A., Lozach, J., Glass, C.K., and Rosenfeld, M.G. (2008). Histone H2A monoubiquitination represses transcription by inhibiting RNA polymerase II transcriptional elongation. Molecular cell *29*, 69-80.

Zink, B., and Paro, R. (1989). In vivo binding pattern of a trans-regulator of homoeotic genes in Drosophila melanogaster. Nature *337*, 468-471.

Zofall, M., and Grewal, S.I. (2006). Swi6/HP1 recruits a JmjC domain protein to facilitate transcription of heterochromatic repeats. Molecular cell *22*, 681-692.

Appendix A: Primers used in this study

RNAi knockdown of dKDM4A and LacZ in S2 Cells

Primer Name	Sequence
dKDM4A RNAi-F	TAATACGACTCACTATAGGGAGAtggaatcctcaatcctcgtc
dKDM4A RNAi-R	TAATACGACTCACTATAGGGAGAcaatggatgtgaacgaaacg
LacZ RNAi-F	gcTAATACGACTCACTATAGGCCAAACatgaccatgattacgccaagct
LacZ RNAi-R	gcTAATACGACTCACTATAGGCCAAACgtcccattcgccattcaggc

RT-PCR and real-time RT-PCR (qRT-PCR)

Primer Name	Sequence
dKDM4A-F	TCGAAGCGTTGGATCGAGTA
dKDM4A-R	ACAGGGCAGTTCATTCCATA
rp49-F	ATGTGTATTCCGACCACGTTACAAGA
rp49-R	AAGAAGCGCACCAAGCACTTCA
dKDM4A qRT-F	ACTTTGGCATGTGGAAGAGC
dKDM4A qRT-R	GGCATTGCATTCCTGGTAGT
rp49 qRT-F	GACGCTTCAAGGGACAGTATCTG
rp49-qRT-R	AAACGCGGTTCTGCATGAG

H3K36me3 or HP1a ChIP-qPCR

Primer Name	Sequence
Scp1-F	GCAGAACCCATCAGCAAAAT
Scp1-R	AGGGAATTGCTTTTCCGAGT
Nipped-A-F	TTGCGACAAGACAAGTCAGG
Nipped-A-R	CAGTTTGTGGAGCGTGCTTA
CG40263-F	TACCAACGCCCTGAATTCTC
CG40263-R	CCTCGCTTCTTCGTGGTAAG
Cht3-F	CGTGGGAGCATTTAGTTGGT
Cht3-R	ATGTACAGCCACCCAGAAGG
intergenic-F	AATTGCATCGCAACACAATGAG
intergenic-R	TCGTGAAATGTTTGCTACTGGAATA

Appendix B: MudPIT analysis of dKDM4A purification

	dKDM4A			control		
Description	**P**	**S**	**SC (%)**	**P**	**S**	**SC (%)**
dKDM4A	**36**	**1086**	**73.74**	**X**	**X**	**X**
p16-ARC	7	33	68.21	X	X	X
Hsp23	10	43	67.74	X	X	X
Actin 42A	17	501	65.96	1	2	4.79
Actin 5C	17	507	65.96	1	2	4.79
Hsp26	10	116	60.58	X	X	X
Su(var)2-5	**9**	**227**	**58.25**	**X**	**X**	**X**
Actin-related protein 66B	11	74	50.72	X	X	X
Hsp27	7	87	49.77	X	X	X
Chd64	6	12	48.94	X	X	X
Suppressor of profilin 2	9	52	48.28	X	X	X
Actin 57B	12	377	48.14	1	2	4.79
Heat shock protein cognate	19	174	41.47	X	X	X
Calmodulin	3	8	34.23	X	X	X
Myosin light chain cytoplasmic	4	17	32.65	X	X	X
Arc-p34	8	69	32.56	X	X	X
capping protein beta	6	13	30.8	X	X	X
capping protein alpha	6	21	29.02	X	X	X
alpha-Tubulin	8	26	28.89	X	X	X
Arpc3A	2	19	25.79	X	X	X
Arc-p20	3	15	25	X	X	X
CG10641-PA	5	6	24.88	X	X	X
Hsp68	12	32	24.25	X	X	X
Actin-related protein 14D	6	30	23.35	X	X	X
alpha Spectrin	34	88	22.44	X	X	X
beta-Tubulin	5	26	21.7	X	X	X
CG17293-PA	4	10	21.14	X	X	X
cut up	2	3	20.22	X	X	X
Arpc3B	2	2	20.11	X	X	X
Heat shock protein cognate 3	11	64	19.05	2	3	4.57
His2A	1	2	18.55	X	X	X
Jupiter	2	4	17.77	1	1	6.6
spaghetti squash	2	4	16.67	X	X	X
CG7033-PA	5	13	16.26	X	X	X
cathD	3	5	16.07	X	X	X
T-complex Chaperonin 5	5	8	15.68	X	X	X
HP1b	2	9	15.42	X	X	X
Elongation factor 1alpha48D	4	22	14.25	1	2	2.38
tropomodulin	3	8	13.35	X	X	X
karst	37	84	12.81	X	X	X
CG14224-PA	4	22	12.61	1	3	3.66
ypsilon schachtel	3	4	12.5	X	X	X
C-terminal Binding Protein	3	5	12.18	X	X	X
CG10837-PB	3	5	11.98	17	254	50.11
overgrown hematopoietic organs at 23B	1	1	12.05	1	4	21.69
CG8351-PA	5	8	11.95	X	X	X

CG6444-PA	1	6	11.94	X	X	X
14-3-3epsilon	2	3	11.83	X	X	X
Tcp1-like	4	10	11.67	X	X	X
skpA	1	2	11.73	X	X	X
CG11999-PA	2	4	11.11	X	X	X
alpha actinin	7	11	10.95	X	X	X
CG12265-PA	1	8	10.46	X	X	X
Protein on ecdysone puffs	5	14	10.34	3	7	7.68
Heat shock protein cognate 5	5	9	10.35	X	X	X
peanut	6	10	10.2	X	X	X
pavarotti	6	7	10.15	X	X	X
cdc2-related-kinase	2	7	9.82	1	2	4.65
Lasp	2	4	9.52	X	X	X
lethal (1)	3	3	9.38	X	X	X
CG2158-PA	3	10	8.87	X	X	X
Heterogeneous nuclear ribonucleoprotein at 27C	2	2	8.55	X	X	X
Neosin	2	5	8.36	X	X	X
Cctgamma	3	4	8.27	X	X	X
cryptocephal	1	2	7.87	X	X	X
CG8863-PE	2	5	7.69	X	X	X
CG4164-PA	2	4	7.63	1	1	5.37
Elongation factor 1 beta	1	2	7.28	X	X	X
CG16817-PA	1	4	7.07	X	X	X
Heat shock protein cognate 1	2	27	7.02	X	X	X
Nucleosome remodeling factor - 38kD	1	3	6.8	X	X	X
CG8258-PA	2	5	6.59	X	X	X
shibire	3	3	6.02	X	X	X
Hsp7-Ab	4	4	5.76	X	X	X
CG4747-PA	2	4	5.81	X	X	X
Syndapin	2	3	5.67	X	X	X
CG16972-PA	6	11	5.26	X	X	X
members only	2	3	5.13	X	X	X
RacGAP50C	3	3	4.96	X	X	X
Ski6	1	1	4.88	3	7	17.07
CG8289-PA	1	2	4.76	X	X	X
14-3-3zeta	1	2	4.84	X	X	X
Myosin 61F	3	7	4.58	X	X	X
poly U binding factor	2	2	4.55	2	9	3.92
Septin-2	1	10	4.53	X	X	X
RhoGAP92B	2	4	4.32	X	X	X
Rae1	1	2	4.34	X	X	X
CG13096-PA	2	2	4.11	X	X	X
cheerio	7	9	3.9	X	X	X
Heat shock protein cognate 2	2	2	3.79	X	X	X
RNA-binding protein S1	1	2	3.74	X	X	X
beta Spectrin	6	10	3.62	X	X	X
glorund	1	7	3.58	X	X	X
smallminded	2	2	3.5	X	X	X
coracle	3	5	3.42	X	X	X
Z4	2	2	3.11	X	X	X
abstrakt	1	2	3.07	1	1	2.1
U2 small nuclear riboprotein auxiliary factor 50	1	2	3.13	X	X	X
Eb1 CG3265-PC	1	4	3.05	X	X	X
hu li tai shao	2	4	3.03	X	X	X
CG6995-PA	1	2	3	X	X	X
CG3838-PA	1	4	2.99	X	X	X

DnaJ-like-1	1	2	2.99	X	X	X
twins	1	4	2.81	X	X	X
dilute class unconventional myosin	3	4	2.68	X	X	X
CG9373-PA	1	4	2.69	X	X	X
zipper	3	5	2.58	X	X	X
female lethal d	1	2	2.61	X	X	X
specifically Rac1-associated protein 1	2	2	2.48	X	X	X
DNA replication-related element factor	1	2	2.4	X	X	X
Collagen type IV	2	2	2.3	X	X	X
Fimbrin	1	2	2.19	X	X	X
Trithorax-like	1	2	2.23	X	X	X
rad50	2	3	2.15	X	X	X
SRm160	1	1	2.1	1	1	1.68
Cortactin	1	2	2.15	X	X	X
CLIP-190	2	3	1.78	X	X	X
DDB1	1	2	1.84	X	X	X
scraps	1	2	1.61	X	X	X
Chromator	1	1	1.62	1	2	1.94
misshapen	1	2	1.46	X	X	X
HEM-protein	1	4	1.51	X	X	X
serpent	1	2	1.36	X	X	X
Nup214	1	3	1.17	X	X	X
CG18811-PA	1	2	1.25	X	X	X
CG31938-PA	X	X	X	4	20	26.29
Rrp4 CG3931-PA	X	X	X	3	12	18.79
CG8928-PA	X	X	X	2	2	11.95
Eps-15	X	X	X	8	34	11.01
Csl4 C	X	X	X	1	3	10.78
CG6543-PB	X	X	X	2	2	10.17
CG10984-PA	X	X	X	3	12	9.69
CG31974-PA	X	X	X	2	19	8.41
CG17002-PB	X	X	X	2	3	8.08
karyopherin alpha3	X	X	X	2	2	6.42
CG14005-PA	X	X	X	1	2	5.99
CG15415-PA	X	X	X	3	6	5.7
CG7692-PA	X	X	X	4	18	5.21
Otefin	X	X	X	1	2	5.19
Dis3	X	X	X	3	9	4.28
ebi	X	X	X	2	3	3.57
Dynamin associated protein 160	X	X	X	1	6	2.73
Total Spc	541	4291		83	458	

P: Unique peptide; S: Spectra: SC: Sequence coverage

Appendix C: MudPIT analysis of dKDM4B purification

	dKDM4B			Control		
Description	**P**	**S**	**SC (%)**	**P**	**S**	**SC (%)**
Actin 5C	22	498	71.54	14	35	52.66
Eukaryotic initiation factor 4B	26	1560	55.34	22	188	49.89
Actin 57B	16	421	48.94	12	21	39.63
Actin 42A	22	100	71.54	14	35	52.66
Myosin light chain cytoplasmic	8	120	68.03	5	12	42.86
Heat shock protein cognate 4	24	336	45.01	5	8	12.44
spaghetti squash	7	93	50	5	10	39.08
alpha actinin	44	469	56.2	1	1	1.34
Calmodulin	5	35	41.61	2	2	13.42
dKDM4B	**17**	**79**	**31.19**	**X**	**X**	**X**
Caldesmon-related protein	1	61	3.62	X	X	X
Hsp23	2	11	16.13	X	X	X
zipper	28	94	22.12	3	5	2.28
Nop56	7	21	22.98	X	X	X
Gelsolin	10	29	17.2	X	X	X
Hsp27	3	7	21.6	X	X	X
Myosin 61F	10	31	13.35	2	3	2.73
Myo31DF	12	21	15.83	1	1	1.19
Ribosomal protein L30	1	2	10.81	X	X	X
hoi-polloi	2	2	26.77	X	X	X
Fibrillarin	2	5	11.34	X	X	X
abstrakt	1	8	2.75	X	X	X
CG8578	3	5	8.59	1	1	2.78
Ribosomal protein L14	1	2	6.02	X	X	X
CG30428	2	3	12.17	X	X	X
polyA-binding protein	4	7	11.36	X	X	X
capping protein alpha	2	3	10.84	4	9	24.13
CG7993	1	3	4.69	X	X	X
SF2	1	2	3.92	X	X	X
B52	1	2	4.26	X	X	X
nop5	3	3	8.22	X	X	X
lark	2	2	8.24	X	X	X
dilute class unconventional myosin	3	8	2.73	X	X	X
Rrp6	1	3	1.33	X	X	X
tumbleweed	1	2	1.76	X	X	X
FK506-binding protein 1	1	1	3.64	X	X	X
CG30349	1	1	1.77	X	X	X
Nup358	3	4	1.89	X	X	X
Rs1	1	1	1.15	X	X	X
l(2)k09022	1	1	0.76	X	X	X
Heat shock protein cognate 3	33	1195	51.52	5	10	12.2
Protein disulfide isomerase	22	661	57.06	3	5	7.86
tropomodulin	12	525	34.41	3	6	8.56
CG15415	24	397	34.2	5	9	8.18
Arc-p34	9	120	33.89	1	2	4.98
CG10641	8	69	47	3	5	20.74

CG12265	8	44	56.86	1	2	10.46
Collagen type IV	48	509	37.38	3	7	3.04
Arc-p20	6	46	45.24	1	1	6.55
viking	49	500	36.39	9	16	7.53
CG6199	19	180	28.71	2	2	3.61
Suppressor of profilin 2	13	73	55.7	1	1	5.31
prolyl-4-hydroxylase-alpha EFB	10	80	22.55	3	5	7.27
stubarista	6	35	42.59	1	1	6.3
Elongation factor 1alpha48D	8	56	26.57	1	2	1.73
ebi	9	49	20.43	2	6	6.14
squid	4	18	21.75	2	3	10.06
ATP synthase-beta	7	28	18.61	1	2	2.77
SSRP	9	35	17.29	2	2	3.6
CG8928	2	6	15.72	1	1	9.43
CG6543	2	7	11.86	1	1	6.44
alpha Spectrin	26	56	16.19	6	8	3.4
capping protein beta	3	6	17.39	7	13	37.68
CG18811	8	19	11.76	1	1	1.25
dre4	7	20	8.82	2	3	2.32
glorund	1	8	3.58	1	1	2.22
Rrp42	2	3	7.77	1	2	5.07
karst	17	31	5.73	4	4	1.41
Rrp4	1	1	5.37	1	2	4.03
Su(var) 3-9	1	1	3.37	1	2	4.21
Hsp70Ab	3	0	5.92	X	X	X
BM-40-SPARC	16	1226	65.79	X	X	X
Annexin IX	14	371	52.16	X	X	X
p16-ARC	8	94	68.21	X	X	X
CG13117	4	67	59.09	X	X	X
CG31974	9	211	26.44	X	X	X
Eb1	12	132	54.98	X	X	X
Actin-related protein 14D	13	144	43.91	X	X	X
Arpc3A	6	56	45.26	X	X	X
Actin-related protein 66B	13	123	45.93	X	X	X
cheerio	75	614	52.04	X	X	X
Heat shock protein cognate 5	27	176	52.04	X	X	X
Dynein light chain 90F	3	25	36.04	X	X	X
Cytoplasmic dynein light chain 2	2	20	37.08	X	X	X
CG13335	8	52	43.88	X	X	X
VhaAC39	10	65	44.86	X	X	X
lethal (1)	2	27	17.2	X	X	X
ERp60 C	15	59	49.18	X	X	X
Glutactin	24	161	33.53	X	X	X
CG17272	3	22	29.53	X	X	X
14-3-3zeta	5	30	30.65	X	X	X
14-3-3epsilon	8	5	50.76	X	X	X
CG11999	4	29	23.15	X	X	X
Hsp68	19	79	42.99	X	X	X
Ef1gamma	12	55	38.75	X	X	X
Ribosomal protein S28b	1	8	18.46	X	X	X
overgrown hematopoietic organs at 23B	2	10	33.73	X	X	X
Protein phosphatase 1alpha at 96A	6	37	29.97	X	X	X
Eps-15	28	139	37.91	X	X	X
Elongation factor 1 beta	6	28	39.08	X	X	X
alpha-Tubulin at 84B	7	48	26.67	X	X	X
CG14482	2	6	56.14	X	X	X

CG3884	5	30	27.27	X	X	X
Chd64	6	19	49.47	X	X	X
karyopherin alpha3	6	48	21.21	X	X	X
CG4164	7	33	28.25	X	X	X
Arpc3B	2	14	22.29	X	X	X
Chitinase-like	10	40	35.62	X	X	X
beta-Tubulin at 56D	11	20	33.11	X	X	X
Su(var)2-5	4	17	33.01	X	X	X
CG31938	7	19	41.38	X	X	X
CG9338	1	12	6.12	X	X	X
Vha100-2	11	68	19.06	X	X	X
Female sterile (2) Ketel	9	72	15.16	X	X	X
Neosin	6	29	23.45	X	X	X
Heterogeneous nuclear ribonucleoprotein at 27C	7	32	28.03	X	X	X
Vacuolar H[+]-ATPase 55kD B subunit	9	36	31.02	X	X	X
CG9328	3	13	24.44	X	X	X
C-terminal Binding Protein	14	2	40.55	X	X	X
Ribosomal protein LP2	1	7	15.04	X	X	X
CG34132	3	5	51.19	X	X	X
HP1b	3	14	20	X	X	X
Heat shock protein 60	7	33	21.12	X	X	X
CG1749	8	23	27.48	X	X	X
Tim8	1	5	12.5	X	X	X
14-3-3epsilon	8	2	49.61	X	X	X
skpA	3	9	19.14	X	X	X
Receptor mediated endocytosis 8	31	132	17.32	X	X	X
Ribosomal protein LP1	2	6	31.25	X	X	X
CG8863	6	21	23.82	X	X	X
apontic	4	25	10.22	X	X	X
Vha68-2	10	31	24.92	X	X	X
CG15098	1	9	11.83	X	X	X
CG2158	9	27	27.13	X	X	X
CG14224	6	26	16.45	X	X	X
Pendulin	6	24	16.28	X	X	X
VhaM9.7-2	1	4	12.36	X	X	X
Dynamin associated protein 160	12	45	21.2	X	X	X
C-terminal Binding Protein	14	1	47.67	X	X	X
Dis3	8	43	12.02	X	X	X
CG14207	3	8	32.24	X	X	X
CG3074	6	18	24.13	X	X	X
CG10527	5	12	28.72	X	X	X
Mec2	3	14	12.29	X	X	X
supercoiling factor	6	13	30.7	X	X	X
Hdac3	3	17	10.27	X	X	X
Eukaryotic initiation factor 4E	3	9	22.58	X	X	X
Ribosomal protein S12	2	5	20.14	X	X	X
Glycoprotein 93	10	28	19.19	X	X	X
poly U binding factor 68kD	7	22	18.84	X	X	X
Ferritin 1 heavy chain homologue	3	7	25.37	X	X	X
CLIP-190	24	55	21.12	X	X	X
CG9577	2	10	11.22	X	X	X
Vacuolar H[+]-ATPase 26kD E subunit	4	7	22.57	X	X	X
CG2852	4	6	28.78	X	X	X
Translationally controlled tumor protein	1	5	6.98	X	X	X
enhancer of rudimentary	1	3	16.35	X	X	X
14-3-3epsilon	8	1	50.38	X	X	X

Vacuolar H[+] ATPase 16kD subunit	1	4	11.32	X	X	X
CG31999 CG31999-PA	10	23	16.25	X	X	X
Ski6	3	6	18.29	X	X	X
CG14273	1	6	5.95	X	X	X
CG15602	2	8	8.48	X	X	X
CG34191	2	2	49.43	X	X	X
cathD	4	9	16.33	X	X	X
Hrp59	4	14	9.97	X	X	X
lethal (2) 09851	3	10	12.5	X	X	X
CG5335	4	7	19.31	X	X	X
Rrp46	2	5	13.73	X	X	X
CG17002	2	9	8.08	X	X	X
Z4	6	20	13.65	X	X	X
Dihydroorotate dehydrogenase	2	8	8.4	X	X	X
CG5664	6	14	12.66	X	X	X
UDP-glucose-glycoprotein glucosyltransferase	12	30	13.11	X	X	X
Vap-33-1	2	5	13.01	X	X	X
CaBP1	3	8	10.85	X	X	X
CG6891	2	3	14.11	X	X	X
Hsp83	5	13	10.18	X	X	X
terribly reduced optic lobes	32	83	10.72	X	X	X
Vha100-1	6	15	10.47	X	X	X
Cyclophilin 1	1	4	6.17	X	X	X
Heat shock protein cognate 1	4	9	8.74	X	X	X
CG2918	6	16	9.32	X	X	X
Rpd3 C	4	9	12.09	X	X	X
CG14476	7	15	10.39	X	X	X
CG12948	1	4	7.14	X	X	X
CG17293	4	5	19.56	X	X	X
CG10672	3	5	11.36	X	X	X
enabled	5	13	10.49	X	X	X
Moesin	4	10	7.09	X	X	X
CG10191	2	6	8.7	X	X	X
Ran GTPase activating protein	5	9	11.74	X	X	X
Calreticulin	3	6	11.82	X	X	X
Ribosomal protein L23	1	2	10.71	X	X	X
downstream of receptor kinase	2	3	12.8	X	X	X
CG10984	4	9	12.66	X	X	X
ran CG1404-PB	2	3	15.74	X	X	X
mitochondrial single stranded DNA-binding protein	1	2	9.59	X	X	X
Decapping protein 1	2	5	6.72	X	X	X
CG1637	3	6	9.33	X	X	X
mitochondrial transcription factor B2	3	6	9.07	X	X	X
delta-coatomer protein	4	7	12.03	X	X	X
CG6751	4	6	16.34	X	X	X
CG31915	2	8	5.88	X	X	X
CG15747	3	5	11.89	X	X	X
CG10131	2	4	6.98	X	X	X
CG30382	2	3	8.61	X	X	X
REG	1	3	5.31	X	X	X
CG9796	2	3	16.8	X	X	X
Cleavage stimulation factor 64 KDa subunit	3	5	11.69	X	X	X
CG6724	3	5	11.43	X	X	X
smallminded	5	11	9.53	X	X	X
CG6904	3	8	5.95	X	X	X
lava lamp	14	32	7.95	X	X	X

DNA replication-related element factor	5	8	10.3	X	X	X
Nipsnap CG9212-PC	2	3	11.72	X	X	X
Vacuolar H[+]-ATPase SFD subunit	3	5	9.83	X	X	X
CG32032	2	3	6.64	X	X	X
Jupiter	1	2	6.81	X	X	X
Heterogeneous nuclear ribonucleoprotein at 87F	2	4	9.87	X	X	X
nmdyn-D7	1	4	3.88	X	X	X
mad2	2	2	11.59	X	X	X
Hsp26	1	2	7.21	X	X	X
stress-sensitive B	1	3	3.85	X	X	X
Receptor of activated protein kinase C 1	2	3	9.12	X	X	X
Aac11	2	5	5.04	X	X	X
CG2063	1	3	6.15	X	X	X
Smrter	13	33	6.91	X	X	X
Peroxiredoxin 2540	1	2	4.55	X	X	X
bellwether	2	5	5.07	X	X	X
Vacuolar H[+] ATPase 44kD C subunit	2	4	8.14	X	X	X
Nucleosome remodeling factor - 38kD	1	3	4.73	X	X	X
CG9086	7	16	6.09	X	X	X
kugelkern	2	5	5.26	X	X	X
belphegor	2	5	5.63	X	X	X
thioredoxin peroxidase 2	1	2	4.13	X	X	X
Actin-related protein 87C	2	3	8.24	X	X	X
bigmax	1	2	4.72	X	X	X
coracle	4	13	4.59	X	X	X
CG18789	2	3	7.29	X	X	X
Rrp45	2	3	8.25	X	X	X
Ribosomal protein L23A	1	2	3.97	X	X	X
CG34417	4	6	6.96	X	X	X
Down syndrome cell adhesion molecule	8	14	5.5	X	X	X
CG4169	1	3	3.64	X	X	X
Succinate dehydrogenase B	1	2	4.04	X	X	X
CG8778	2	2	9.7	X	X	X
unkempt	2	4	5.34	X	X	X
CG9917	1	2	4.32	X	X	X
CG10722	1	4	1.99	X	X	X
Traf3	2	3	5.97	X	X	X
vulcan	1	4	2.48	X	X	X
CG7946	2	3	6.74	X	X	X
CG7920	1	3	4.61	X	X	X
CG14629	1	2	5.02	X	X	X
Mtr3	2	2	12.58	X	X	X
CoRest	1	4	2.13	X	X	X
twins	2	3	5.21	X	X	X
Elongation factor 2b	3	5	6.28	X	X	X
rasputin	2	4	4.49	X	X	X
CG8516	2	5	4.26	X	X	X
CG6766	1	3	3.62	X	X	X
coro	3	3	6.82	X	X	X
CG7671	1	2	3.63	X	X	X
CG12547	3	4	7.39	X	X	X
CG8258	2	3	4.95	X	X	X
Transcription factor IIA L	1	2	5.46	X	X	X
CG3061	1	2	7.57	X	X	X
CG8029	1	2	3.17	X	X	X
CG13349	1	2	3.86	X	X	X

selenide,water dikinase	1	2	3.52	X	X	X
CG30084	5	6	8.95	X	X	X
CG10932	2	2	10.98	X	X	X
CG9911	1	2	3.4	X	X	X
CG8232	4	6	5.4	X	X	X
CG1837	1	2	2.64	X	X	X
Autophagy-specific gene 1	2	4	4.07	X	X	X
CG12262	1	2	3.58	X	X	X
Heat shock protein cognate 2	4	2	8.53	X	X	X
MRG15	1	2	3.07	X	X	X
short stop	18	41	2.98	X	X	X
Chromatin assembly factor 1 subunit	1	2	6.28	X	X	X
CG6842	1	2	2.71	X	X	X
CG9342	3	4	4.63	X	X	X
beta-Tubulin at 60D	7	1	18.06	X	X	X
Heat shock factor	1	3	2.73	X	X	X
CG11486	1	3	2.54	X	X	X
CG14805	1	2	2.37	X	X	X
cap binding protein 80	3	3	4.5	X	X	X
growl	1	2	2.99	X	X	X
Cctgamma	2	2	5.33	X	X	X
lingerer	3	5	3.85	X	X	X
Su(var)2-10	1	2	3.25	X	X	X
rhea	6	10	3.49	X	X	X
Lysyl-tRNA synthetase	1	2	2.79	X	X	X
CG7408	1	2	5.3	X	X	X
l(2)37Cb	2	3	3.8	X	X	X
Calpain-B	2	3	3.57	X	X	X
CG18616	1	2	2.2	X	X	X
short wing	1	2	2.2	X	X	X
CG12065	2	2	5.09	X	X	X
Ced-12	1	2	1.38	X	X	X
CG13366	2	3	2.01	X	X	X
Host cell factor	3	4	2.67	X	X	X
Stromalin	2	3	2.93	X	X	X
barentsz	1	2	1.84	X	X	X
CG5726	1	2	1.83	X	X	X
CG6509	4	5	3.44	X	X	X
CG11870	2	3	2.71	X	X	X
CG6522	1	2	1.72	X	X	X
scraps	2	3	2.1	X	X	X
O-glycosyltransferase	2	2	3.21	X	X	X
sec24	2	2	2.28	X	X	X
CG32306	2	2	1.59	X	X	X
His2A	X	X	X	1	1	7.26
Histone H2A variant	X	X	X	1	1	6.38
CG15220	X	X	X	1	2	12.5
CG4769	X	X	X	1	2	5.21
Glyceraldehyde 3 phosphate dehydrogenase 2	X	X	X	1	3	4.22
CG7616	X	X	X	1	2	1.97
Total SpC	1803	19799		244	1447	

P: Unique peptide; S: Spectra: SC: Sequence coverage

Appendix D: Differential gene expression analysis

Gene	mt1	mt2	wt1	wt2	fc (mt/WT)	log2 fc	t_pval
CG13532	0.05	0.03	11.88	11.06	0.00	-8.20	3.62E-02
Kdm4A	0.66	0.83	73.58	70.37	0.01	-6.60	1.24E-02
Nos	0.36	0.05	23.68	0.07	0.02	-5.86	5.78E-01
GluClalpha	0.09	1.00	10.24	15.57	0.04	-4.55	1.87E-01
CG14502	0.88	0.86	11.28	10.27	0.08	-3.64	8.27E-03
CG4398	1.50	1.40	16.25	15.70	0.09	-3.46	1.64E-03
CG32816	2.44	3.02	30.46	28.34	0.09	-3.43	1.61E-02
CG18586	1.72	1.63	18.00	16.13	0.10	-3.35	3.21E-03
CG13375	0.79	0.60	6.97	6.94	0.10	-3.32	3.70E-02
CG42651	2.28	1.77	18.27	18.70	0.11	-3.19	3.54E-02
CG34353	2.39	2.25	20.50	21.67	0.11	-3.18	4.13E-04
dpr6	1.96	1.84	12.53	13.85	0.14	-2.80	2.01E-03
CG11200	3.99	4.08	26.81	26.41	0.15	-2.72	8.95E-05
P5cr	2.45	1.88	11.12	12.55	0.18	-2.45	2.31E-02
iab-4	14.58	15.29	76.94	77.06	0.19	-2.37	9.06E-03
RhoGAP100F	1.12	0.64	3.64	4.71	0.21	-2.24	7.02E-02
CG4991	1.25	1.60	6.70	5.44	0.23	-2.09	1.28E-02
CR31044	1.69	1.57	6.92	6.34	0.25	-2.02	1.91E-03
CG8503	7.02	7.57	29.61	25.86	0.26	-1.93	8.97E-03
CG9752	14.07	12.58	50.66	41.92	0.29	-1.80	1.56E-02
sec13	37.05	41.95	126.72	138.03	0.30	-1.74	6.32E-03
Sec61beta	71.53	71.51	218.50	208.65	0.33	-1.58	1.34E-02
CG17209	6.23	6.61	19.22	18.65	0.34	-1.56	3.96E-03
alpha-Est5	12.38	11.34	35.11	32.36	0.35	-1.51	3.37E-03
CG6463	25.14	28.76	71.60	80.62	0.35	-1.50	7.80E-03
CG2993	2.75	2.47	7.23	6.85	0.37	-1.43	1.15E-02
CR32205	1.88	1.84	4.23	5.67	0.38	-1.41	9.45E-02
CG2812	4.35	5.34	11.75	13.54	0.38	-1.38	2.30E-02
CG11206	1.41	0.70	2.13	3.36	0.39	-1.38	1.61E-01
Tim10	29.93	9.65	59.39	42.40	0.39	-1.36	2.88E-01
CG7381	5.32	4.43	11.62	12.62	0.40	-1.31	3.23E-02
Mis12	4.27	5.61	12.94	11.30	0.41	-1.29	5.36E-02
CG6927	1.30	1.31	3.35	2.77	0.43	-1.23	7.10E-02
CG8180	2.03	2.62	6.01	4.81	0.43	-1.22	4.01E-02
CG9344	9.01	10.87	22.23	23.79	0.43	-1.21	4.64E-02
CG30428	7.29	7.59	18.44	15.72	0.44	-1.20	4.86E-02
Ppcs	5.32	5.74	13.21	12.00	0.44	-1.19	6.63E-03
Rbp9	5.11	4.33	10.85	10.49	0.44	-1.18	5.51E-02
CG5602	15.33	15.31	34.59	34.16	0.45	-1.17	4.54E-03
Aats-arg	11.79	11.54	26.80	25.55	0.45	-1.17	6.23E-03
CG4565	1.54	1.02	3.36	2.25	0.46	-1.13	1.14E-01
CG3097	2.06	2.86	5.41	5.24	0.46	-1.11	1.29E-01
CG14425	6.22	8.91	14.58	18.05	0.46	-1.11	8.82E-02
osk	4.98	4.47	11.35	8.95	0.47	-1.10	6.06E-02
Mef2	11.74	12.83	26.01	26.31	0.47	-1.09	3.45E-02
aret	11.97	11.02	26.48	21.98	0.47	-1.08	4.59E-02
Adh	9.96	9.47	20.70	20.09	0.48	-1.07	4.24E-03
Picot	1.90	1.75	3.58	4.03	0.48	-1.06	1.52E-02

GstD1	13.10	12.42	28.90	22.60	0.50	-1.01	9.87E-02
Tsp29Fb	3.94	3.87	2.05	1.84	2.01	1.01	4.51E-02
Prm	10.26	9.20	4.51	5.18	2.01	1.01	1.76E-02
Tm2	17.29	16.19	8.27	8.34	2.02	1.01	2.77E-02
GV1	3.30	1.93	1.18	1.40	2.03	1.02	2.15E-01
CG30291	47.18	45.70	23.31	22.34	2.03	1.02	2.01E-03
CG4872	14.13	12.91	6.46	6.76	2.05	1.03	1.49E-02
CG5399	6.47	6.35	3.52	2.71	2.06	1.04	1.11E-01
CG12607	6.50	4.51	2.45	2.89	2.06	1.04	1.19E-01
CG32243	34.14	30.35	16.22	14.77	2.08	1.06	1.22E-02
CG15282	8.97	9.06	4.69	3.96	2.08	1.06	7.24E-02
CG6579	3.46	2.11	1.03	1.64	2.08	1.06	1.65E-01
CG8311	26.61	25.51	12.53	12.43	2.09	1.06	1.49E-02
CG13067	15.52	14.90	7.13	7.39	2.10	1.07	1.46E-03
CG5080	13.15	14.12	6.41	6.53	2.11	1.08	2.10E-02
CG15449	5.89	6.55	2.69	3.20	2.11	1.08	2.98E-02
CG10625	5.48	3.61	2.28	2.02	2.11	1.08	1.57E-01
CG11327	2.36	3.30	1.16	1.52	2.12	1.08	7.94E-02
CG8654	24.16	23.74	11.80	10.79	2.12	1.08	3.13E-02
Nap1	492.24	462.99	227.47	222.81	2.12	1.09	1.43E-02
CG17290	19.78	15.75	7.86	8.80	2.13	1.09	5.39E-02
CG17032	4.99	5.09	2.19	2.51	2.14	1.10	5.27E-02
CG30458	7.11	6.52	3.63	2.67	2.17	1.12	1.04E-01
CG13679	6.88	8.41	2.15	4.88	2.17	1.12	2.70E-01
CG5958	3.37	3.01	1.47	1.46	2.18	1.12	4.55E-02
Ndg	3.42	3.60	1.60	1.62	2.18	1.12	1.18E-02
Gasp	5.62	4.27	2.75	1.78	2.18	1.13	1.12E-01
CG7298	7.00	6.93	3.26	3.11	2.18	1.13	1.38E-02
CG4229	4.42	4.49	1.74	2.26	2.23	1.16	9.95E-02
CG13731	5.53	5.13	2.25	2.51	2.24	1.16	1.09E-02
Idgf2	32.95	30.85	14.33	14.15	2.24	1.16	2.14E-02
TpnC73F	6.73	7.17	3.19	3.01	2.24	1.16	2.94E-03
l(2)34Fc	7.12	5.26	2.42	3.08	2.25	1.17	5.76E-02
CG13059	12.36	11.09	5.78	4.63	2.25	1.17	4.67E-02
Muc26B	3.19	3.17	1.44	1.38	2.26	1.17	1.42E-02
CG5177	8.07	6.84	3.79	2.81	2.26	1.18	6.41E-02
Idgf3	7.62	8.04	3.50	3.38	2.27	1.19	3.26E-03
CG12011	9.82	12.70	5.00	4.86	2.28	1.19	9.58E-02
Ccp84Ae	3.96	3.54	1.33	1.95	2.29	1.19	1.18E-01
CG2852	762.33	774.65	326.65	344.03	2.29	1.20	1.14E-02
CG32694	4.09	3.16	1.71	1.44	2.30	1.20	4.50E-02
CG30392	8.38	7.50	3.20	3.70	2.30	1.20	1.50E-02
CG10953	38.15	37.86	13.92	19.00	2.31	1.21	1.15E-01
TwdlL	6.35	6.00	2.71	2.63	2.31	1.21	6.43E-03
CG9449	4.23	4.42	2.10	1.61	2.33	1.22	9.09E-02
bl	515.48	537.63	235.44	210.54	2.36	1.24	2.27E-02
CG16884	8.19	6.38	2.78	3.37	2.37	1.25	3.68E-02
spdo	2.94	4.19	1.40	1.60	2.37	1.25	9.89E-02
CG15739	4.16	3.78	1.66	1.67	2.38	1.25	3.52E-02
CR31808	3.11	2.69	1.37	1.06	2.38	1.25	4.78E-02
obst-E	5.92	4.50	2.35	2.01	2.39	1.26	5.07E-02
CG5326	3.62	2.79	1.44	1.22	2.41	1.27	4.13E-02
CG9628	4.33	3.39	1.69	1.51	2.41	1.27	5.06E-02
CG1368	10.92	12.47	4.48	5.16	2.42	1.28	1.19E-02
CG16885	8.41	6.45	2.88	3.24	2.43	1.28	5.82E-02
CG9279	3.96	4.19	1.72	1.62	2.44	1.29	2.25E-03

Ppn	5.41	5.49	1.95	2.50	2.45	1.29	8.59E-02
CG14621	48.70	49.49	19.61	20.23	2.46	1.30	2.09E-03
CG8888	2.69	3.16	1.09	1.23	2.51	1.33	1.41E-02
Lmpt	4.65	4.69	1.20	2.49	2.53	1.34	2.24E-01
Pmi	8.92	6.77	2.54	3.64	2.54	1.34	5.91E-02
Fas3	3.15	3.74	1.40	1.30	2.55	1.35	3.30E-02
CG14191	3.20	2.61	1.34	0.94	2.55	1.35	6.77E-02
TwdlW	4.03	2.24	1.61	0.82	2.57	1.36	1.67E-01
CG3244	16.60	12.12	6.29	4.85	2.58	1.37	4.67E-02
Cyp6d4	5.06	5.62	2.44	1.68	2.59	1.37	1.00E-01
CG33205	6.81	6.52	2.28	2.78	2.64	1.40	5.44E-02
Khc	37.95	38.12	14.48	14.11	2.66	1.41	6.74E-03
Ccp84Ad	3.21	3.82	1.19	1.42	2.69	1.43	1.54E-02
CG13041	5.60	5.16	2.92	1.06	2.70	1.43	2.69E-01
CG13063	7.66	6.48	2.33	2.64	2.84	1.51	1.29E-02
modSP	7.19	7.33	2.48	2.62	2.85	1.51	8.11E-03
Ccp84Ag	7.35	5.70	2.23	2.32	2.87	1.52	7.05E-02
CG4476	3.90	4.24	1.53	1.28	2.89	1.53	2.45E-02
CG6357	14.49	13.42	5.03	4.43	2.95	1.56	1.03E-02
Phk-3	6.94	6.56	2.85	1.68	2.98	1.58	1.43E-01
Cpr62Bc	5.61	4.97	1.90	1.64	2.98	1.58	8.33E-03
CG13066	6.35	5.37	1.42	2.50	2.99	1.58	1.32E-01
TwdlM	22.62	21.21	7.56	7.03	3.00	1.59	2.12E-03
CG9083	6.93	4.14	3.27	0.38	3.03	1.60	3.73E-01
CG32667	2.29	3.32	1.28	0.53	3.10	1.63	1.88E-01
CG13047	4.38	4.33	1.50	1.30	3.11	1.64	3.77E-02
CG4115	5.52	4.49	1.98	1.10	3.24	1.70	1.21E-01
CG42694	5.94	5.52	2.05	1.48	3.25	1.70	7.42E-02
TwdlC	3.03	2.16	1.14	0.46	3.26	1.70	1.87E-01
Cpr64Ad	6.62	5.61	2.41	1.34	3.26	1.71	1.30E-01
Dbi	11.78	10.59	2.64	4.18	3.28	1.71	1.05E-01
Surf1	8.49	9.00	3.20	2.13	3.28	1.72	1.00E-01
CG8316	3.67	3.18	1.10	0.97	3.31	1.73	6.79E-03
CG33981	24.21	21.55	7.18	6.54	3.34	1.74	4.66E-03
CG13068	5.90	7.84	2.55	1.53	3.37	1.75	7.91E-02
Msr-110	4.28	3.73	1.27	1.07	3.41	1.77	9.36E-03
CG13678	4.09	3.17	1.03	1.06	3.48	1.80	6.34E-02
Lcp65Ag1	3.33	3.44	1.40	0.48	3.60	1.85	2.30E-01
Verm	8.03	6.51	2.34	1.69	3.61	1.85	3.18E-02
TwdlF	7.20	4.20	2.98	0.08	3.73	1.90	4.05E-01
Serp	3.67	2.88	0.94	0.73	3.90	1.96	1.61E-02
Pio	4.90	4.54	0.96	1.45	3.91	1.97	8.50E-02
CG1503	22.36	22.44	5.04	5.68	4.18	2.06	2.62E-02
CG6567	11.63	11.55	2.94	2.55	4.22	2.08	3.11E-02
Osi20	4.70	2.87	1.59	0.16	4.33	2.11	3.26E-01
CG17816	8.44	7.26	2.53	1.07	4.36	2.12	1.61E-01
Cpr65Ec	3.37	3.47	0.77	0.78	4.42	2.14	2.52E-04
CG13049	3.20	1.85	0.90	0.24	4.42	2.14	2.03E-01
Cpr51A	13.84	10.76	3.38	2.14	4.45	2.16	4.97E-02
TwdlD	12.22	8.93	3.66	0.96	4.57	2.19	2.22E-01
Ipod	3.74	2.36	1.15	0.18	4.57	2.19	2.76E-01
CG9380	9.33	9.06	2.42	1.45	4.75	2.25	1.00E-01
Osi15	5.59	3.68	1.71	0.24	4.75	2.25	2.86E-01
Cpr65Ea	26.12	19.37	6.71	2.73	4.82	2.27	1.41E-01
CG15022	7.88	4.68	1.94	0.65	4.85	2.28	1.56E-01
Osi14	3.06	2.34	0.92	0.13	5.16	2.37	2.76E-01

CG7675	4.24	3.84	0.93	0.61	5.25	2.39	6.84E-02
mthl6	6.25	5.59	1.23	1.02	5.27	2.40	9.23E-03
Osi19	3.96	2.66	1.17	0.04	5.45	2.45	3.50E-01
ect	3.83	3.36	0.85	0.46	5.48	2.45	1.00E-01
CG2962	16.44	10.89	4.21	0.65	5.62	2.49	2.55E-01
Osi6	16.73	12.63	3.72	1.40	5.74	2.52	1.43E-01
CG30101	4.43	3.16	0.84	0.38	6.22	2.64	9.16E-02
CG14147	3.05	2.26	0.57	0.19	6.99	2.81	1.40E-01
Lcp65Af	4.40	4.30	0.47	0.48	9.20	3.20	5.44E-05
CG9184	4.88	6.92	0.23	0.89	10.53	3.40	1.46E-01
TpnC4	3.02	2.02	NA	0.23	10.91	3.45	NA
TepII	9.87	8.52	0.23	0.30	34.37	5.10	5.59E-03
CG11034	9.77	10.74	0.32	0.22	37.99	5.25	2.47E-02
mol	41.77	40.72	0.78	0.60	59.73	5.90	1.94E-02
kek1	11.97	14.38	0.28	0.12	65.47	6.03	5.11E-02

- mt1, mt2, WT1 and WT2 represent FPKM value from two biological repeats of dKDM4A mutant and wild-type embryos.
- fc: fold change, average FPKM mt/WT

Appendix E: Genes with increased H3K36me3 levels in dKDM4A mutant embryos

CG10132	CG7456	CG30148	CG8908	CG32350	CG10296	CG4606	CG12737
CG10699	CG7595	CG30149	CG8946	CG32369	CG10612	CG4910	CG12773
CG11023	CG8222	CG30150	CG9068	CG32374	CG10618	CG5023	CG12991
CG11326	CG8475	CG30194	CG9204	CG32407	CG1090	CG5099	CG13316
CG11327	CG8506	CG30259	CG9313	CG32448	CG10979	CG5237	CG13360
CG11527	CG8552	CG30265	CG9325	CG32451	CG1105	CG5400	CG13760
CG12283	CG8851	CG30286	CG9380	CG32484	CG11069	CG5455	CG14408
CG12676	CG9098	CG30287	CG9416	CG32485	CG11120	CG5730	CG1500
CG12789	CG9175	CG30392	CG9480	CG33275	CG11168	CG5737	CG15199
CG13284	CG9227	CG30438	CG9815	CG33291	CG11502	CG5760	CG15641
CG13793	CG9258	CG30440	CG9850	CG33484	CG11626	CG5873	CG15642
CG13794	CG9395	CG30463	CG9858	CG33965	CG11821	CG5948	CG1567
CG14029	CG9664	CG30471	CG9864	CG34244	CG11878	CG5959	CG15890
CG14039	CG9961	CG30483	CG12559	CG34342	CG11891	CG6040	CG1643
CG14937	CG9964	CG30484	CG15848	CG34416	CG11896	CG6118	CG16902
CG14938	CG40040	CG30485	CG17514	CG40050	CG11908	CG6127	CG1749
CG15385	CG11055	CG30488	CG40080	CG40053	CG11909	CG6184	CG1751
CG15400	CG10051	CG3257	CG40084	CG40452	CG12224	CG6342	CG17762
CG15444	CG10073	CG33150	CG40085	CG4144	CG12250	CG6356	CG18102
CG15627	CG10079	CG33151	CG40211	CG42255	CG12402	CG6490	CG18104
CG15824	CG10109	CG33183	CG40212	CG42278	CG12800	CG6706	CG18130
CG15828	CG10117	CG33554	CG40263	CG42337	CG13419	CG6969	CG1998
CG17124	CG10128	CG3356	CG40270	CG42377	CG13648	CG6972	CG2174
CG17211	CG10153	CG33724	CG40311	CG4321	CG13656	CG7034	CG2467
CG17224	CG10200	CG33988	CG40461	CG4357	CG13837	CG7077	CG3078
CG17264	CG10241	CG34192	CG40498	CG4432	CG13850	CG7079	CG32538
CG17265	CG10242	CG34195	CG41233	CG4684	CG13855	CG7125	CG32593
CG17348	CG10243	CG34197	CG41252	CG4821	CG14358	CG7126	CG32702
CG17378	CG10255	CG34222	CG41254	CG4942	CG14372	CG7146	CG32791
CG17490	CG10392	CG34350	CG41265	CG4999	CG14395	CG7208	CG32816
CG17544	CG10396	CG34405	CG41323	CG5087	CG14521	CG7431	CG3342
CG17941	CG10444	CG3541	CG10140	CG5414	CG14608	CG7432	CG33968
CG18028	CG10497	CG3548	CG10269	CG5528	CG14670	CG7675	CG34346
CG18140	CG10505	CG3565	CG1066	CG5618	CG14899	CG7794	CG34359
CG18405	CG10737	CG3570	CG11249	CG6024	CG14900	CG7896	CG34411
CG18507	CG10751	CG3682	CG11259	CG6611	CG15186	CG7940	CG34417
CG18559	CG10808	CG3955	CG11348	CG6767	CG15531	CG7998	CG3600
CG18783	CG11175	CG40129	CG1146	CG6821	CG15594	CG8129	CG3626
CG18854	CG11209	CG4051	CG11801	CG6885	CG16791	CG8136	CG3926
CG2671	CG11217	CG42321	CG1200	CG6895	CG17025	CG8507	CG3954
CG2903	CG11430	CG42391	CG12038	CG7018	CG17121	CG8516	CG42237
CG2964	CG11807	CG4329	CG12169	CG7158	CG17819	CG8790	CG42248
CG2969	CG11895	CG4533	CG1228	CG7447	CG17820	CG9388	CG4293
CG2976	CG11949	CG4832	CG12414	CG7458	CG18048	CG9698	CG4396
CG3131	CG12052	CG4840	CG1275	CG7507	CG1842	CG9728	CG4547
CG3164	CG12140	CG4975	CG13239	CG7571	CG18473	CG9743	CG4557
CG31641	CG12263	CG4984	CG13458	CG7924	CG18599	CG9855	CG5310
CG31719	CG12490	CG5065	CG13676	CG7962	CG1945	CG9918	CG5529
CG31720	CG12758	CG5174	CG13679	CG7972	CG1954	CG9990	CG6847
CG31792	CG12857	CG5330	CG13698	CG8065	CG1976	CG15831	CG6867
CG31897	CG12868	CG5335	CG13708	CG8100	CG1988	CG40138	CG6867
CG31957	CG12908	CG5411	CG13895	CG8177	CG2023	CG40158	CG7178
CG3212	CG12926	CG5431	CG14109	CG8308	CG2031	CG40159	CG7537
CG32972	CG13326	CG5473	CG14957	CG8540	CG2128	CG40368	CG7727
CG33196	CG13424	CG5489	CG14993	CG8564	CG2239	CG41075	CG8146

CG3327	CG13431	CG5532	CG14997	CG8607	CG31000	CG41133	CG8909
CG33296	CG13432	CG5594	CG14998	CG8634	CG31020	CG41249	CG8959
CG3399	CG13521	CG5819	CG15020	CG8641	CG31022	CG41286	CG9095
CG34007	CG13569	CG6280	CG15822	CG8742	CG31028	CG41298	CG9108
CG34182	CG1429	CG6355	CG16711	CG9149	CG31030	CG41300	CG9201
CG3762	CG15072	CG6362	CG16992	CG9279	CG31051	CG41335	CG9413
CG3769	CG15078	CG6530	CG16993	CG9295	CG31052	CG11155	CG9518
CG3779	CG15100	CG6646	CG16998	CG9299	CG31086	CG11231	CG9533
CG3921	CG15651	CG6671	CG17084	CG9391	CG31103	CG1507	CG9578
CG40006	CG15844	CG7576	CG17181	CG9614	CG31219	CG32019	CG9581
CG4026	CG15860	CG7759	CG17334	CG9628	CG31221	CG33521	CG9650
CG4158	CG16786	CG8089	CG17687	CG9670	CG31323	CG33653	CG9817
CG4238	CG16827	CG8095	CG18023	CG17023	CG31371	CG17626	CG9902
CG4644	CG17390	CG8098	CG18214	CG17374	CG3153	CG40091	CG2893
CG5075	CG17508	CG8250	CG1869	CG17594	CG32474	CG40092	CG40444
CG5125	CG17575	CG8394	CG18769	CG40337	CG32491	CG40108	
CG5149	CG1794	CG8403	CG18808	CG40413	CG32944	CG40195	
CG5322	CG18604	CG8405	CG32032	CG40467	CG33547	CG40378	
CG5803	CG18812	CG8405	CG32055	CG41050	CG34157	CG41087	
CG6093	CG1975	CG8424	CG32071	CG41248	CG34290	CG41327	
CG6105	CG1975	CG8425	CG32072	CG41283	CG34402	CG41520	
CG6729	CG2078	CG8428	CG32096	CG41347	CG3593	CG10362	
CG7052	CG2269	CG8430	CG3217	CG41348	CG3822	CG10986	
CG7068	CG2679	CG8443	CG32227	CG41511	CG3937	CG11417	
CG7075	CG2682	CG8453	CG32228	CG10038	CG42335	CG12141	
CG7234	CG2812	CG8547	CG32242	CG10041	CG42390	CG12199	
CG7384	CG30095	CG8632	CG32284	CG10047	CG42457	CG12311	
CG7400	CG30116	CG8841	CG32301	CG10097	CG4393	CG12348	
CG7438	CG30145	CG8859	CG32305	CG10170	CG4509	CG12531	